INVESTIGATING THE MACHINING CHARACTERISTICS OF TITANIUM ALLOYS USING ULTRASONIC MACHINING

A thesis submitted
in fulfillment of the requirements
for the award of the degree
of

DOCTOR OF PHILOSOPHY

By

RUPINDER SINGH

DEPARTMENT OF MECHANICAL ENGINEERING
THAPAR INSTITUTE OF ENGINEERING AND TECHNOLOGY
(DEEMED UNIVERSITY)
PATIALA-147 004 (INDIA)
2006

PREFACE

This research work was carried out by the author under the guidance of Dr. J.S. Khamba, Assistant Professor in the Department of Mechanical Engineering at Thapar Institute of Engineering and Technology (Deemed University) Patiala 147 004 (India).

Ultrasonic drilling machine, surface finish measuring instruments, weighing machine, brazing apparatus and other facilities available in the Department of Mechanical Engineering at T.I.E.T. Patiala (Deemed University) were used for this research work. Also, some instruments like perthometer and image analyzer available at Research & Development Centre for Bicycle & Sewing Machine, Ludhiana (Punjab) were used for the investigation of ultrasonically machined samples.

Several research papers were published out of this research work. **The list of Journals/Conferences in which the papers find place is given below:**

1. Singh Rupinder and Khamba J.S. (2006), "Ultrasonic machining of titanium and its alloys: A review", *Journal of material processing technology*, Vol. 173, No.2, pp 125-135.
2. Singh Rupinder and Khamba J.S. (2006), "Effect of toughness on machining characteristics in ultrasonic assisted drilling", *Journal of manufacturing technology today*, Vol. 5, No.4, pp 11-14.
3. Singh Rupinder and Khamba J.S. (2005), "Titanium alloys machining characteristics comparison using alumina slurry in ultrasonic assisted drilling", *Journal of manufacturing technology today*, Vol. 4, No.1, pp 18-20.
4. Singh Rupinder and Khamba J.S. (2005), "Modeling the machining characteristics of titanium alloys using ultrasonic machining: Buckingham-Π approach", Proceedings of 14th ISME international conference on Mechanical engineering in knowledge age, at Delhi College of Engineering, Delhi, India, Dec12-14, 2005, pp 464-469.

5. Singh Rupinder and Khamba J.S. (2005), "An experimental investigation on machining characteristics of titanium alloys using USM", Proceedings of Stainless Steel conference and expo. 2005, Maastricht, the Netherlands, Nov 08-10, 2005, pp 261-264.
6. Singh Rupinder and Khamba J.S. (2005), "Development in USM for drilling of titanium alloys", Proceedings of national conference on advances in condensed matter physics (ACMP-05), T.I.E.T. Patiala, India, Feb 11-12, 2005, pp 333-339.
7. Singh Rupinder, Khamba J.S. and Grewal J.S. (2005), "Machining characteristics optimization using Taguchi technique in ultrasonic drilling of titanium alloys", Proceedings of international conference on emerging technologies in intelligent system and control (EISCO-2005), Kumaraguru College of Tech. Coimbatore, India, Jan 05-07, 2005, pp 81-87.
8. Singh Rupinder and Khamba J.S. (2004), "Tool manufacturing technique in ultrasonic drilling machine", *Journal of manufacturing technology Today,* Vol-3, No.1, pp 05-07.
9. Singh Rupinder and Khamba J.S. (2004), "Study of machining characteristics of titanium alloys in ultrasonic machining", Proceedings of the 21st AIMTDR conference, Vellore Institute of Technology, Tamilnadu, India, Dec 20-22, 2004, pp 155-160.
10. Singh Rupinder and Khamba J.S. (2004), "Machining characteristics comparison of titanium alloys in ultrasonic assisted drilling", Proceedings of international conference on recent advances in composite materials (ICRACM2004), Institute of Technology, B.H.U (Banaras) India, Dec 17-19, 2004, pp 438-442.
11. Singh Rupinder and Khamba J.S. (2004), "Comparison of machining characteristics of titanium alloys: Effect of slurry in ultrasonic machining process", Proceedings of global congress on manufacturing and management, the international conference on manufacturing and management (GCMM-2004), Vellore Institute of Technology, Tamilnadu, India, Dec 08-10, 2004, pp 54-58.

12. Singh Rupinder and Khamba J.S. (2004), "Effect of slurry temperature on ultrasonic machining of titanium alloys, Souvenir of 18th national convention of metallurgical and materials engineers, I.E (I), Jaipur, (Rajasthan), India, Oct11-12, 2004.
13. Singh Rupinder, Khamba J.S. and Singh N. (2004), "Latest in brazing for tool making in USM process", Proceedings of annual convention of ISTE section & national seminar, at BBSBEC, Fatehgarh Sahib, (Punjab) India, March 12, 2004, pp 77-79.
14. Singh Rupinder and Khamba J.S. (2003), "Silicon carbide slurry effect in ultrasonic assisted drilling of titanium alloy (TITAN15)", *Journal of manufacturing technology today*, Vol-2, No. 7, pp 08-11.
15. Singh Rupinder and Khamba J.S. (2003), "Investigating the machining characteristics of titanium (Titan31) alloy using ultrasonic machining", Proceedings of 13th national conference of Indian Society of Mechanical Engineers (ISME-2003), IIT Roorkee, (Uttranchal) India, Dec 30-31, 2003, pp 59.
16. Singh Rupinder and Khamba J.S. (2003), "Ultrasonic assisted drilling of titanium (Titan-15) using Carbide, HSS and SS Tool", Proceedings of international conference on emerging technologies (ICET), KIIT, (Bhuvneswar) India, Dec19-21, 2003, pp 67.
17. Singh Rupinder and Khamba J.S. (2003), "Comparing the machining characteristics of titanium with cylindrical & conical horn in ultrasonic drilling", Proceedings of national conference on recent development in mechanical engineering (NCME-2003), T.I.E.T., Patiala, India, Oct 31-Nov 01, 2003, pp 619-620.
18. Singh Rupinder and Khamba J.S. (2003), "Effect of alumina (White Fused) slurry in ultrasonic drilling of titanium Alloy (Titan15)", Proceedings of national conference on emerging technologies (NCMRT-2003), TIET Patiala, India Sep19-20, 2003, pp 75-79.

19. Singh Rupinder and Khamba J.S. (2003), "Silver brazing for tool preparation in ultrasonic machining process" , Proceedings of national workshop on welding technology in India-Present status and future trends, S.L.I.E.T., Longowal, (Punjab) India, April 25-26, 2003, pp 61-63.
20. Singh Rupinder and Khamba J.S. (2003), "A frame work for modeling the machining characteristics of titanium alloys using USM", Proceedings of international conference on digital aided modelling & simulation (DAMS 2003), CIT, Coimbatore, India, Jan 06-08, 2003, pp 91.
21. Singh Rupinder and Khamba J.S. (2002), "Investigation of titanium alloys for machining characteristics using ultrasonic machining process", Souvenir of 47th congress of the Indian Society of Theoretical & Applied Mechanics (ISTAM), IIT, Guwahati, India, Dec 23-26, 2002, pp 64.
22. Singh Rupinder (2002), "Ultrasonic machining for tough materials & its application in mechanical industry", Proceedings of 4th national symposium (NSRS4) of research scholars on metals & materials, IIT, Madras, India, Sep 27-28, 2002, pp 31.

The list of Journals/Conferences in which the papers are communicated is given below:

1. Singh Rupinder and Khamba J.S. (2006), "Surface roughness optimization in Ultrasonic Machining of Titanium and its Alloys", communicated to 22nd AIMTDR, Indian Institute of Technology Roorkee, India, Dec 21-23, December 2006.
2. Singh Rupinder and Khamba J.S. (2006), "Robust design for modeling MRR in USM of titanium", accepted at international conf on Advances in Mechanical Engineering (AME-2006), BBSBEC, Fatehgarh Sahib, Punjab (India) Dec 01-03, 2006.
3. Singh Rupinder and Khamba J.S. (2005), "Ultrasonic machining of pure titanium", communicated to *Machining science and technology journal* (Taylor and Francis publications).

4. Singh Rupinder and Khamba J.S. (2005), "Macro-model for ultrasonic machining of titanium and its alloys: designed experiments", communicated to *Journal of Engineering Manufacture* (Proc. of IMechE Part B).
5. Singh Rupinder and Khamba J.S. (2005), "Investigation for ultrasonic machining of titanium and its alloys", communicated to *Journal of material processing technology* (Elsevier publications).
6. Singh Rupinder and Khamba J.S. (2005), "Mathematical modeling of tool wear rate in ultrasonic machining of titanium", communicated to *Journal of material processing technology* (Elsevier publications).

Rupinder Singh

ACKNOWLEDGEMENT

The author wishes to express his deep sense of gratitude to Dr. J.S.Khamba, Assistant Professor in the Department of Mechanical Engineering, Thapar Institute of Engineering and Technology, Patiala, for having given me an opportunity to do research in the area of ultrasonic machining with special reference to titanium alloys and for the inspiring guidance given throughout this research work.

Heartfelt thanks are due to Dr. S.C Saxena (Director, T.I.E.T Patiala) and Dr. S.B. Singh (Principal, Guru Nanak Dev Engineering College, Ludhiana) for their encouragement and support during this research work.

The author wishes to place on record his profound gratitude to Dr. K. K. Raina (Dean, Research and Sponsored Projects, T.I.E.T, Patiala), Dr. R. G. Tathgir, Dr. N. K. Nayar, and Dr. S. K. Mahapatra (Head, Department of Mechanical Engineering, T.I.E.T, Patiala), Dr. H.K. Grewal (Professor & Head, Department of Computer Science & Engineering, Guru Nanak Dev Engineering College, Ludhiana), and Dr. Harpreet Singh Rai (Sr. Lecturer, Department of Civil Engineering, Guru Nanak Dev Engineering College, Ludhiana) for their motivation provided to him throughout the period of research.

The author is grateful to Mr. B.S. Sangha (General Manager, Research & Development Centre for Bicycle & Sewing Machine, Ludhiana) for granting permission to use image analyzer and surface finish measuring instruments to conduct tests on some of his samples.

The author wishes to profusely thank Mr. Trilok Singh, Mr. Sohan Lal and Mr. Sukhdev Chand (Lab Superintendents, Machine Tool Lab, Department of Mechanical Engineering, Thapar Institute of Engineering and Technology, Patiala) for providing all the possible assistance and co-operation during the course of experimental work.

Special thanks are due to Dr. Lalit Kumar Sharma (Scientist & Head In-charge, Central Glass & Ceramic Research Institute, Noida) for providing powdered slurry and other consumables.

The author shall ever remain indebted to Mr. Charlie Wilhite (SONIC-MILL, Albuquerque, NM), and Ms. Lata M. Phadke (Phadke Associates, Inc., Colts Neck, NJ) for their technical advice. Institution of Engineers (India) is gratefully acknowledged for the financial help, without which the research work could not have been completed.

Grateful thanks are due to faculty and staff of Department of Mechanical Engineering at T.I.E.T. Patiala and at Guru Nanak Dev Engineering College, Ludhiana for providing encouragement and moral support from time to time.

My firm faith in the Almighty God has led me to face all problems with a smile, and helped me to cross all the bridges which came my way during this journey of success.

Last, but not the least, my parents deserve special mention for their love, affection and blessings showered on me to undertake and successfully complete this research work leading to Ph. D. degree. Special ones deserve special acknowledgement.

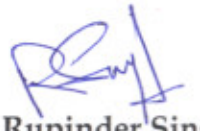

Rupinder Singh

CERTIFICATE

Certified that the thesis entitled, **"INVESTIGATING THE MACHINING CHARACTERISTICS OF TITANIUM ALLOYS USING ULTRASONIC MACHINING"** which is being submitted by Mr. Rupinder Singh, to Department of Mechanical Engineering, Thapar Institute of Engineering and Technology (Deemed University) Patiala, in fulfillment of the requirements for the award of the degree of **DOCTOR OF PHILOSOPHY**, is a record of bonafide research work carried out by him under my guidance and supervision. The matter presented in this thesis has not been submitted either in part or full to any other University or Institute for the award of any degree.

Jaimal S. Khamba

(Dr. J.S. Khamba)

Assistant Professor

Department of Mechanical Engineering

Thapar Institute of Engineering and Technology (Deemed University) Patiala-147004

Supervisor

ABSTRACT

Today, titanium and its alloys are extensively used for aerospace, industrial and consumer applications. In addition to aircraft engines and airframes, titanium alloys are also used in the applications like: missiles; spacecraft; chemical and petrochemical production; plant for hydrocarbon production and processing; power generation; desalination; nuclear waste storage; pollution control; ore leaching and metal recovery; offshore, marine deep-sea applications, and ship components; armor plate applications; anodes, automotive components, food and pharmaceutical processing; recreation and sports equipment; medical implants and surgical devices etc. These alloys are branded as difficult to machine materials and the conventional machining processes are unable to provide good machining. Commercially these alloys are machined by non-conventional Electric Discharge Machining (EDM), which is giving good material removal rate however accuracy and surface finish are some problematic areas. Another non-conventional machining process i.e. Ultrasonic machining (USM) is widely used to make holes and cavities in hard or brittle work-pieces by using shaped tools, high frequency mechanical motion, and an abrasive slurry. This process is giving good accuracy and surface finish for such materials. So, the study was aimed to carry out research on ultrasonic machining of titanium alloys (as work material) while machining with USM using different tool materials to know their impact on material removal rate (MRR), tool wear rate (TWR), and to model these characteristics for their applications in manufacturing industry. In the current study the work has been limited to commercially pure titanium (TITAN15, ASTM Gr.2) and titanium alloy (TITAN31, ASTM Gr.5), as work material, in combination with six different tool materials (Stainless steel; High speed steel; High carbon steel; Titanium; Tungsten carbide; Diamond) for experimentation. The results showed that the response variables (out put parameters) were strongly influenced by the control factors (input parameters).

ABSTRACT

Today, titanium and its alloys are extensively used for aerospace, industrial and consumer applications. In addition to aircraft engines and airframes, titanium alloys are also used in the applications like: missiles; spacecraft; chemical and petrochemical production; plant for hydrocarbon production and processing; power generation; desalination; nuclear waste storage; pollution control; ore leaching and metal recovery; offshore, marine deep-sea applications, and ship components; armor plate applications; anodes, automotive components, food and pharmaceutical processing; recreation and sports equipment; medical implants and surgical devices etc. These alloys are branded as difficult to machine materials and the conventional machining processes are unable to provide good machining. Commercially these alloys are machined by non-conventional Electric Discharge Machining (EDM), which is giving good material removal rate however accuracy and surface finish are some problematic areas. Another non-conventional machining process i.e. Ultrasonic machining (USM) is widely used to make holes and cavities in hard or brittle work-pieces by using shaped tools, high frequency mechanical motion, and an abrasive slurry. This process is giving good accuracy and surface finish for such materials. So, the study was aimed to carry out research on ultrasonic machining of titanium alloys (as work material) while machining with USM using different tool materials to know their impact on material removal rate (MRR), tool wear rate (TWR), and to model these characteristics for their applications in manufacturing industry. In the current study the work has been limited to commercially pure titanium (TITAN15, ASTM Gr.2) and titanium alloy (TITAN31, ASTM Gr.5), as work material, in combination with six different tool materials (Stainless steel; High speed steel; High carbon steel; Titanium; Tungsten carbide; Diamond) for experimentation. The results showed that the response variables (out put parameters) were strongly influenced by the control factors (input parameters).

LIST OF TABLES

LIST OF FIGURES

LIST OF APPENDICES

CONTENTS

CHAPTER 1

INTRODUCTION

The human race has distinguished itself from all other forms of life by using tools and intelligence to create items that serve to make life easier and more enjoyable. Through the centuries, both the tools and the energy sources to power these tools have evolved to meet the increasing sophistication and complexity of mankind's needs. Initially, tools were powered by muscles; either human or animal. However as the power of water, wind, steam, and electricity were harnessed, mankind was able to further extend manufacturing capabilities with new machines, with greater accuracy, and faster rates.

With the development of technology, the scientists and technologists in the field of manufacturing face more and more challenges. The difficulty in adopting the traditional manufacturing processes can be attributed mainly to the following three basic sources:

(i) New materials with low machinability.

(ii) Dimensional accuracy requirements.

(iii) Higher production rate and economy.

Many new materials and alloys that have been developed for specific uses possess a very low machinability. Producing complicated geometries in such materials becomes extremely difficult with the traditional methods. Also, sometimes the combination of the material properties and the job dimensions is such that it makes the use of traditional processes impossible. Examples of these types of jobs are, machining a complicated turbine blade made of super alloys, and producing holes and slots (both through and blind) in materials such as glass and semiconductors. So, drilling a non-circular hole or a micro hole becomes problematic (and sometimes impossible) if the traditional processes are used. Apart from the situations cited, higher production rate and economic requirements may demand the use of non traditional (or unconventional) machining processes.

The basic objective of all machining operations is to remove the excess material to obtain the desired shape and size. Yet in the past 50 years, different non traditional manufacturing processes have been invented and successfully implemented in production. The reason that there are such a large number of non-traditional processes is the same as there are such a large number of

conventional processes; each process has its own characteristic attributes and limitations, hence no one process is the best for all manufacturing situations. Table 1.1 shows the possible machining processes using the different types of energy and various methods of material removal.

Table 1.1 Unconventional Machining Processes

Unconventional machining processes			
Energy type	**Mechanics of material removal**	**Energy source**	**Process**
	Plastic shear	Mechanical motion of tool/ job	Conventional machining
Mechanical	Erosion	Mechanical/ fluid motion	Ultrasonic machining (USM) Abrasive jet machining (AJM)
Electrochemical	Ion displacement	Electric current	Electrochemical machining (ECM)
Mechanical and electrochemical	Plastic share and ion displacement	Electric current and mechanical motion	Electrochemical grinding (ECG)
Chemical	Corrosive reaction	Corrosive agent	Chemical machining (CHM)
	Fusion and vaporization	Electric spark	Electric discharge machining (EDM)
		High speed electrons	Electron beam machining (EBM)
Thermal	Fusion and vaporization	Powerful radiation	Laser beam machining (LBM)
		Ionized substance	Ion beam machining (IBM)
			Plasma arc machining (PAM)

Quite often, nontraditional manufacturing processes are able to provide a capability that simply cannot be met with conventional techniques. These non-traditional machining processes are sometimes applied to increase productivity either by reducing the number of overall manufacturing operations required to produce a product or by performing operations faster than the previously used method. In other cases, non traditional processes are used to reduce the number of rejects experienced by the traditional manufacturing method by increasing repeatability, reducing in-process breakage of fragile work pieces, or by minimizing detrimental effects on work piece properties.

Because of the aforementioned attributes, non-traditional manufacturing processes have experienced steady growth since their introduction. An increasing growth rate for these processes

in the future is assured, as these processes possess virtually unlimited capabilities when compared with conventional processes. Great advances have been made in the past few years in increasing the removal rates of some of these processes, and there is no reason to believe that this trend will not continue in the future.

The implementation of non traditional manufacturing processes will continue to increase as manufacturing engineers, product designers, and metallurgical engineers become increasingly aware of the unique capabilities and benefits that non traditional manufacturing processes provide.

1.1 ULTRASONIC MACHINING

Ultrasonic machining (USM) is a mechanical material removal process used to make holes and cavities in hard or brittle work-pieces by using shaped tools, high frequency vibrations, and an abrasive slurry. This process is generally associated with low material removal rates; however its application is not limited by the electrical or chemical characteristics of the work-piece material. Because the process is non-chemical and non-thermal, materials are not altered either chemically or metallurgically [1]. The process is able to effectively machine all materials harder than HRc 40, whether or not the material is an electrical conductor or an insulator [2-8]. Holes as small as 76μm in diameter can be machined, however, the depth to diameter ratio is limited to about 3:1[4, 8]. The USM process begins with the conversion of low- frequency electrical energy to a high-frequency electrical signal, which is then fed to a transducer [1, 9-14]. The transducer converts high frequency electrical energy into mechanical vibrations, which are then transmitted through an energy-focusing device that is horn/tool assembly [15-17]. This causes the tool to vibrate along its longitudinal axis at high frequency (usually $\geq$ 20 kHz) [1, 9]. The tool vibrates with total amplitude of only a few hundredths of a millimeter in a direction parallel to the axis of tool feed [1, 16, 17]. For efficient material removal to take place, the tool and tool holder must be designed with consideration given to mass and shape so that resonance can be achieved within frequency range capability of the USM machine. Typical power ratings range from 50-3000W [18] and can reach up to 4000W in some machines [9]. A controlled static load is applied to the tool. An abrasive slurry (composing a mixture of abrasive material; for example silicon carbide, boron carbide, alumina, etc. suspended in oil or water) is pumped around the cutting zone [9]. The

vibration of the tool causes the abrasive particles held in slurry between the tool and the work piece, to impact the work-piece surface causing material removal by micro chipping [19]. Figure 1.1 shows the basic elements of an USM set up using either a magnetostrictive or piezoelectric transducer with brazed and screwed tooling [1, 20].

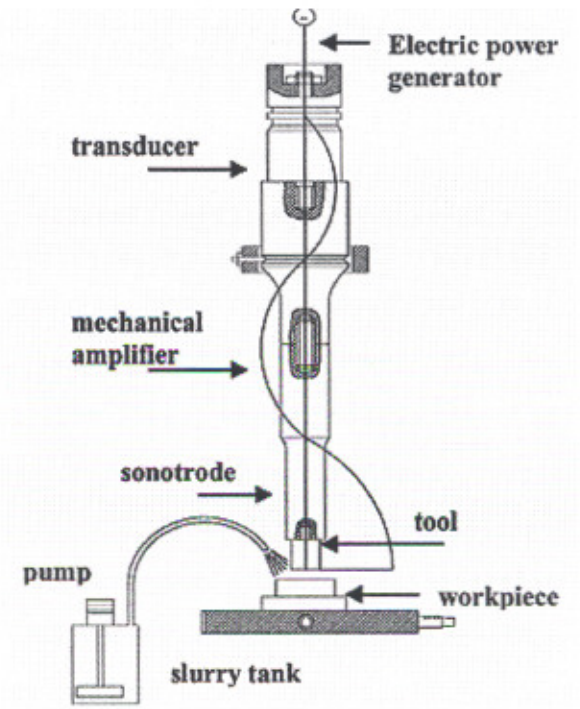

Figure 1.1 Basic elements of USM [20]

Variations on this basic configuration include: -

- A variation of USM, known as rotary ultrasonic machining (RUM), involves the use of rotating diamond-plated tools or drilling, milling, and threading operations [1,9]. The construction of RUM machines is nearly identical to USM machines except for the addition of a 0.37-0.56 kW (1/2-3/4 HP) rotary spindle motor capable of rotating up to 5000 rpm [9, 21]. The ultrasonic power required for the RUM process is considerably less than that used for USM; RUM machines typically are rated at 300 W or less [1].
- USM combined with electrical discharge machining (EDM) [13, 15, 17, 22, 23].

- Ultrasonic assisted turning is claimed to reduce machining time, work piece residual stresses and strain hardening, and improve work piece surface quality and tool life compared to conventional turning [8, 23-24].
- There are also non-machining ultrasonic applications such as cleaning, plastic/metal welding, chemical processing, coating and metal forming [1, 9].

1.2 TITANIUM AND ITS ALLOYS

Titanium has been recognized as an element (Symbol Ti; atomic number 22; and atomic weight 47.9) for at least 200 years. Titanium products available in both commercially pure and alloy grades, can be grouped into three categories according to the predominant phase or phases in their microstructure namely; alpha, alpha-beta, and beta. Although each of these three general alloy types requires specific and different mill processing methodologies, each offers a unique combination of properties, which may be advantageous for a given application. However, commercial production of titanium had not begun until 1950's. At that time, titanium was recognized for its strategic importance as a unique lightweight, high strength alloy [25, 26]. Today titanium alloys are common, readily available engineering metals that compete directly with stainless and specialty steels, copper alloys, nickel based alloys and composites. In addition to its attractive high strength- to-density characteristics for aerospace use, titanium's exceptional corrosion resistance derived from its protective oxide film has motivated extensive application in seawater, marine, brine and aggressive industrial chemical service over the past fifty years. Today, titanium and its alloys are extensively used for aerospace, industrial and consumer applications. In addition to aircraft engines and airframes, titanium is also used in the following applications: missiles; spacecraft; chemical and petrochemical production; hydrocarbon production and processing; power generation; desalination; nuclear waste storage; pollution control; ore leaching and metal recovery; offshore, marine deep-sea applications, and navy ship components; armor plate applications; anodes, automotive components, food and pharmaceutical processing; recreation and sports equipment; medical implants and surgical devices; as well as many other areas.

These alloys are branded as difficult-to-machine materials but have high utility in manufacturing sector [27]. Poor thermal conductivity of Titanium alloys retard the dissipation of heat generated,

creating, instead a very high temperature at the tool work-piece interface and adversely affecting the tool life [28]. Titanium is chemically reactive at elevated temperature and therefore the tool material either rapidly dissolves or chemically reacts during the traditional machining process resulting in chipping and pre-mature tool failure [27]. Compounding of these characteristics is the low elastic modulus of Titanium, which permits greater deflection of the work piece and once again adds to the complexity of machining [27, 29]. The Machinability of commercially pure grades of titanium has been compared by veteran shop men to that of 18-8 stainless steel, with the alloy grades of titanium being some what harder to machine [26]. Commercially pure and alloyed titanium can be turned with little difficulty; however the milling of titanium is more difficult operation than that of turning (using H.S.S tool). The cutter mills only during a part of each revolution and the chips tend to adhere to the teeth during that portion of the revolution and each tooth does not cut. Successful drilling is accomplished by using drills of proper geometry and by maintaining maximum drilling force to ensure continuous cutting. It is important to avoid the drill ride on the titanium surface in conventional drilling operation since the resultant work hardening makes it difficult to re-establish the cut [26, 30, 31]. So the conventional machining processes are unable to provide good machining characteristics to titanium alloys [28]. Commercially, these alloys are machined by non-conventional Electric Discharge Machining (EDM), which is giving good material removal rate. However, accuracy and surface finish are some problematic areas [32, 33]. The combined process of EDM with USM, improved the machining efficiency and accuracy [34]. In Ultrasonic assisted cutting, the chip, and work face are periodically separated leading to lower temperature/ forces, there by increasing tool life [35]. The problem of length of unsupported section of drill has been solved easily using USM. Here the portion of drill is no longer and still allows the chips to flow unhampered out of the hole [36, 37]. This permits application of maximum cutting pressure, as well as rapid drill removal to clear chips and drill re-arrangement without breakage.

1.3 OBJECTIVES AND ISSUES

The study was aimed to carry out research on ultrasonic machining of titanium alloys (as work material) using different tool materials to know their impact on material removal rate (MRR), tool wear rate (TWR), and to model these characteristics for their application

in manufacturing industry. The following issues have been taken up during this research work.

- The process capability of ultrasonic machining has been discussed for conventional work and tool materials.

- Machining properties of commercially pure titanium, (TITAN 15, ASTM Gr.2) and titanium alloy, (TITAN31, ASTM Gr.5) have been explored in combination with six different tool materials; namely, Stainless Steel (S.S.), High Speed Steel (H.S.S.), High Carbon Steel (H.C.S.), Titanium (Ti), Tungsten Carbide (WC), and Poly Crystalline Diamond (P.C.D.) in ultrasonic machining.

- Tool wear of aforesaid tool materials has been studied in machining of pure titanium and titanium alloys.

- Relationship between different machining parameters (slurry grit-size, slurry concentration, slurry type, slurry temperature, tool material, work material, power rating) and material properties (material removal rate, tool wear rate and surface roughness) has been established in this regard.

- The results achieved have been modeled for their application in manufacturing industry.

1.4 SCOPE OF THE WORK

The work has been limited to commercially pure titanium, TITAN15 (ASTM Gr.2) and titanium alloy, TITAN31 (ASTM Gr.5), as work material, in combination with six different tool materials (S.S., H.S.S., H.C.S., Ti, WC, P.C.D.) for experimentation. Machining characteristics of titanium and its alloy have been explored for their use in manufacturing industry. The typical composition of titanium and its alloy used is as follows:

Table 1.2 Chemical Analysis (%) TITAN 15 (ASTM Gr 2) {UTS 491 MPa}

C	H	N	O	Fe	Ti
0.006	0.0007	0.014	0.140	0.05	Balance

Table 1.3 Chemical Analysis (%) TITAN 31 (ASTM Gr 5) {UTS 994 MPa}

C	H	N	O	Al	V	Fe	Ti
0.019	0.0011	0.007	0.138	6.27	4.04	0.05	Balance

1.5 OVERALL METHODOLOGY OF THE STUDY

The overall research work is divided in to four phases.

(i) Detailed literature survey

(ii) Design of experiments (D.O.E)

(iii) Experimentation

(iv) Modeling the results

Literature on ultrasonic machining and its constituent aspects have been reviewed extensively to design a methodology for carrying out analysis on machining characteristics of titanium and its alloys. The literature survey has been focused on the various aspects of ultrasonic machining covering economic and technical viability. D.O.E phase uses the results of literature survey. In the beginning of D.O.E phase, pilot experiments have been performed for preliminary study of titanium and its alloys machining capabilities with USM. The various machining conditions, their ranges and levels have been selected based upon results of pilot study.

Based upon the finding of the Pilot study, experiments have been designed to determine the MRR of titanium pure (TITAN15, ASTM Gr.2) and titanium alloy (TITAN31, ASTM Gr.5) with different tool materials (S.S, H.C.S, H.S.S., WC, Ti and P.C.D.) under established environmental conditions. Accordingly tool wear of aforesaid tool materials used in combination with titanium and its alloys, as work material has been established. Taguchi Technique for Robust design, using L18 orthogonal arrays has been used for design of experiment.

The experimentation has been done on 500W ultrasonic drilling machine, Sonic Mill U.S.A. The impact of input parameters on material removal rate (MRR), tool wear rate (TWR) and surface roughness (SR) has been established for machining of titanium and its alloys with aforesaid tool materials.

- Type of slurry used
- Concentration of slurry
- Grain size of slurry particle
- Temperature of slurry
- Power rating of ultrasonic drilling machine

The results showed that the response variables (out put parameters) were strongly influenced by the control factors (input parameters). So, the results obtained after experimentation have been modeled using both "MACRO" and "MICRO" modeling approach. This has been followed by Taguchi, L18 Orthogonal arrays approach for macro modeling and Buckingham-π theorem for micro modeling for implementation of various control factors in manufacturing industries to achieve the desired levels of performance.

1.6 ORGANIZATION OF THE THESIS

The thesis has been divided into seven chapters. Brief description of the contents of each chapter is as under:

Chapter 1 brings out the need and importance of ultrasonic machining of titanium alloys, with their impact on productivity and performance. An overview of USM and problems associated with machining of titanium and its alloys particularly for manufacturing industry has been provided. Significant issues like various control factors affecting the

process have been listed out. Objectives and scope of study and overall methodology adopted have also been briefly outlined.

Chapter 2 outlines the literature review on theory of ultrasonic machining, parameters involved in ultrasonic machining and machining problems of titanium and its alloys. The description of control factors, signal and noise factors and response variable has been made.

Chapter 3 discusses preliminary study for selection of factors levels by pilot experimentation. The actual experimentation procedure, test date report, and observational data as per Taguchi designed experiments have been described.

Chapter 4 highlights results of designed experiments, followed by further discussion. The discussion is based upon analysis of experimental data.

Chapter 5 outlines modeling of results. Both macro and micro modeling approach has been adopted. Macro model has been developed using Taguchi approach and micro model has been developed using Buckingham π theorem.

Chapter 6 is all about conclusions of this research work. This chapter also highlights limitation of the study, and scope of future work in this area.

This chapter is followed by references.

CHAPTER 2

LITERATURE REVIEW

2.1 INTRODUCTION

A comprehensive review of literature on diverse aspects of ultrasonic machining, and machining characteristics of titanium and its alloys has been presented here. It had helped to identify the areas explored in this study.

2.2 REVIEW OF LITERATURE

The history of USM began with a paper by R.W. Wood and A.L. Loomis in 1927 [9, 38, 39] and the first patent was granted to American engineer Lewis Balamuth in 1945 [3, 9, 40, 41]. USM has been variously termed ultrasonic drilling; ultrasonic abrasive machining; ultrasonic cutting; ultrasonic dimensional machining and slurry drilling [9]. However, from early 1950s it was commonly known either as ultrasonic impact grinding or USM [4, 10, 11, 40]. Since its invention, USM has developed into a process that has been relied upon to solve some of the manufacturing community's toughest problems [1].

2.2.1 Tooling considerations in USM

The tool was shaped conversely to the desired hole or cavity and positioned near, but not touching, the surface of the work piece [1], generally manufactured by silver brazing [42, 43]. Many USM applications were involved in drilling where a tool of either simple or complex cross section penetrated axially in to the work piece, to produce either a through or blind hole of the required dimensions [1, 9]. For three-dimensional cavity, a process analogous to die sinking was generally employed [3, 6, 39, 44-47], see figure 2.1.

Rutan [48] reported that special tools were used to simultaneously produce a multitude of holes in precise patterns. This gang drilling technique had significantly increased productivity without compromising quality.

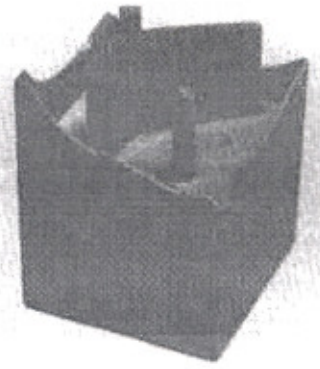

Figure 2.1 Silicon nitride turbine blade counter-sunk using USM [3]

Although USM volumetric material removal rates were relatively low, the process remained economically competitive because of its ability, with a single pass of the tool, to generate complex cavities or multiple holes in work piece materials that were too hard or fragile to machine by alternate processes, see figure 2.2.

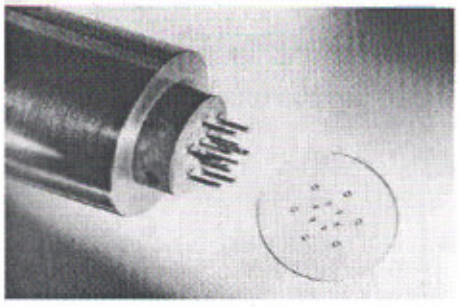

Figure 2.2 USM gang drill tool for drilling 12 holes simultaneously [48].

Figure 2.3 shows a 0.64 mm thick aluminum oxide substrate used by the electronics industry. USM was used to simultaneously drill 930 holes 0.64 mm in diameter and 30 holes 1.53 mm in diameter. The entire operation was performed in 8.5 minutes, using an array of stainless steel hypodermic needles as the tool and 320-grit boron carbide as the abrasive. This process time equated to approximately 0.5 sec/hole [49]. In a similar application, 2176 square holes measuring 0.79 mm on a side were simultaneously made in a 1.01 mm thick carbon plate in 10 minutes. Because such a large number of holes were made simultaneously, an alternative process that drills one hole at a time would have to generate holes at rate of 3.6 holes per second to be able to match the rate of USM [1].

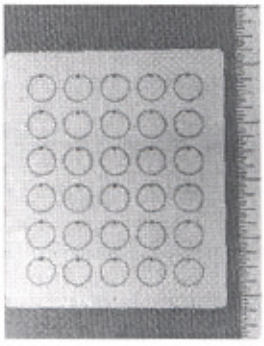

Figure 2.3. Aluminum oxide substrate drilled using USM [9].

Using this technique, graphite electrode for EDM was shaped in 30 minutes instead of the 20 hours required by copy milling [50-53]. The problem of using tools of complex form, however, was that they were not subjected to same machining rate over whole of their working surface and experienced differential wear rate, both of which affected the product shape [9, 54]. In addition, there were problems in tuning a complex tool to achieve maximum performance compared to basic tool [9].

An alternative approach was to use a simple "pencil" tool and contour machine the complex shape with a CNC programme. Figure 2.4 shows hypodermic needle that was used to ultrasonically drill small holes through a silicon nitride (Si_3N_4) work piece [55]. Recently, this technique has been investigated in a number of countries including the UK, France, Switzerland, Japan, etc. [9, 19]. A few CNC controlled rotary USM systems are available commercially such as the SoneX 300 from Extrude Hone Limited (France); and the ErosonicUS400/US800 from Erosonic AG (Switzerland) [9]. Most successful ultrasonic machining applications involve drilling holes or machining cavities in non-conductive ceramic materials.

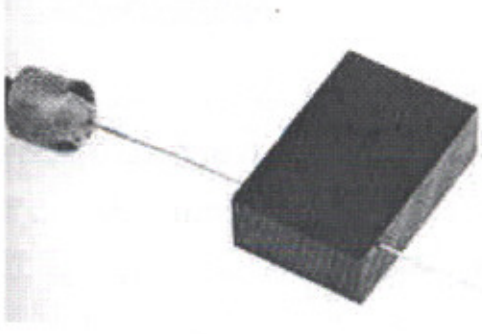

Figure 2.4 Silicon nitride machined by hypodermic needle using USM [55].

A novel use for USM has been the multi-step process for fabricating silicon nitride (Si_3N_4) turbine blades, see figure 2.5. The technique removes a large volume of material that would otherwise have been removed by the much slower technique of pantograph profile grinding [55]. Completed Si_3N_4 turbine blades are shown in figure 2.6 [56]. The selection of USM as a manufacturing process usually occurred because no other process was capable of performing the task. The alternative process would have required substantially longer process times [1].

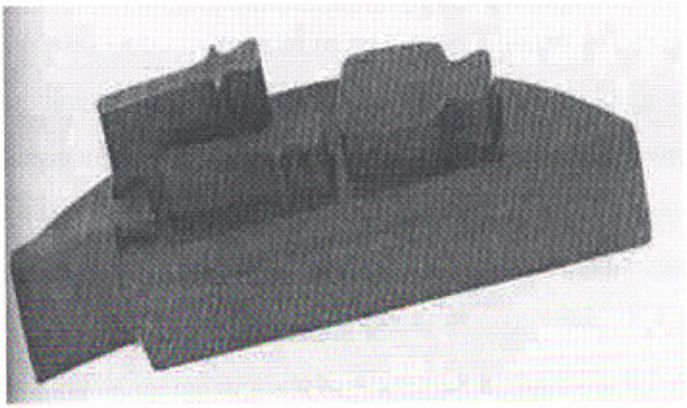

Figure 2.5 Silicon nitride turbine blade blank machined using USM [55].

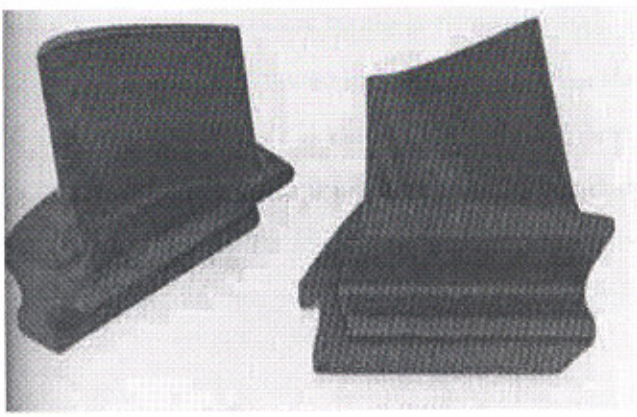

Figure 2.6 Ceramic turbine blade machined using USM [56].

As regards to rotary ultrasonic machining (RUM) applications, most popular use was for drilling high aspect ratio holes in hard, brittle materials. Current capabilities include hole diameters from 0.51 to 38.1 mm at depths up to 305 mm. Aspect ratios up to 200:1 can be achieved using roughing and finishing passes [1]. An example of deep holes drilled through glass, along with the tool used to produce them is shown in figure 2.7.

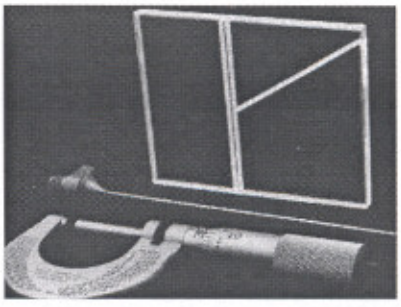

Figure 2.7 Thin tool for deep, intersecting holes through glass [1].

Although the initial cost of USM/RUM equipment is higher than conventional drilling, milling, and thread-grinding equipment, this difference can be quickly offset by the savings realized from extended tool life, increased productivity, and reduced work piece breakage [1].

2.2.2 Basic elements of USM

The machines for USM range from small tabletop-sized units to large-capacity machine tools. In addition to the part-size capacity of a USM machine, suitability for a particular application is also determined by the power rating [1]. Figure 2.8 shows compact 500W USM machine for small, light- weight work piece [57].

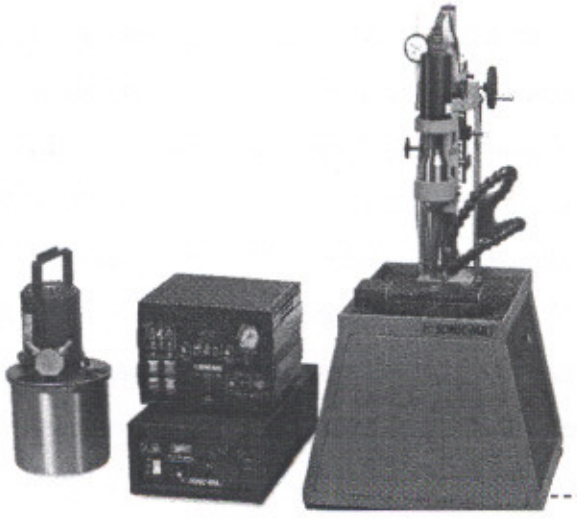

Figure 2.8 Compact 500W USM machine for small, light- weight work piece [57]

The material removal rate is directly related to power capability of the USM machine. All USM machines share common subsystems regardless of the physical size or power [1].The most

important of these subsystems are the power supply, transducer, tool holder, tool and abrasives [9].

2.2.2.1 Ultrasonic Power Supply

The power supply for USM is more accurately characterized as a high power sine-wave generator that offers the user control over both the frequency and power of the generated signal [1]. It converts low-frequency (60Hz) electrical power to high frequency (approximately 20 kHz). This electrical signal is supplied to the transducer for conversion in to mechanical motion [1, 9].

2.2.2.2 Ultrasonic Transducer

In the case of USM transducer, electrical energy is converted in to mechanical motion [1, 9, 37, 58]. With a conventional generator system, the tool and horn are set up and mechanically tuned by adjusting their dimensions to achieve resonance [9]. Recently, resonance following generators have become available which automatically adjust the out put high frequency to match the exact resonance of the horn/tool assembly [2].

They can also accommodate any small error in set up and tool wear, giving minimum acoustic energy loss and very small heat generation [16]. The power supply depends on the size of transducer [18]. Two types of transducers used for USM are based on two different principle of operation, piezoelectric and magnetostrictive [1]. Piezoelectric transducers used for USM generate mechanical motion through the piezoelectric effect by which certain materials, such as quartz or lead zirconate titanate [59-62]. Piezoelectric transducers, by nature, exhibit extremely high electromechanical conversion efficiency (up to 96%) [1, 9, 59, 63-64, 65], which eliminates the need for the water-cooling of the transducer [1]. These transducers are available with power capabilities up to 900W. Figure 2.9 shows the converter for compact 500W USM machine [57]. Magnetostrictive transducers are usually constructed from a laminated stack of nickel or nickel alloy sheets. These types of transducers are rugged but have electromechanical conversion efficiencies ranging from only 20 to 35% [1].

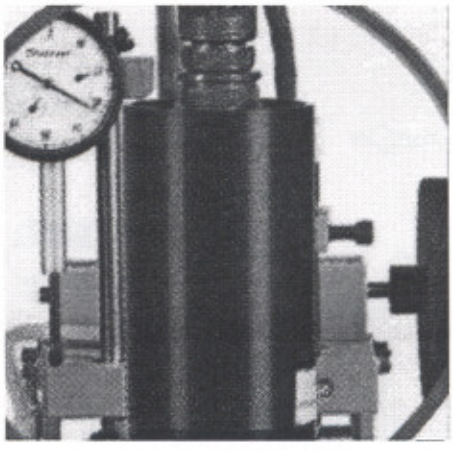

Figure 2.9 Converter for compact 500W USM machine [57].

2.2.2.3 Tool Holder

The function of tool holder is to attach and hold the tool to the transducer. Additionally, the tool holder also transmits the sonic energy to the tool, and in some applications, also amplifies the length of the stroke at the tool [1,]. Figure 2.10 shows the amplitude coupling for compact 500W USM machine [57]. Tool holders are attached to the transducer by means of a large, loose-fitting screw [1, 57].

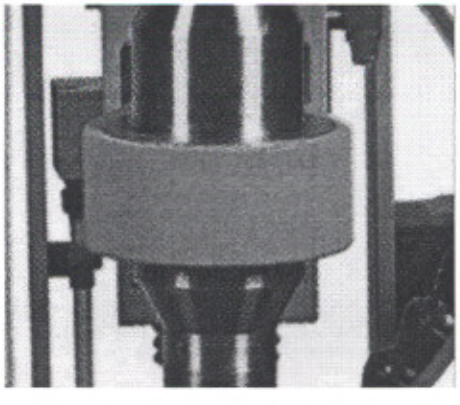

Figure 2.10 Amplitude coupling for compact 500W USM machine [57]

Half hard copper washers are used between the transducer and tool holder to dampen and cushion the interface, which further reduces the chances of unwanted ultrasonic welding [1]. Figure 2.11 shows the amplifying tool holders, and mechanically attached tools used for USM [57].

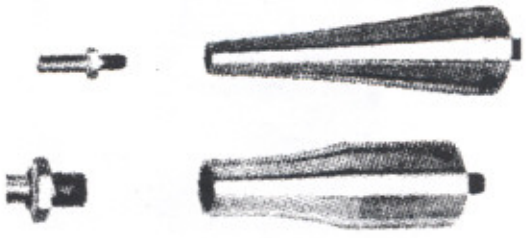

Figure 2.11 Amplifying tool holders for USM [57]

The horn is variously referred to as an acoustic coupler, velocity/mechanical transformer, tool holder, concentrator, stub or sonotrode. The oscillation amplitude at the face of the transducer is too small (0.001-0.1 μm) [65, 66, 67] in order to achieve any reasonable cutting rate, therefore, the horn is used as an amplification device [38, 68]. Figure 2.12 shows different horn designs with and without additional tool heads [69].

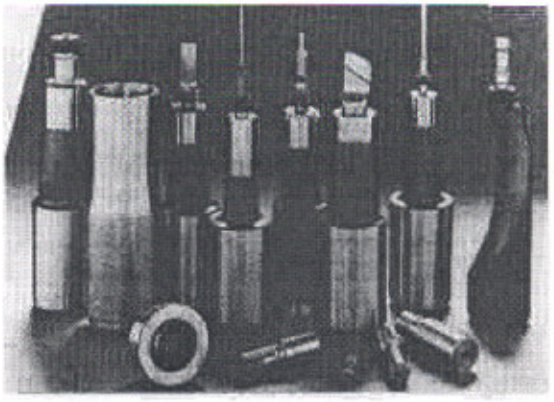

Figure 2.12 Different horn designs with and without additional tool heads [69].

Tool holders are available in two configurations: non- amplifying and amplifying. Non-amplifying tool holders are cylindrical and result in the same stroke amplitude at the out put end as at the input end. Amplifying tool holders have a modified cross section, as shown in figure 2.11 and are designed to increase the amplitude of the tool stroke as much as 600% [1, 57]. The material used should have high wear resistance, good elastic and fatigue strength properties, and

have optimum values of toughness and hardness for the application [39, 65, 70]. Tungsten carbide, Silver steel, and Monel are commonly used tool materials [9]. Polycrystalline diamond (PCD) has recently been detailed for the machining of very hard work piece material such as hot iso-statically pressed silicon nitride [71]. Tool can be attached to the horn by either soldering or brazing, screw/taper fitting [9, 43]. Also, the actual tool configuration can be machined on to the end of the horn [1, 39, 9, 18, 51, 72-74]. Threaded joints are conventionally used because of quick and easy tool changing, however problems can occur such as self-loosening, loss of acoustic power, fatigue failure etc. [75].

2.2.2.4 Tools and Abrasives

To minimize tool wear, tools should be constructed from relatively ductile materials such as stainless steel, brass and mild steel [1, 9]. However the difficulties with very ductile material like aluminum can be traced due to its short tool life. This difficulty can be eliminated by using low carbon steel and stainless steel as tool material. Depending upon the abrasive used, the work-piece material, work-piece/tool wear ratio can range from 1:1 to 100:1 [1, 37, 58]. The tool is normally held against the work piece by a static load exerted via a counter weight/ static weight, spring, pneumatic/hydraulic or solenoid feed system [39, 21, 67, 70, 76]. For optimum results, the system should maintain a uniform working force while machining and be sufficiently sensitive to over come the resistance due to the cutting action [68, 73]. Static load values of about 0.1-30N are typically used [9]. The force is particularly critical when drilling small holes less than 0.5 mm diameter as bending of the tool can occur under too high a load. The transport medium for the abrasive should possess low viscosity with a density approaching that of the abrasive, good wetting properties and, preferably, high thermal conductivity and specific heat for efficient cooling, water meets most of these requirements [9, 40, 68]. The abrasive material is mixed with water to form the slurry. The most common abrasive concentration is 50% by weight [1, 57]; however this can vary from 30-60%. Thinner mixtures are used to promote efficient flow when drilling deep holes or when forming complex cavities [1, 40, 67, 70, 77, 78]. Once abrasive has been selected and mixed with water, it is stored in a reservoir at the USM machine and pumped to the tool- work piece interface by re-circulating pumps at rate up to 26.5 L/min [1, 57].

2.2.3 Material removal mechanisms

Shaw [18] and Miller [79], Cook [80], Rosenberg [3] and others [46, 66, 81, 82] have done extensive work on the mechanism of material removal. Most of the work is on machining mechanism of hard and brittle material [33, 36, 37]. These mechanisms are detailed in figure 2.13 and comprise of: -

- Material abrasion by direct hammering of the abrasive particles against the work piece surface [6, 17, 18, 44, 53, 63, 67, 73, 79, 83];
- Micro chipping by impact of the free moving abrasive particles [18, 40, 44, 53, 73, 83, 84];
- Cavitation effect from the abrasive slurry [6, 18, 40, 45, 53, 84];
- Chemical action associated with the fluid employed [18, 40].

The individual or combined effect of the above mechanisms resulted in work-piece material removal by shear [23, 73, 78, 85], by fracture (for hard or work hardened material) [78] and displacement of material at the surface, without removal, by plastic deformation [23], which occurred simultaneously at the transient surface [9]. With porous materials like graphite, as opposed to hardened steels and ceramics, cavitation erosion was a significant contributor to material removal [6, 18, 40, 44, 83]. Markov [80] and others [18,39] considered that cavitation erosion and chemical effects were of secondary significance with the majority of work piece material acting essentially to weaken the work piece surface, assist the circulation of the abrasive and the removal of debris.

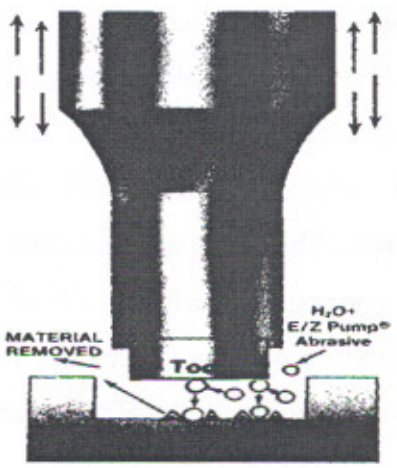

Figure 2.13 USM material removal mechanisms [57]

The experimental verification has shown that the MRR decreased with the ratio of work piece hardness and tool hardness. Thus, if work piece hardness increases it is expected that the tool hardness is also increased. The choice of tool material is one of the most important decisions, for making maximizing MRR and minimizing tool cost.

Kainth et al [81] outlined the mechanism of material removal in ultrasonic machining as shown in figure 2.14. USM results in ∂t penetration in to the tool and ∂w penetration in to the work-piece.

∂t = Penetration in to tool

∂w = Penetration in to work piece

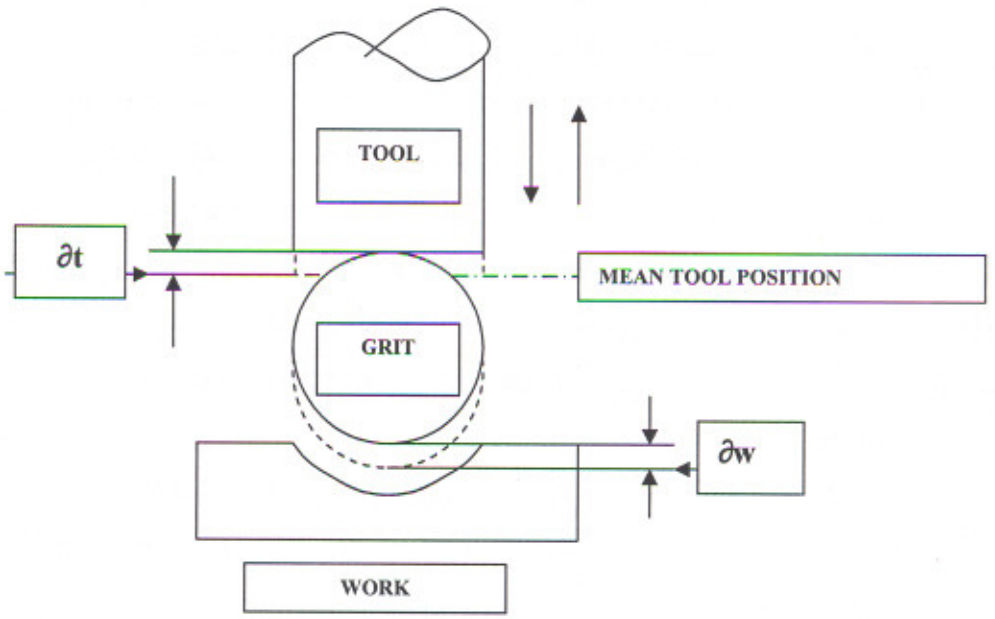

Figure 2.14 Schematic diagram of Impact ultrasonic machining [81].

This is an extension of Shaw model [18]. The theory that supports the ultrasonic machining process is neither complete nor non-controversial. Several investigators [3, 18, 46, 66, 79-82] have explained the process in different ways. However, Shaw [18] proposed a comprehensive theory of USM. This theory highlighted mainly hammering action of abrasive particles and impact of free abrasive particles on the work-piece. The cavitation erosion and chemical action associated with fluid employed was assumed to be secondary factor. Miller [79] derived expression for MRR assuming that the abrasive particles are of

cubical shape. This model for MRR included plastic deformation, work hardening and chipping.

Rosenberg [3] concluded that MRR is primarily due to hammer blows by the tool on the abrasive in contact with the work surface (similar to conclusions arrived by Shaw [18]). Saha and Bhattacharya [86] conducted an exhaustive study for developing a comprehensive analytical model for estimation of MRR and also investigated the mechanism of MRR by considering the major influencing parameters. The experimental results highlighted that fall in MRR at higher static loads occur. Zhao et al has found that bending vibration-cutting bar (BCB) plays a very important role in the ultrasonic vibration cutting systems. The design of BCB must meet requirements of resonance of both transversal and longitudinal vibration components. Also two-stage amplification function of the step shaped BCB is verified [87]. Nishimura concluded that the efficiency of machining depends on the impulsive force of machining and vibration displacement of the tool tip [9]. Riddi and Roch [88], Bulat [89] and Willard [90] reported that the cavitation bubbles formed during the ultrasonic oscillations produce a pressure more than 1000 kgf/cm^2 on the work-piece surface when they collapse. This pressure rise causes some material removal. Goetze [91] reported that for tools with equal contact area, there is an increase in penetration rate for tools with larger perimeters leading to more MRR; the effect is mainly due to difficulty of adequately distributing the abrasive slurry over the machining zone [15, 68, 92, 93].

2.2.4 Process parameters

The major USM process variables effecting material removal rate, accuracy, and surface-finish are ultrasonic power, amplitude of vibrations, abrasive size and frequency [1, 9]. Koops [94] and others [95, 96] investigated the influence of the wear of the abrasive powder on the technological indices of USM and provided cause and effect diagram of material removal rate (MRR) and tool wear rate (TWR), see figure 2.15.

The affect of process parameters can be studied independently based upon, work-piece properties; slurry properties; tool characteristics and operating parameters.

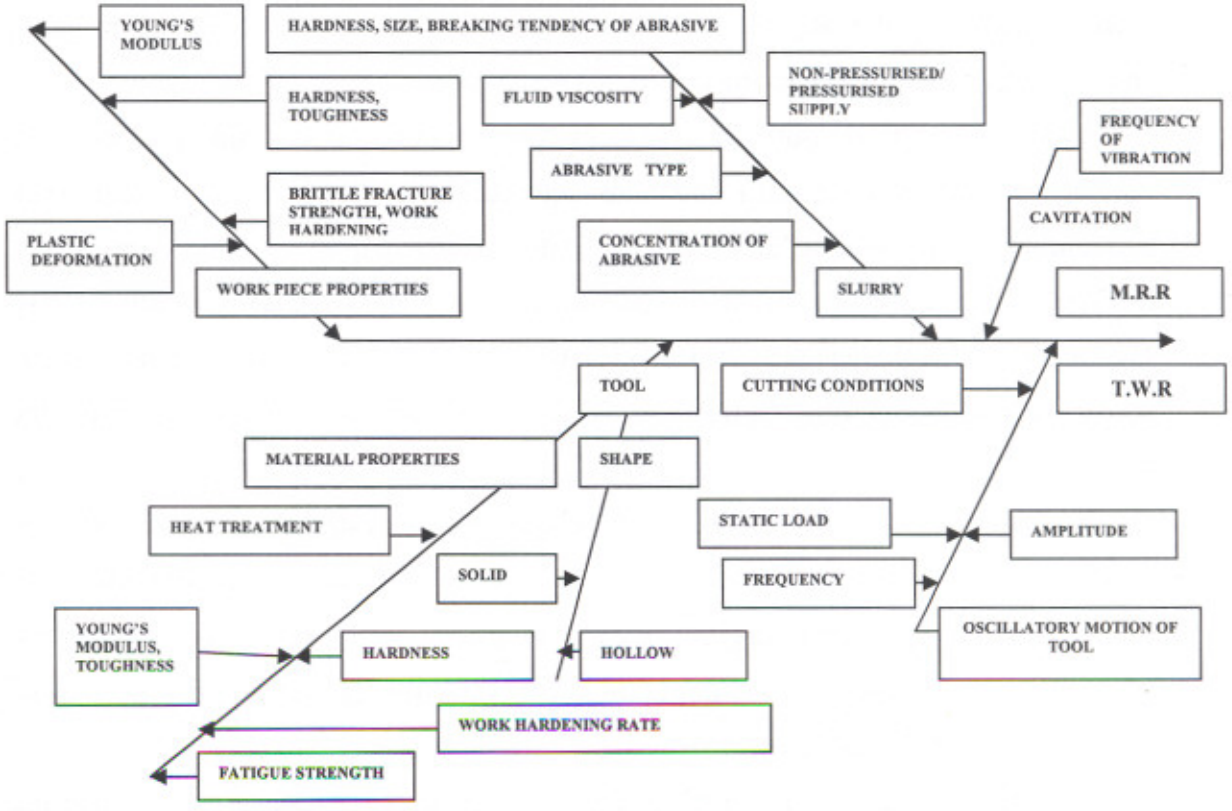

Figure2.15 Cause and effect diagram of MRR and TWR [94]

2.2.4.1 Work-piece properties

Kremer and Mackie [97] outlined applications of USM on ceramic materials as impact grinding process. The material removal mechanism reported involves both erosion and grinding. Zhang outlined MRR analysis selecting 99.5% Al_2O_3 ceramic as work material [98]. The experimental simulation of the process mechanics, in an attempt to analyze micro removal of ceramic material Al_2O_3 in precision machining, outlined by Rajurkar et al [99]. Results show that low impact forces cause only structural disintegration and particle dislocation. The high impact force contributes to cone cracks and subsequent crater damage.

Kennedy and Skaar outlined general review for improving machining of ceramics. This paper explored non-traditional machining methods like USM, EDM and gave an assessment of research needed for industrial application [100]. USM of ceramics has

been outlined by Spur et al [101]. This paper deals with application of USM and resulting problems concerning the finishing of ceramic materials.

Haun and Schulze [102] outlined new technique for ultrasonic machining of complex ceramic components i.e. tooth restorations, introducing a multi part tool system. They also outlined new ceramic machining route to create complex ceramic components. Hocheng et al outlined machinability of zirconia ceramics in ultrasonic drilling [103]. The material is removed at several cubic millimeters per minute with 0.5-micrometer average surface roughness. Optimal machining conditions were established with the above performance indices.

The problem of drilling small diameter (less than equivalent to 1 mm) cooling holes in electrically non-conductive ceramic coated nickel alloy using combined USM and EDM has been studied by Thoe et al [104]. By adjusting the operating parameters during the transition from ceramic to nickel machining, it was possible to maintain the integrity of any intermediate bonding layer.

Guzzo et al. [105] highlighted relation- ship between quartz crystal orientation and the surface quality obtained by USM. Scanning electron microscopy analysis shows that brittle micro cracking is the main wear mechanism involved with material removal. Kai and Takahira highlighted micro ultrasonic machining by the application of work-piece vibration [106]. Using this set up, successes have been achieved in machining micro holes in quartz, glass and silicon.

Zhixin [107] outlined combined machining of USM and EDM for advanced ceramics. The combined machining technique can be applied to machine all conductive, hard and brittle materials with efficiency and surface integrity. Zhixin et al. [108] studied a new technology of USM and EDM. The experimental results show that its efficiency is over three times than that of USM, and surface integrity is not significantly different in case of brittle material. Micro ultrasonic machining and its application in micro electro-mechanical system (MEMS) was outlined by Sun [109]. The combination of wire electric discharge grinding (WEDG), EDM and USM on micro ultrasonic machine also makes possible the machining. Pei et al. [110] outlined rotary ultrasonic machining (RUM),

which is hybrid-machining process, combining material removal mechanism of diamond grinding and ultrasonic machining. Deng and Lee [111] studied surface integrity in EDM, USM and Diamond saw cutting of ceramic composites. With in most machining conditions, the ultrasonic machined and diamond saw cut specimen behaved fairly consistently, and the flexural strength were higher than that of EDM specimen. Ya et al. [112] have also outlined an experimental investigation at RUM. The investigation shows that compared with conventional USM, RUM have higher MRR, and can be combined with CNC technology in hard and brittle machining.

Diepold and Obermeier [113] compared ultrasonic drilling method with two other procedures for machining holes (Sand Blasting and laser machining). A process was developed to smoothen the walls of the drilled holes with different concentration of hydrofluoric acid.

2.2.4.2 Slurry properties

The abrasive particle size strongly influences the MRR and surface finish. As particle size increases MRR increases proportionally and surface finish is decreased [1, 9, 95, 96, 114-116]. Khairy [83] outlined assessment of some dynamic parameters for USM. The mechanism underlying the micro-chipping action in USM identified as mainly localized hammering and free impact by abrasive grains in the slurry [117-121].

Kazantsev [122] claimed that forced delivery of the slurry increased the output of USM five fold without the need to increase grit size or machine power. The abrasive particle size strongly influences the MRR and surface finish. As particle size increases MRR increases proportionally and surface finish is decreased [1, 9, 95, 96]. The temperature of slurry also affects the surface finish of the work piece obtained [123-128].

Kennedy et al. [15] and others [129-133] pointed out the difficulty of machining a flat at the bottom of a hole because of uneven slurry distribution across the machining face, resulting in fewer active grits at the tool centre. When the work piece is a hard material, a slightly better surface finish can be obtained than with a material of lower hardness, value as low as 0.4 micron are obtainable [2]. Dam et al. [134] suggested that better surface finish is obtained when feed rates and depths of cut are decreased. A decrease in abrasive

grain size during USM leads to lower Ra value [9]. In addition, the accuracy of the machined hole is improved [6, 11, 39, 78] and a better surface finish is obtained on the bottom face than on the walls of the cavity [2, 3, 133].

2.2.4.3 Tool characteristics

Tool wear is an important variable in USM, affecting both MRR and hole accuracy [93, 124,125]. The complex tool wear pattern in USM can be divided into longitudinal wear [74, 125, 126] and lateral/side/diametral wear [88, 91] some of which will occur as a result of cavitation or suction wear [88, 127-129]. Adithan [74] and Venkatesh [130] reported maximum tool wear at a particular static load, which may be considered optimum for the point of view of maximum MRR [9]. Tool wear is affected by work piece hardness and can also be affected by the toughness of work piece [131]. If the hardness of the tool increases by work hardening, the penetration of the abrasive grains into the tool will decrease resulting in higher work piece MRR. In addition, material removal from the periphery of the work zone will be greater so that a convex surface will be formed in the work piece. This causes plastic deformation of the centre of the tool face, forming a dish [9]. It has been found that the degree of hardening is highest at the periphery and lowest at the centre for the tool material [132]. As a result, soft materials, e.g. copper and brass, are unsuitable as tools since they develop burrs at large oscillatory amplitudes [18, 68].

Komaraiah et al. [132] and others [93, 126] have shown that tool materials can be ranked in order of superiority as follows: Nimonic 80A> thoriated tungsten > silver steel > stainless steel > maraging steel > titanium > mild steel. Neppiras [39] using other tool materials gave the following ranking: tungsten carbide > brass > mild steel > silver steel > stainless steel > copper. Tool with diamond tips have been shown to have good material removal characteristics and extremely low wear rate [2].

Several authors have reviewed the theory and art of designing the tool/ horns, but it is not as yet fully understood [3,123,135-139]. Detailed guidelines for tool design are described by Rozenberg et al [3]. Traditional methods of acoustic horn design are based upon differential equation which considers the equilibrium of an infinitesimal element under

the action of elastic and inertia forces, which is then integrated over the horn length to achieve resonance [123, 136]. Typical design includes cylindrical, stepped, conical and exponential types [7, 136, 140]. Tuning is normally done from the transducer (screw thread end) where a tuning allowance of 10-15 mm should be made [72, 136, 141]. Recently, finite element modeling (FEM) has been used [7, 123, 136] to design axi-symmetric horn shapes. The analysis can take into consideration the weight of the tool [9]. FEM has also been used to access the working stress to ensure safe stress limits [135]. Dam et al. [134] claimed that a horn can be designed which converts the longitudinal ultrasonic action into a mixed lateral and longitudinal vibration mode. This lateral motion obviously aids contouring work [9, 134].

Sharma et al. [142] outlined a new longitudinal mode ultrasonic transducer with an eccentric horn for micro machining. The device can produce an angular vibration of the order of 40 kHz at the cutting tip attached to the end of the horn. The vibrating tip was to be used for precision machining of straight micro-grooves, which are difficult to achieve using existing precision machine tools. The appearance of the machined surface is excellent compared with that of surface obtained in conventional groove machining.

2.2.4.4 Operating parameters

Power primarily determines the mass of the tool-tool holder combination that can be utilized for an application and also determines the frontal-cutting area of the tool. The more power available in a USM machine, the larger the frontal-cutting area that can be supported [1]. The amplitude (ξ) of the tool motion affects the removal rate and determines the maximum size of the abrasive particles that can be used [1, 9]. Ideally the amplitude should be equal to the mean diameter of the abrasive grit used in order to optimize cutting rate [2, 5, 6, 52].

Hocheng [103] performed assessment of ultrasonic drilling of carbon/silicon carbide (C/SiC) composite material. The effect of various parameters of ultrasonic drilling, including abrasives, volume ratio, electric current, down force on MRR, hole clearance, edge quality and tool wear are presented and discussed. The amplitude (ξ) of the tool motion affects the removal rate and determines the maximum size of the abrasive particles that can be used [1, 9]. Ideally the amplitude should be equal to the mean

diameter of the abrasive grit used in order to optimize cutting rate [2, 5, 6, 52]. Shaw [18] showed that MRR $\alpha\ \xi^{3/4}$ while other researchers [79, 91, 120] have advocated that MRR $\alpha\ \xi$, and yet other [3, 14, 15, 78, 121] have suggested that MRR $\alpha\ \xi^{2}$ at constant frequency and static load.

Rosenberg et al. [3] and Kainth et al. [81] have shown that, in practice, an increase in static load from zero, with other parameters constant, yields an approximately linear relationship between MRR and static load. Koops [94] indicated that the use of a smaller that optimal value (based on MRR) for the static load is better for reducing abrasive wears and increasing tool life.

Ramu et al. outlined machining performance of toughened zirconia ceramic and cold compact alumina ceramic in ultrasonic drilling. The behavior of certain tool material and work material combinations with respect to penetration rate and tool wear under the influence of different parameters in ultrasonic drilling were discussed [114]. Zahra et al. highlighted calibrated methods for ultrasonic on-line monitoring of gradual wear during turning operation, and described a robust method for on-line gradual wear monitoring using ultrasonic signals [115]. Xu and Han [116] outlined piezoelectric actuator based active error compensation of precision machining. Experimental cutting results have shown that the cutting tool developed is satisfactory in terms of improved roundness and surface roughness of machined work-piece.

Zhixin [107] studied the influence of constant machining parameter on MRR. Dam [117] outlined productivity, surface quality and tolerances in ultrasonic machining of ceramics. The investigation shows that tough materials give a low production rate, high tool wear and low surface roughness. For brittle materials relationships are reversed. Wang and Rajurkar [118] outlined dynamic analysis of ultrasonic machining process. The dynamic contact force and stress caused by the impinging of abrasive grits on the work are obtained by solving the three dimensional equation of motion. Wang et al [119] outlined modeling consideration for ultrasonic machining focusing on effect of cavitations for micro finishing along with recent development in USM, future research direction for USM, highlighting USM parameters.

Bellow et al has reported that the high cycle fatigue (HCF) properties of some material can be enhanced through the creation of compressive residual stresses on the USM-machined surfaces [143].This is similar to the effect on HCF properties resulting from shot-peening operations.

Babitsky et al [144] highlighted ultrasonic assisted turning of aviation materials through simulation and experimental study. The suggested finite-element model provides numerical comparison between conventional and ultrasonic turning of inconel 718 in terms of stress/strain state, cutting forces and contact conditions at the work-piece/ tool interface.

2.2.5 Machining properties

Murakawa and Masahiko [145] outlined turning of beta-titanium alloys (Ti-15V-3Cr-3Sn-3Al and Ti-15Mo-5Zr-3Al) with iron cutting grade carbide tools. Effects on machinability aspects, including surface integrity and tool life were studied respectively for the case of two-dimensional, continuous and intermittent turning operation. Tool life of a carbide tool subjected to turning operation of these alloys was substantially improved.

Lin et al [34] described machining characteristics of titanium alloy (Ti-6Al-4V) using a combination process of EDM with USM. The EDM and USM mechanism was integrated to improve the machining efficiency and accuracy. During the experiments, parameters such as dielectric type, abrasive size, concentration of abrasive in dielectric fluid, discharge peak current and pulse duration were changed to explore their effect on MRR, electrode wear rate, surface roughness and thickness of the recast layer.

2.3 PROCESS CAPABILITIES OF CONVENTIONAL TOOL AND WORK MATERIAL

USM is a valuable process for precision machining of hard, brittle materials. Although USM is not limited by high-hardness materials, it is limited by the softness of material. Work piece material softer than HRc 40 result in prohibitively long cycles. The best machining rates can be obtained on material harder than HRc 60. Materials such as

carbides, ferrites, germanium, ceramics, glass, and tungsten are representative of those that are difficult to process conventionally and can benefit the most from the USM process. When performing drilling operations, USM can produce holes as small as 0.076 mm (0.003 in) in diameter. The best tolerance that can be obtained is ±0.025 mm (±0.001 in); how ever with special considerations given to slurry delivery and abrasive selection, tolerances of ±0.007 mm (±0.0003 in) can some-times be achieved. Holes of up to 51-mm (2-in) deep can be drilled without employing special techniques. When optimum flushing techniques are employed, hole-depth capabilities can be extended to 152 mm (6 in) with aspect ratios of up to 40:1. When the USM-drilling depth exceeds 12.7 mm (0.5 in), the MRR is greatly reduced because of lack of efficient slurry flow through the cutting gap. Penetration rates, ranging from 0.025-25 mm/min (0.001-1.00 in/min) vary depending upon the shape being machined, the parameters, and work piece material properties. Surface finish is governed primarily by the abrasive particle size. The best surfaces finishes result when using 800-grit abrasives and are on the order of 0.25 μ (10 μin.). The roughest surface finishes results from using the larger particle sizes and average approximately 0.75 μ (30μin.). Because USM is a non thermal material removal process, material properties remain essentially unaltered. Table 2.1 shows typical performance characteristics of 700W USM with a cold rolled steel and 32 micron boron carbide abrasive [146].

Currently, principal fields of application of USM are in the following areas:

1. Manufacture of hard alloy wire drawing, punching and blanking dies, also making small complicated dies and punches of steel.
2. Machining semi-conducting materials such as germanium and silicon.
3. Machining ferrite and other special metallo-ceramic materials used in electrical installations.
4. Making instruments and optical parts of glass, quartz, fluoride and barium Titanate.
5. Making components of porcelain and special ceramics.

6. Cutting accurate sallow holes of rectangular or other section in cemented and nitride steel.
7. Cutting of industrial diamonds.
8. Grinding glass, quartz and ceramics.
9. Cutting holes with curved or spiral center line and cutting threads in glass and mineral or metallo-ceramic.

Table 2.1 Typical performance characteristics (Obtained from a 700W USM with a cold rolled steel and 32 micron boron carbide abrasive)

Material	Ratio of MRR to TWR	Max. machining area (cm^2)	Average penetration rate (mm/min)
Glass	100:1	25.8	3.81
Ceramic	75:1	19.4	1.51
Germanium	100:1	22.6	2.16
WC	1.5:1	7.7	0.25
Tool Steel	1:1	5.6	0.13
Mother of Pearl	100:1	25.8	3.81
Synthetic Ruby	2:1	5.6	0.51
Carbon-graphite	100:1	19.4	2.00
Ferrite	100:1	22.6	3.18
Quartz	50:1	19.4	1.65
B_4C	2:1	5.6	0.20
Glass bonded mica	100:1	22.6	3.18

Table 2.2 shows abrasive cutting power of commonly available abrasive powders with their hardness values and table 2.3 shows the list of materials successfully machined by USM [146].

Table 2.2 Abrasive Cutting power

Abrasive	Knoop hardness	Relative cutting power
Diamond	6500-7000	1.0
Cubic Boron Nitride (CBN)	4700	0.95
Boron Carbide (B_4C)	2800	0.50-0.60
Silicon Carbide (SiC)	2480-2500	0.25-0.45
Aluminum Oxide (Al_2O_3)	2000-2100	0.14-0.16

Table 2.3 List of materials successfully machined by ultrasonic

Agale	Formica	Ruby
Aluminum	Garnet	Sapphire
Aluminum Oxide	Germanium	Silicon
Barium Titanate	Glass	Silicon Carbide
Beryllium Oxide	Glass-bonded Mica	Silicon Nitrate
Boron Carbide	Graphite	Stainless Steel (hardened)
Boron Composites	Hardened Steel	Stealite
Brass	High Pressure Laminates	Tool Steel
Calcium	Limestone	Ti-alloys
Carbides	Lithium-Fluoride	Tungsten
Carbon	Micarta	Tungsten Carbide
Ceramics	Molybdenum	Thorium Oxide
Composite	Molybdenum disilicate	Uranium Carbide
Cold rolled steel	Plaster of Paris	Zirconium Oxide
Febony	Pyrolytic Graphite	
Ferrite	Quartz	

For conventional tool and work material the operational summary is shown in table 2.4.

Table 2.4 Operational summary

Power	200-4000 Watt
Frequency	15-30 kHz (most common-20 kHz)
Abrasive	
Type	Boron Carbide (frequently)
	SiC (most common)
	Al_2O_3 (may also be used)
Size	Mesh 120-1200 µm 142-6
Concentration	20-60% by volume with water. Sometimes oil may be used for finishing operation.
Flow	Ample (20~5°C)
Amplitude of vibration	5-70 µm (amplitude approx should remain between half to equal mean diameter of abrasive)
Tool tip force	0.45 to 45kg. But generally 4.5 kg.
Tool material	Mild steel, 303 stainless steel, monel, Molybdenum

Over-cut and cutting gap	Twice the grit size (approx)
Area of cut	Up to about 90 mm
Accuracy	± 25 μm (±5 is possible)
Taper	5 μm per mm
Surface roughness, Ra	0.5 to 1.0 μm

2.4 NEED FOR RESEARCH AND AREAS OF STUDY

One area of current development in manufacturing industry involves statistical experimentation as its main tool; in general terms, it is concerned with the application of modern off-line quality control techniques (pre-production or independent of production experimentation and analysis) to product and process engineering. In other words, eliminate the need for mass inspection by building quality into the product and process at the design stage.

This idea was taken up by Professor Genichi Taguchi. He devised a quality improvement technique that uses experimental design methods for efficient characterization of a product or process, combined with a statistical analysis of its variability. This approach allows quality considerations to be included at any early stage of any new venture: in the design and prototype phase for a product; during routine maintenance; or during installation and commissioning of a manufacturing process. The main points of the Taguchi philosophy are:-

1. Change the timing of the application of quality control from on line to off line, so that one can cease to rely on inspection, can build quality into the product and the process, and thus 'do it right first time'.
2. Change the experimental procedures from varying one factor at a time to varying many factors at a time, through statistical experimental design techniques.
3. Change the objectives of the experiments and the definition of quality from 'achieving conformance to specification' to 'achieving the target and minimizing the variability'.

4. Change the attitude for dealing with uncontrollable factors: remove the effect nor the cause, by appropriately tuning the controllable factors.

There are two main aspects to the Taguchi technique. First the behavior of a product or process is characterized in terms of factors (parameters) that are separated into two types:

- Controllable (or design) factors – those whose values may be set or easily adjusted by the designer or process engineer.
- Uncontrollable (or noise) factors, which are sources of variation often associated with the production or operational environment; overall performance should, ideally, be insensitive to their variation (see figure 2.16)

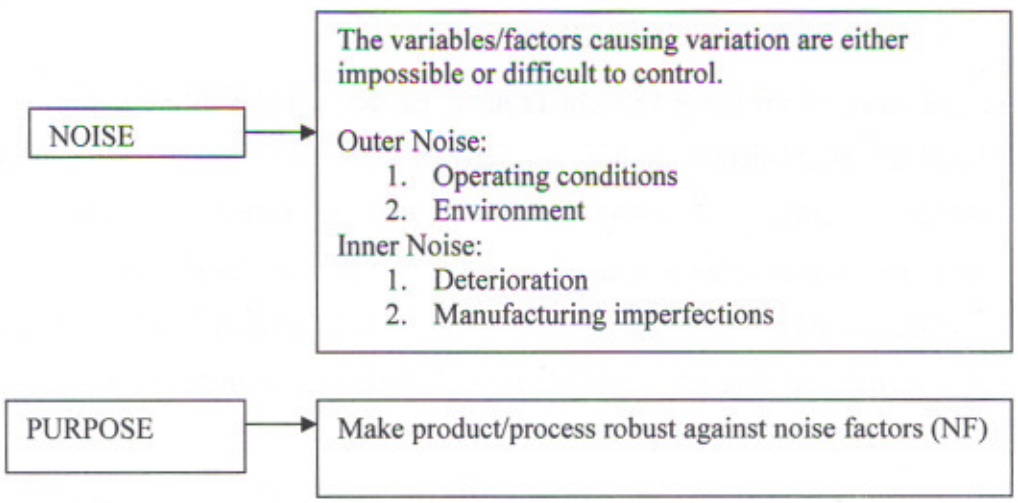

Figure 2.16 Taguchi's definition of noise

Second are the controllable factors, which are divided as shown in figure 2.17. Those factors which affect the average levels of the response of interest, referred to as target control factors (TCF), some times called signal factors. Those factors which affect the variability in the response are variability control factors (VCF); and those factors which affect neither the mean response nor the variability, and can thus are adjusted to fit economic requirements, called the cost factors.

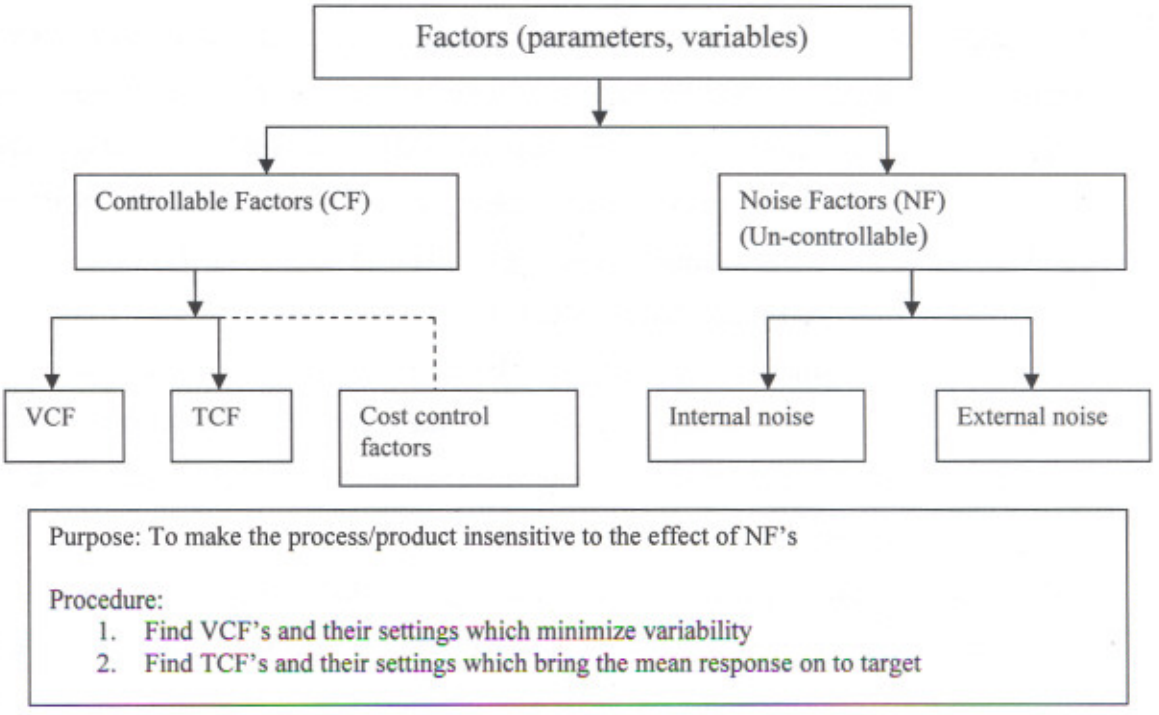

Figure 2.17 Division of factors

It is this concentration on variability which distinguishes the Taguchi approach from traditional tolerance methods or inspection-based quality control. The idea is to reduce variability by changing the variability control factors, while maintaining the required average performance through adjustments to the target control factors [149-150].

2.5 PARAMETER DESIGN

This is the part of the technique which identifies those settings of the controllable factors that reduce performance variation (caused by the noise factors) while keeping the response of interest on target. At this stage one attempt to reduce or remove the effect of the noise factors rather than the noise factors themselves. This effect (variation) is simulated during the experiment, by systematically varying the noise factors at each of the various settings of the controllable factors under study.

The controllable factor settings studied are those suggested by the rows of an experimental design (inner array), usually a fractional orthogonal array; in such a design, every level (setting) of a factor occurs with every level of all other factors the same number of times.

At every level-combination of the controllable factors, some observations should be obtained while changing the settings of the noise factors (assuming of course, that the noise factors can be controlled and changed, at least for the purposes of the experiment). A fractional orthogonal array can then be utilized to determine the level-combinations of the noise factors (outer array). In such a case, the experimenter can simulate the variability (effect) of the noise factors on each controllable-factor setting and determine the setting which minimizes this variability.

2.6 TAGUCHI'S APPROACH FOR DESIGN

There are certain steps which Taguchi suggests to be taken in carrying out experimental studies; these steps, should be followed in the parameter-design stage, and are outlined below:

1. **Define the problem:** Provide a clear statement of the problem to be solved. It is important to establish just what the experiment is aiming to solve.
2. **Determine the objective:** Identify the output characteristics (responses) to be studied and eventually optimized (preferably measurable and with good additivity), and determine the method of measurement. To establish measurement reliability, a separate experiment may be required.
3. **Conduct a brainstorming session:** This is very important stage in performing an experimental study. Managers and operators closely related to the production process or the product under consideration should get together in order to determine the controllable and uncontrollable factors, and to define the experimental range and the appropriate factor levels. Taguchi believes that it is generally preferable to consider as many factors (rather than many interactions) as is economically feasible for the initial screening.
4. **Design the experiment:** Select the appropriate experimental design assigning the controllable factors and their interactions to the columns of the inner array, and the noise factors to the columns of the outer array.
5. **Conduct the experiment:** Perform the experimental trials and collect the experimental data.
6. **Analyze the data:** Evaluate the performance measures for each trial run of the inner array and analyze them using the appropriate statistical analysis techniques.

7. **Interpret the results:** Identify the variability control factors (VCF) and target control factors (TCF) and select their optimal levels. For the VCF the optimal levels are those which minimize the variability in the response, and for TCF they are those which bring the mean response nearest to the target value. Predict the process performance under the optimal conditions.
8. **Run a confirmatory experiment:** It is necessary to confirm, by some follow up experimental trials, that the new parameter settings improve the performance measures over their value at the initial settings. Always run a confirmatory experiment to verify predicted results. A successful confirmation experiment will alleviate concerns about the possibilities of a wrong choice for factor levels and experimental design, wrong assumptions of no interactions or improper assumptions underlying the response model.

If the predicted results from step 7 are not confirmed, or the results are otherwise unsatisfactory, additional experiments may be required, and reiteration of step 3 to step 8 may be necessary.

2.6.1 Description of orthogonal arrays

Orthogonal arrays (OAs) are special experimental designs that require only a small number of experimental trials to discover main factor effects. OAs are "fractional factorial designs" and symmetrical subsets of all combinations of treatments in the corresponding full factorial designs. Before one attempts to select an OA to guide the design optimization experiments, one must answer the following critical questions:

1. How many factors are to be studied?
2. How many treatment levels are possible for each factor?
3. What specific 2-factor interactions are to be investigated?
4. Would one encounter any particular difficulty during the runs (for example some factors may not permit frequent treatment changes)?

The first step in selecting the correct standard OA involves counting the total degree of freedom (dof) present in the study. This count fixes the minimum number of experiments that must be run to study the factors involved. Except in unusual circumstances, the investigator will be able to locate a standard OA fitting his needs.

Taguchi identified several basic OAs which he called "standard OAs". These OAs usually suffice the needs of most design optimization study. After finding the dof, the selection of the appropriate standard OA becomes reasonably straightforward [150].

2.6.2 Steps in robust design

As explained earlier, optimizing a product or process design means determining the best architecture, levels of control factors, and tolerances. Robust design is a methodology for finding the optimum settings of the control factors to make the product or process insensitive to noise factors. It involves eight steps that can be grouped into three major categories of planning experiments, conducting them, and analyzing and verifying the results [151-154].

- **Planning the experiment**

1. Identify the main function, side effects, and failure modes.
2. Identify noise factors and the testing conditions for evaluating the quality loss.
3. Identify the quality characteristics to be observed and the objective function to be optimized.
4. Identify the control factors and their alternate levels.
5. Design the matrix experiment and define the data analysis procedure.

- **Performing the experiment**

6. Conduct the matrix experiment.

- **Analyzing and verifying the experiment results**

7. Analyze the data, determine optimum levels for the control factors, and predict performance under these levels.
8. Conduct the verification (also called confirmation) experiment and plan future actions.

These eight steps make up a robust design cycle.

2.7 CONTROL FACTORS, SIGNAL AND NOISE FACTORS FOR STUDY

The study presented in this research work is based on machining problems associated with titanium and its alloys using USM. The concern is primarily with obtaining the optimum system configuration with minimum expenditure of experimental resources. The P-diagram (Process Diagram) for the process has been shown in figure 2.18.The titanium and its alloys machining is viewed as "black box". The parameters that influence the output are identified and divided in to two classes: Noise factors and Control Factors. The best settings of control factors are determined through experiments. For the analysis *rd Expert* ™ software will be used. The robust design method lends itself well for optimization through the macro modeling approach.

Following output parameters are studied as response variables for analysis:-

1) Name: Material Removal Rate

   Type: Nominal the Best (Ideal Function)

   Response: M.R.R. (gm/min)

2) Name: Tool Wear Rate

   Type: Nominal the Best (Ideal Function)

   Response: T.W.R. (gm/min)

3) Name: Surface Roughness

   Type: Nominal the Best (Ideal Function)

   Response: S.R. (microns)

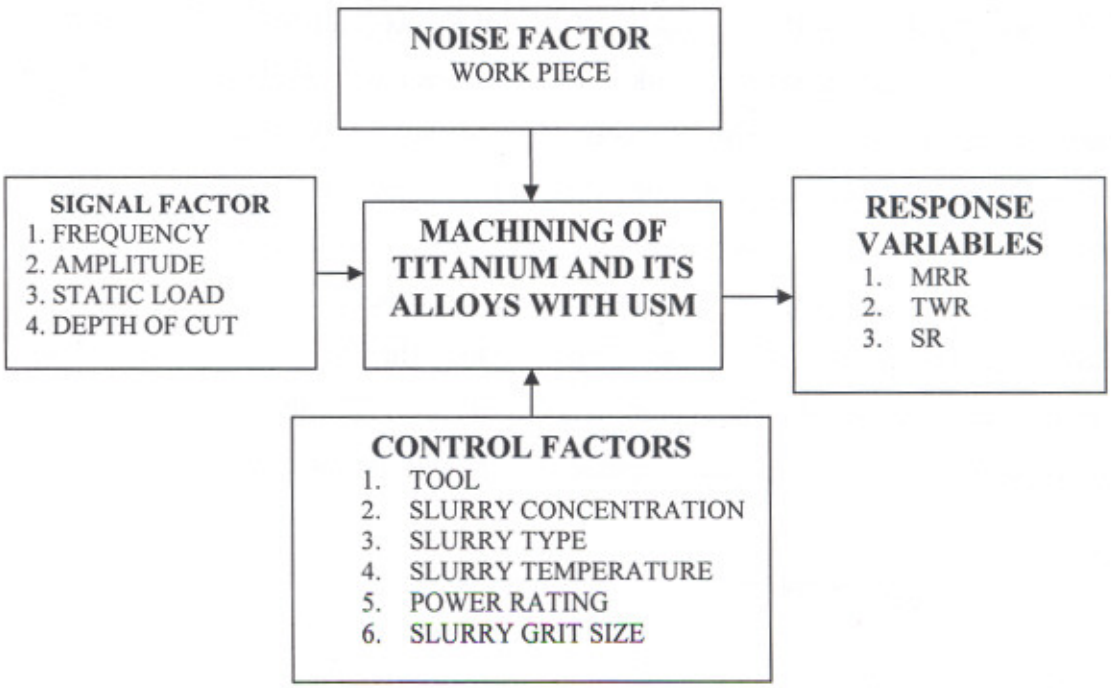

Figure 2.18 P-Diagram for USM of Titanium alloys

The literature review reflected that rate of machining is not a function of load or imposed stress on the tool. There appears to be no simple relationship between the MRR and physical characteristics of work material, such as tensile strength, percentage elongation and micro-hardness or impact strength. Some practical work has been evidenced for machining brittle materials using USM [147-148]. For tough materials, very little effort has been put in to explore the machining capacity of USM. In the present work it is proposed to model machining capacity of tough materials using USM for their applications in manufacturing industry.

This research work is intended to establish the benefits accrued in terms of higher material removal rate and longer tool life with better surface finish, for the manufacturing industry as a result of improvement of machining characteristics of titanium and its alloys while machining with USM.

CHAPTER 3

EXPERIMENTATION

3.1 INTRODUCTION

An experimental set-up having a provision for variation in the process parameters was designed and fabricated [33, 35, 58]. The following size and shape of the work piece was selected based on its availability from the supplier (figure 3.1). The dimensions of the tool were decided keeping in view the limitations of the 'horn shape' to economize the machining operation (figure 3.2).

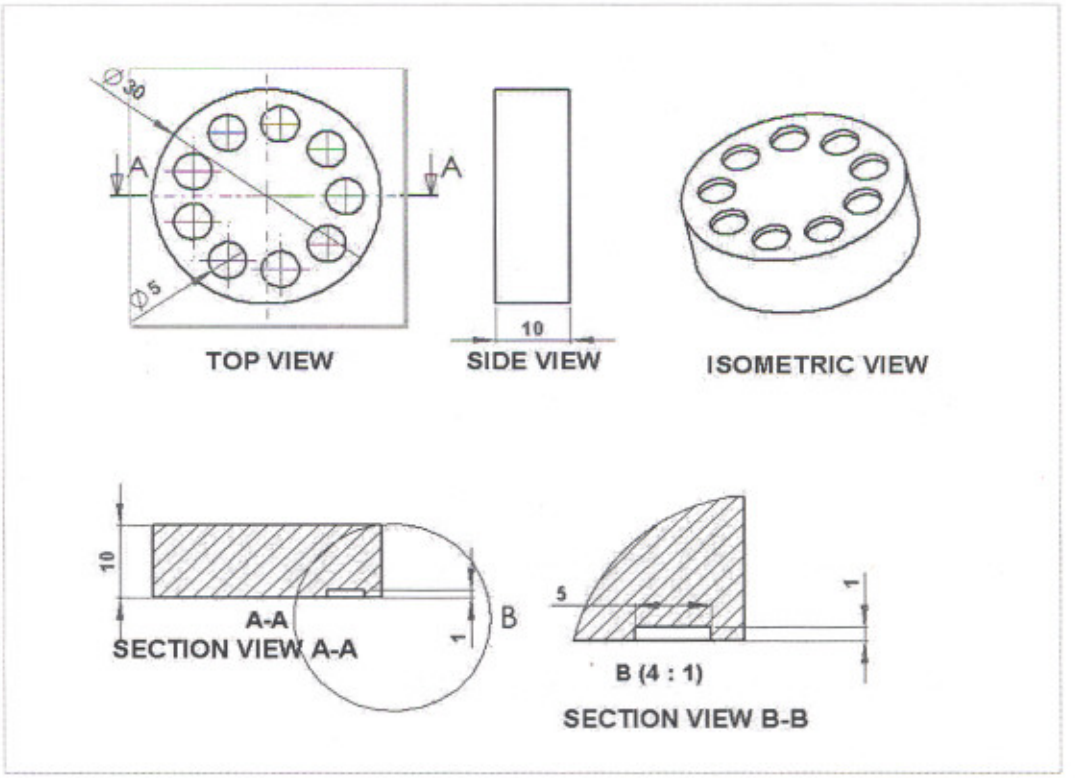

Figure 3.1 Detailed drawing of the work-piece

An electronic balance (Metler, Least count: 0.1mg); and Stop watch (Least count: 0.01 min) was used to determine MRR and TWR. For measuring surface roughness (Pertho-meter, Least count: 0.01 microns) Talysurf was used. In order to understand the effect of

slurry temperature on machining characteristics of titanium and its alloys, the entire set of experiments was carried out in a controlled temperature condition with variation of ± 2°C. The lowest temperature was selected as 10°C; medium level temperature as 27°C; and highest temperature was 60°C. Three repetitions were made for the entire experimentation and corresponding MRR; TWR; SR were recorded.

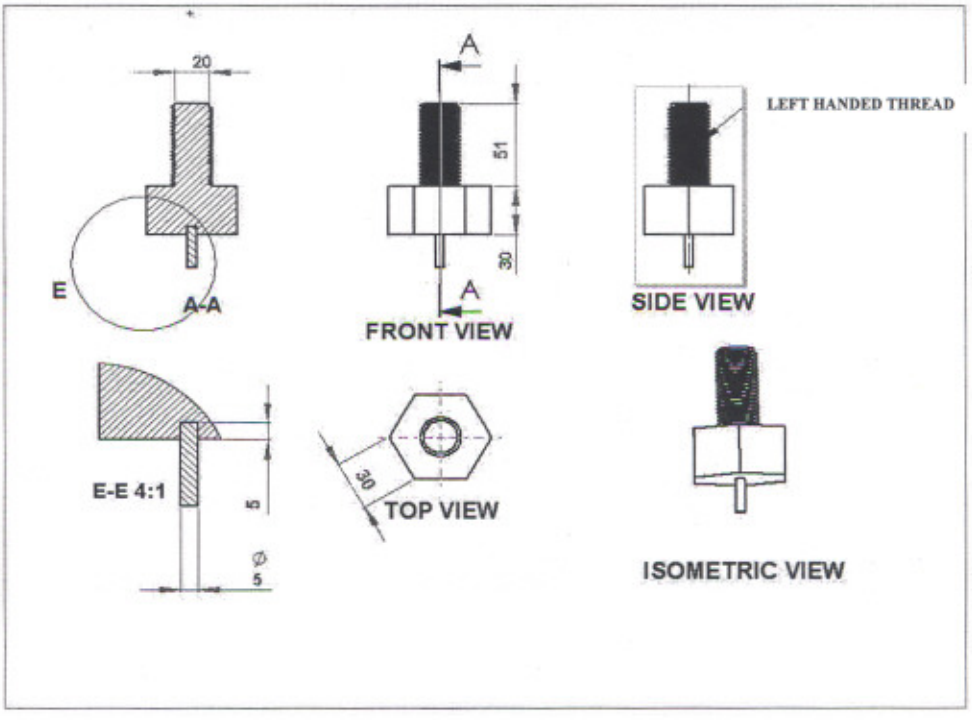

Figure 3.2 Detailed drawing of the tool geometry

3.2 DESCRIPTION OF ULTRASONIC MACHINE

The USM machine tool used for study is of 500W capacity, which consists of an ultrasonic spindle kit; a constant pressure feed system and slurry flow system. Figure 3.3 shows the stationary USM used for study.

Figure 3.3 Ultrasonic machine tool

The ultrasonic spindle kit comprises an ultrasonic spindle, mounted with cylindrical horn of 25.4 mm Ø, a power supply unit. The power supply converts 50 Hz electrical supply to high frequency 20 kHz AC output. This is fed to the piezoelectric transducer located in the spindle. The transducer converts the electrical input in to mechanical vibrations. The amplitude of vibrations is made fixed in range of 0.0253-0.0258 mm with a frequency of 20 kHz +/- 200 Hz (see figure 3.4). The static load for feed rate was fixed at 1.636 kg and slurry flow rate at 26.4 L/min. The replaceable tools used for machining are solid tools made by silver brazing; having same area of cross-section i.e. 5 mm Ø.

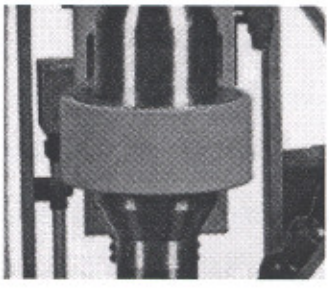

Figure 3.4 Amplitude coupling for compact 500W USM machine

Figure 3.5 schematically illustrates the experimental set-up consisting of temperature control apparatus used with stationary ultrasonic machine. For maintaining low temperature ice is used to lower down slurry temperature and for high temperature heating element is used.

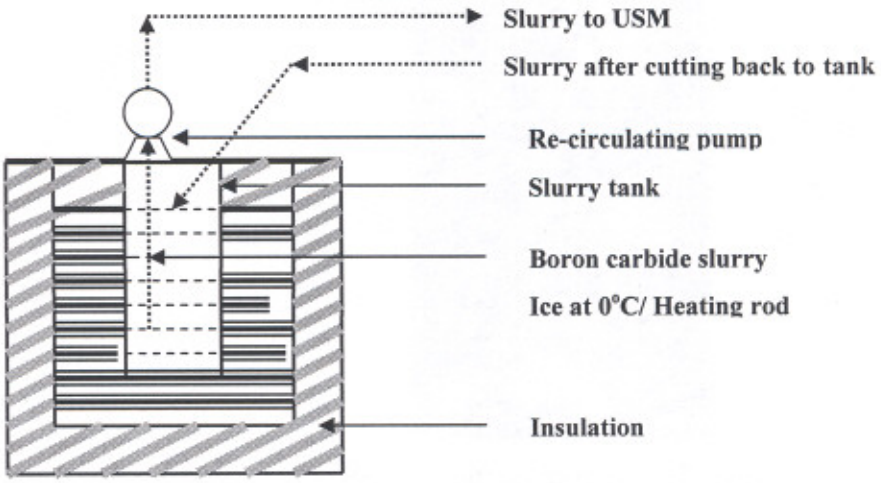

Figure 3.5 Schematic of temperature control apparatus

3.3 PRELIMINARY STUDY TO ASSESS THE EXISTING STATUS

In order to identify the process parameters that affect the quality of components processed by USM, Cause and effect diagram of MRR and TWR [94] was constructed as shown in figure 2.15. The parameters can be classified as follows:

1. Machine based parameters: Ultrasonic power, amplitude and frequency of vibration, medium flow rate, temperature of medium, type of tool material, shape of horn.
2. Media based parameters: Viscosity, grain size (type and shape), concentration of abrasives in the medium.
3. Work-piece based parameters: Geometry of work piece (circular, rectangular or irregular shape etc.), length to diameter ratio, chemical composition of work piece material.

The following six independent parameters have been chosen for this study:

1. Tool material;
2. Slurry concentrations;
3. Slurry types;
4. Slurry temperature;
5. Ultrasonic machine power rating;
6. Slurry grit size.

The ranges of these parameters will be selected on the basis of preliminary experiments conducted by using one variable at a time approach. The work piece selected are Titan15 (pure titanium) and Titan31 (titanium alloy) as it has been reported that chemical composition of work piece material significantly affect the machining properties [25, 33].

3.3.1 Pilot experimentation

The response parameters in the present study were material removal rate (MRR), tool wear rate (TWR) and surface roughness (SR). **MRR** is defined as the difference between the initial weight of work piece and final weight of work piece after processing with USM [67,155]. **TWR** is also defined as the difference between the initial weight of tool and final weight of tool after processing with USM.

Mathematically $MRR = (W_1-W_2)/t$

Where:

'W_1' is initial weight of work-piece in gm (before machining)

'W_2' is final weight of work-piece in gm (after machining)

't' is machining time in min for '01mm' fixed depth of cut in work-piece

Mathematically $TWR = (V_1-V_2)/t$

Where:

'V_1' is initial weight of tool in gm (before machining)

'V_2' is final weight of tool in gm (after machining)

't' is machining time in min for '01mm' fixed depth of cut in work-piece

SR is measured using a surface roughness measuring instrument (Talysurf).The large numbers of experiments were conducted with different input parametric conditions by using one variable at a time approach. The stage of pilot experimentation has been divided into four cases.

Case 1: Slurry used: Silicon Carbide, 320 grit-size at room temperature (25-27°C)

The first case highlights MRR and TWR response variables with silicon carbide slurry of 320 grit-size at room temperature. These out-put variables have been plotted for different tool-work material combinations (refer figure 3.6- 3.27)

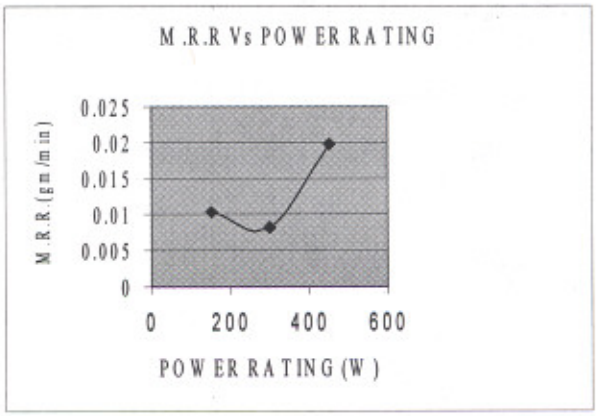

Figure 3.6 M.R.R. Vs Power Rating for Titan15 work piece using Ti tool

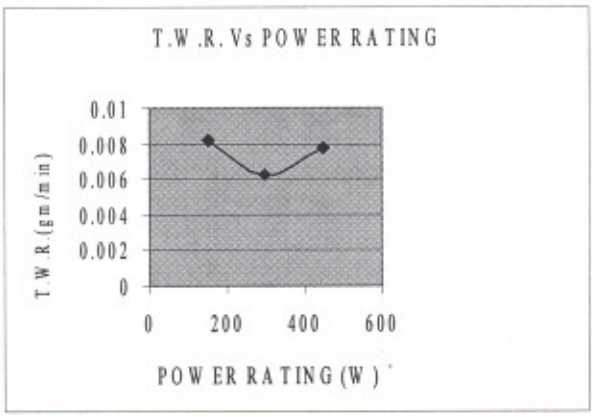

Figure 3.7 T.W.R. Vs Power Rating for Ti tool while machining Titan15 work piece

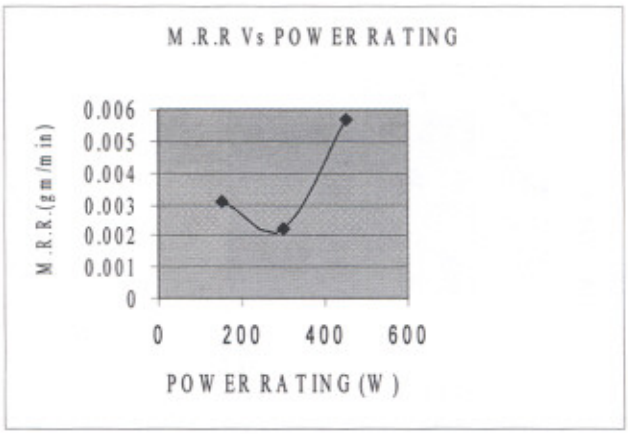

Figure 3.8 M.R.R. Vs Power Rating for Titan15 work piece using S.S tool

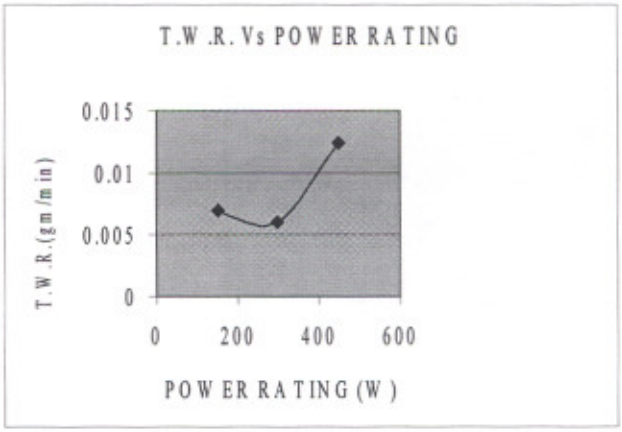

Figure 3.9 T.W.R. Vs Power Rating for S.S tool while machining Titan15 work piece

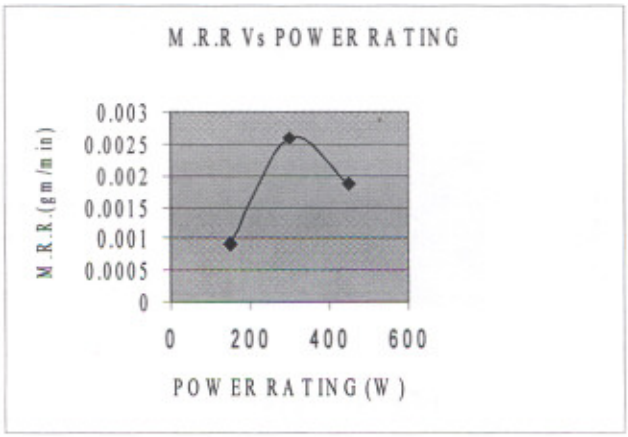

Figure 3.10 M.R.R. Vs Power Rating for Titan15 work piece using H.S.S tool

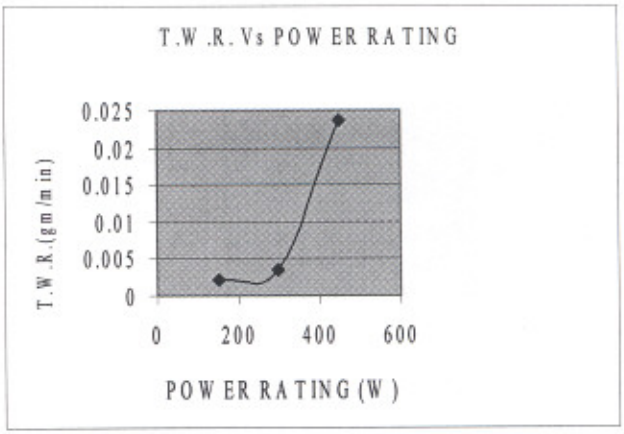

Figure 3.11 T.W.R. Vs Power Rating for H.S.S tool while machining Titan15 work piece

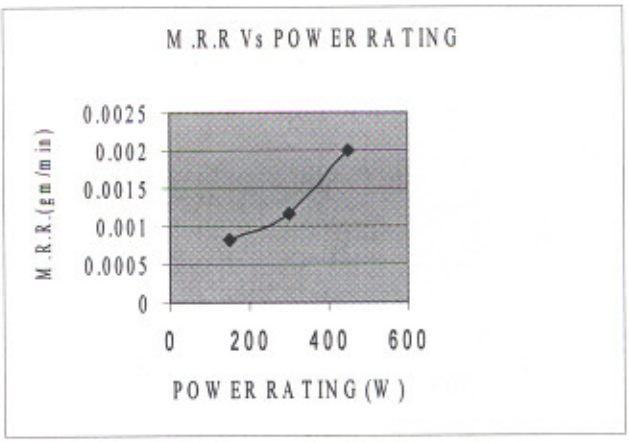

Figure 3.12 M.R.R. Vs Power Rating for Titan15 work piece using H.C.S tool

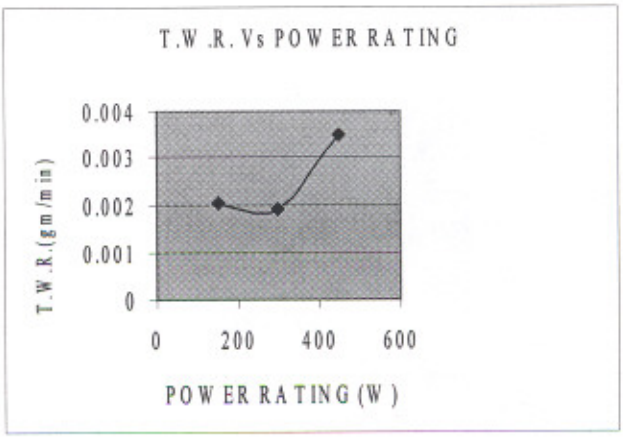

Figure 3.13 T.W.R. Vs Power Rating for HCS tool while machining Titan15 work piece

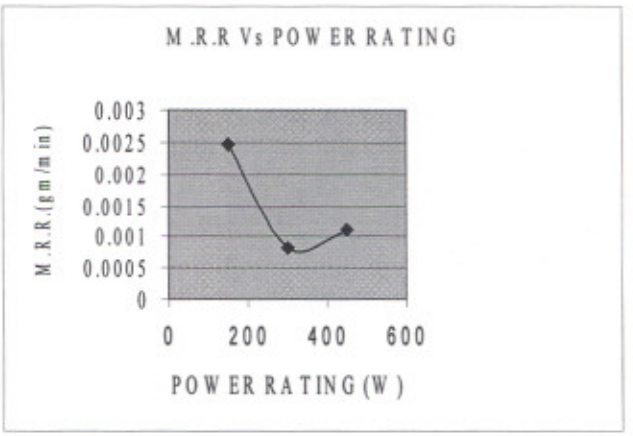

Figure 3.14 M.R.R. Vs Power Rating for Titan15 work piece using WC tool

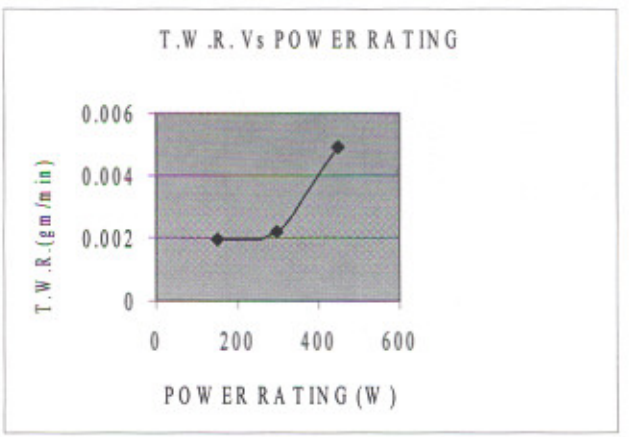

Figure 3.15 T.W.R. Vs Power Rating for WC tool while machining Titan15 work piece

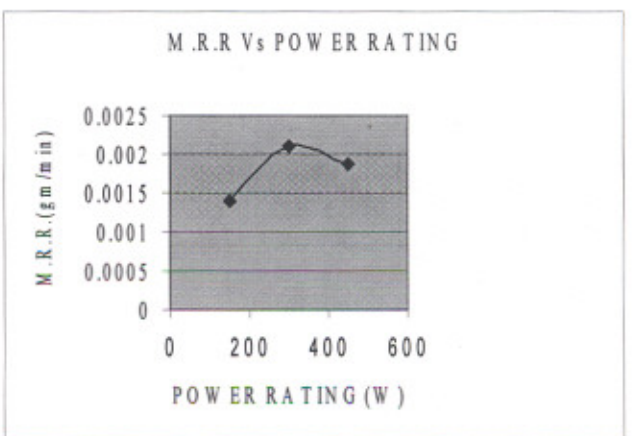

Figure 3.16 M.R.R. Vs Power Rating for Titan15 work piece using PCD tool

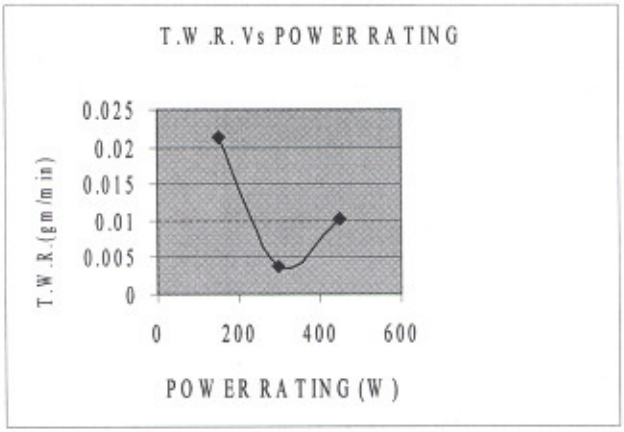

Figure 3.17 T.W.R. Vs Power Rating for PCD tool while machining Titan15 work piece

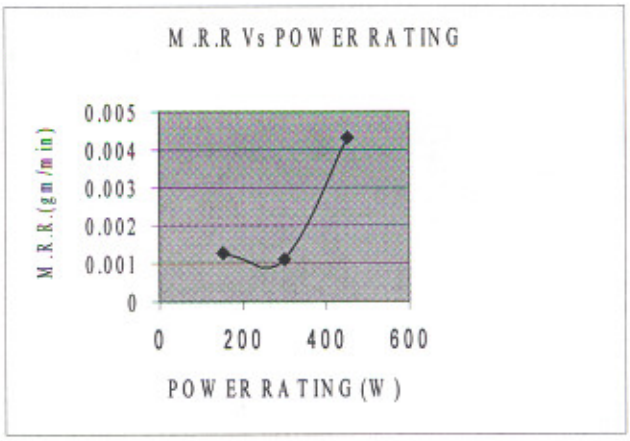

Figure 3.18 M.R.R. Vs Power Rating for Titan31 work piece using H.S.S tool

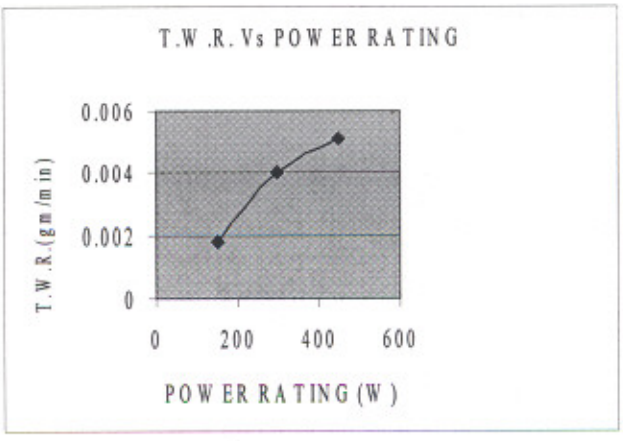

Figure 3.19 T.W.R. Vs Power Rating for H.SS tool while machining Titan31 work piece

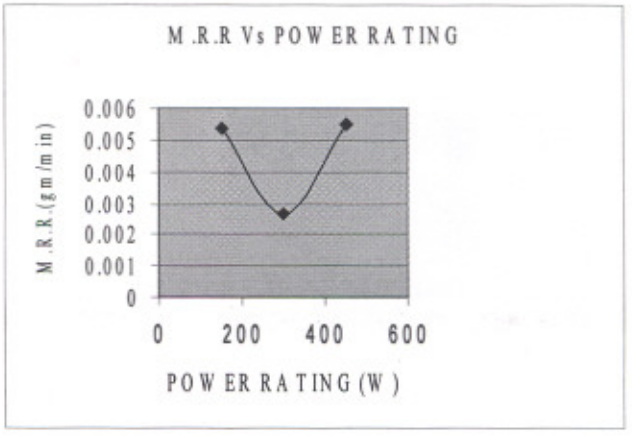

Figure 3.20 M.R.R. Vs Power Rating for Titan31 work piece using Ti tool

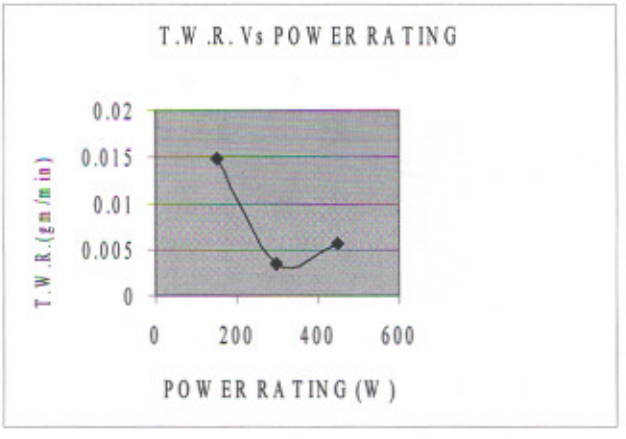

Figure 3.21 T.W.R. Vs Power Rating for Ti tool while machining Titan31 work piece

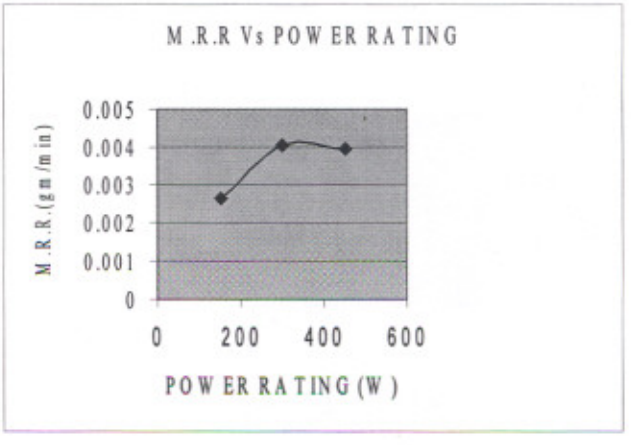

Figure 3.22 M.R.R. Vs Power Rating for Titan31 work piece using S.S tool

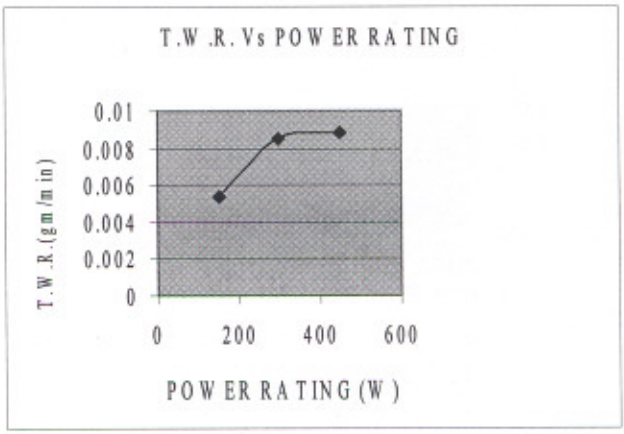

Figure 3.23 T.W.R. Vs Power Rating for S.S tool while machining Titan31 work piece

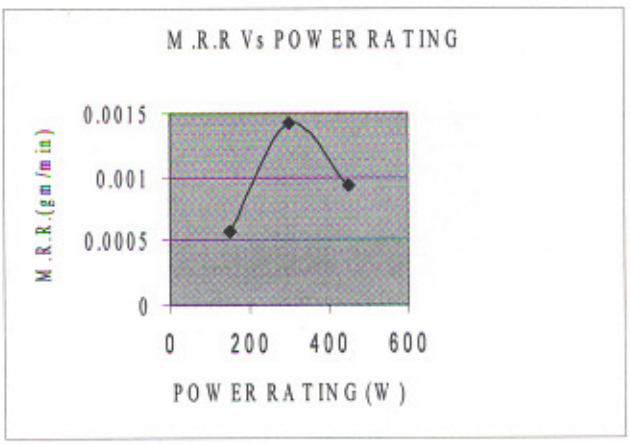

Figure 3.24 M.R.R. Vs Power Rating for Titan31 work piece using WC tool

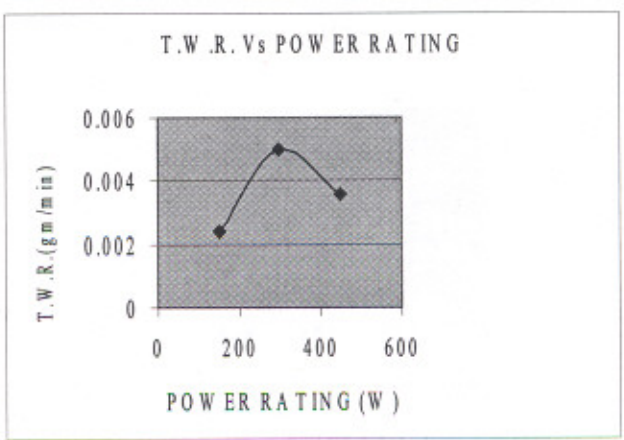

Figure 3.25 T.W.R. Vs Power Rating for WC tool while machining Titan31 work piece

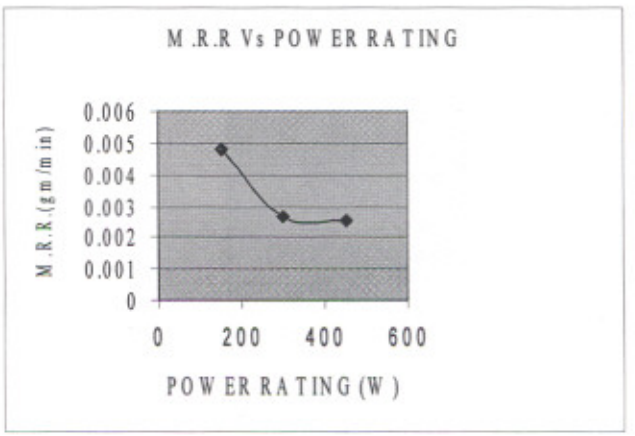

Figure 3.26 M.R.R. Vs Power Rating for Titan31 work piece using PCD tool

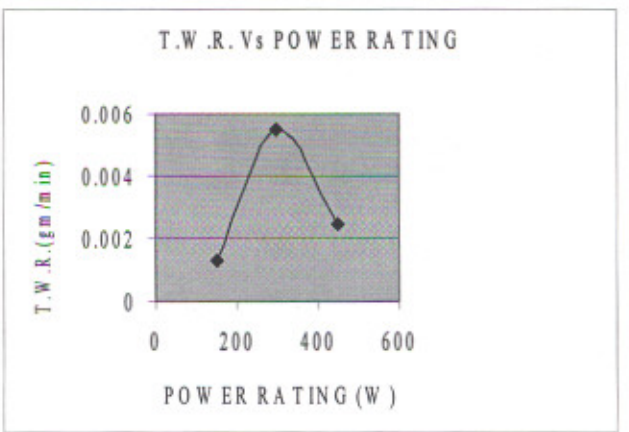

Figure 3.27 T.W.R. Vs Power Rating for PCD tool while machining Titan31 work piece

Case 2: Slurry used: Aluminum Oxide, 320 grit-size at room temperature

For the second case aluminum oxide slurry of 320 grit-size at room temperature has been selected. MRR and TWR have been plotted again for different tool-work material combinations (refer figure 3.28-3.35).

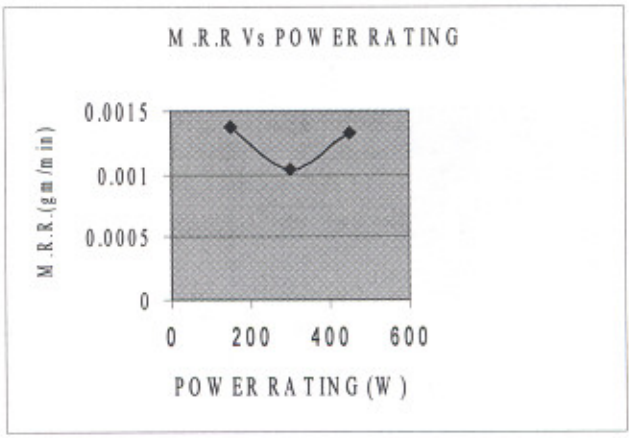

Figure 3.28 M.R.R. Vs Power Rating for Titan15 work piece using S.S tool

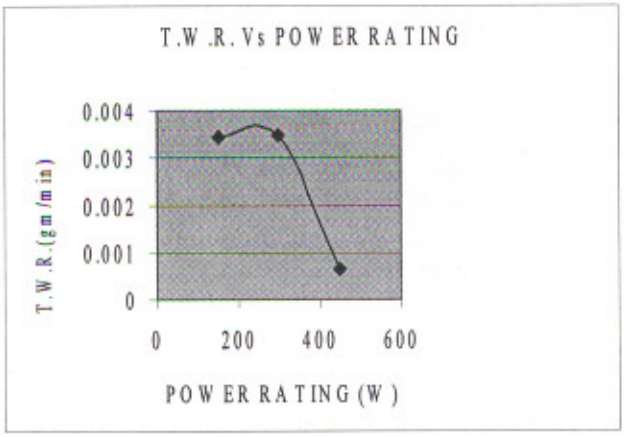

Figure 3.29 T.W.R. Vs Power Rating for S.S tool while machining Titan15 work piece

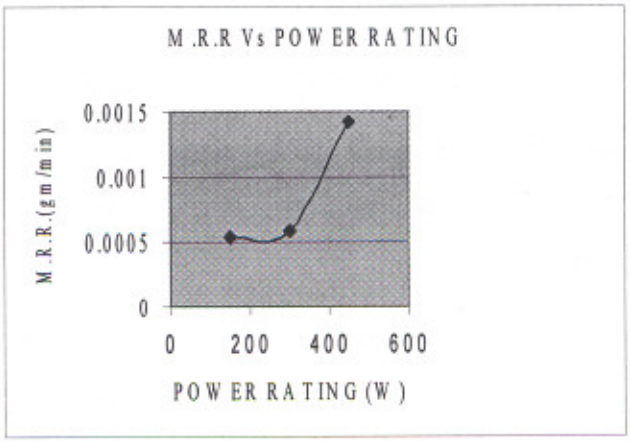

Figure 3.30 M.R.R. Vs Power Rating for Titan15 work piece using H.S.S tool

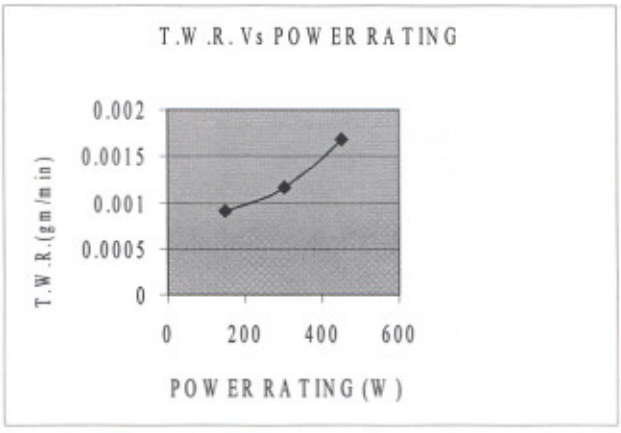

Figure 3.31 T.W.R. Vs Power Rating for H.S.S tool while machining Titan15 work piece

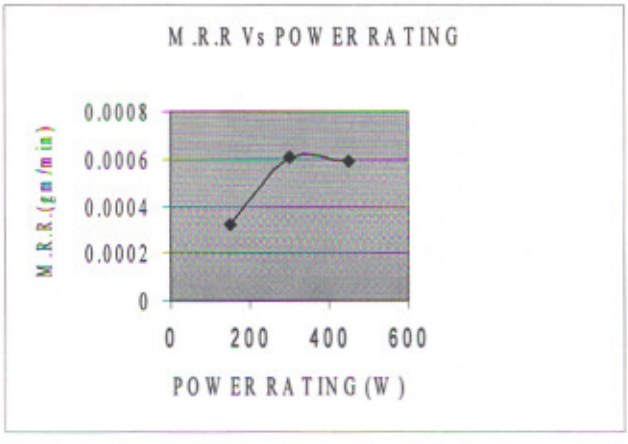

Figure 3.32 M.R.R. Vs Power Rating for Titan31 work piece using WC tool

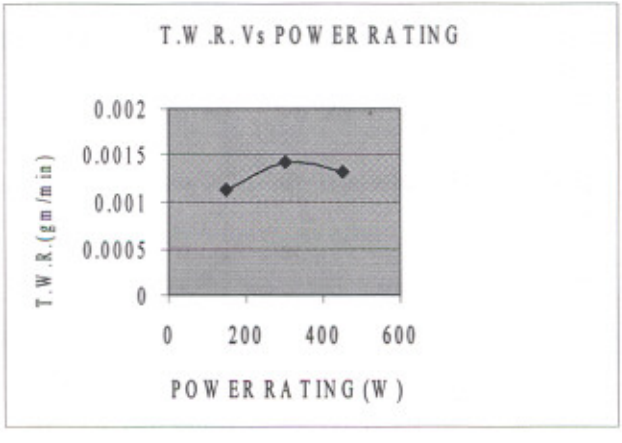

Figure 3.33 T.W.R. Vs Power Rating for WC tool while machining Titan31 work piece

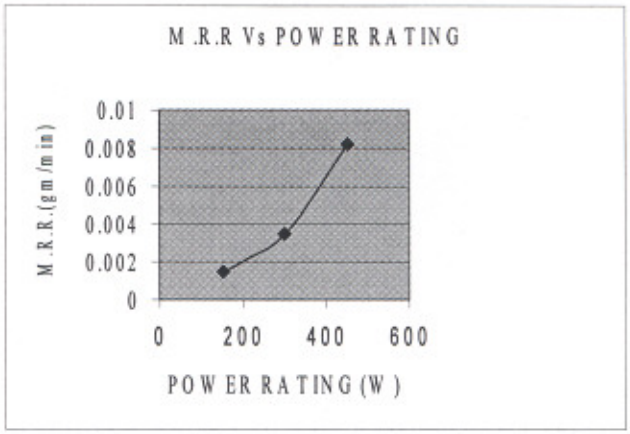

Figure 3.34 M.R.R. Vs Power Rating for Titan31 work piece using Ti tool

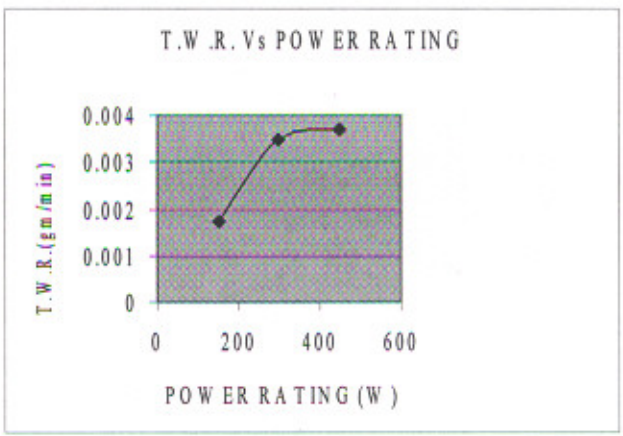

Figure 3.35 T.W.R. Vs Power Rating for Ti tool while machining Titan31 work piece

Case 3: Slurry used: Boron Carbide, 320 grit-size at room temperature

In third case of pilot experimentation stage boron carbide slurry of 320 grit-size at room temperature is selected and response in form of MRR and TWR have been plotted (refer figure 3.36-3.49).

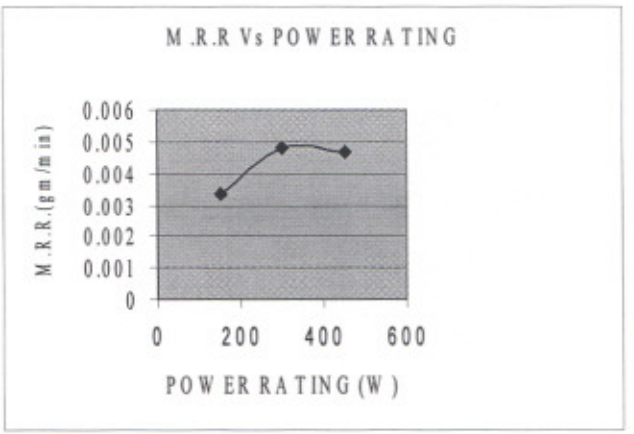

Figure 3.36 M.R.R. Vs Power Rating for Titan31 work piece using S.S tool

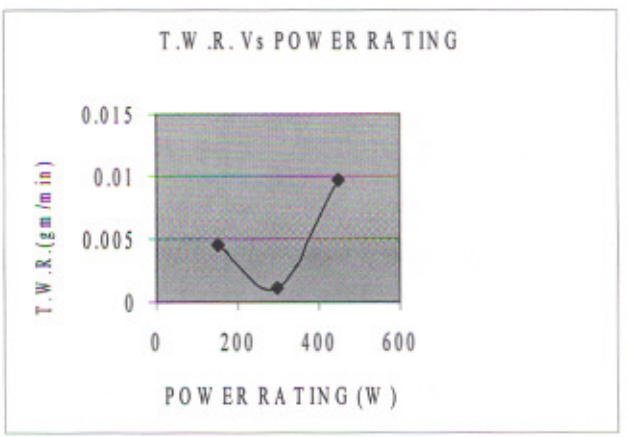

Figure 3.37 T.W.R. Vs Power Rating for S.S tool while machining Titan31 work piece

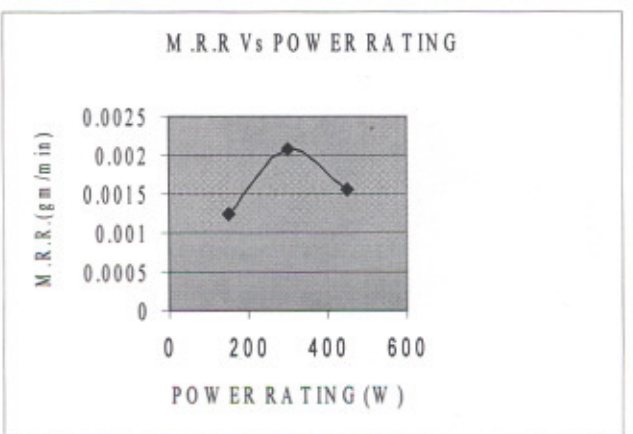

Figure 3.38 M.R.R. Vs Power Rating for Titan31 work piece using H.S.S tool

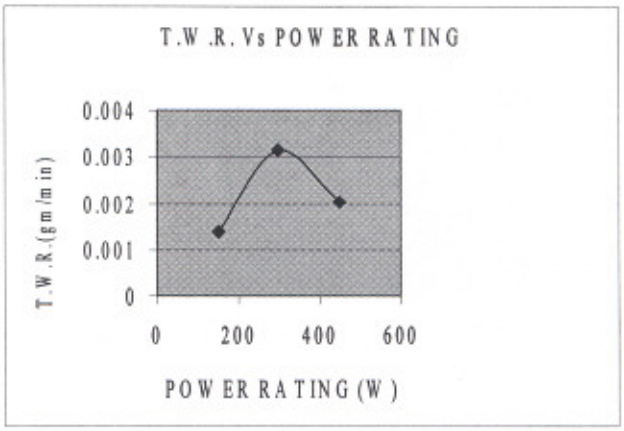

Figure 3.39 T.W.R. Vs Power Rating for H.S.S tool while machining Titan31 work piece

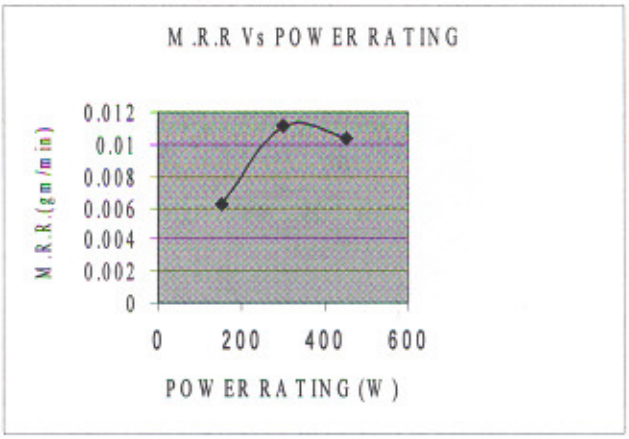

Figure 3.40 M.R.R. Vs Power Rating for Titan31 work piece using Ti tool

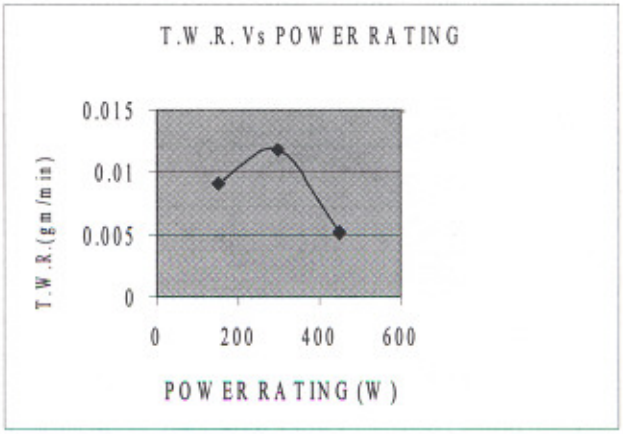

Figure 3.41 T.W.R. Vs Power Rating for Ti tool while machining Titan31 work piece

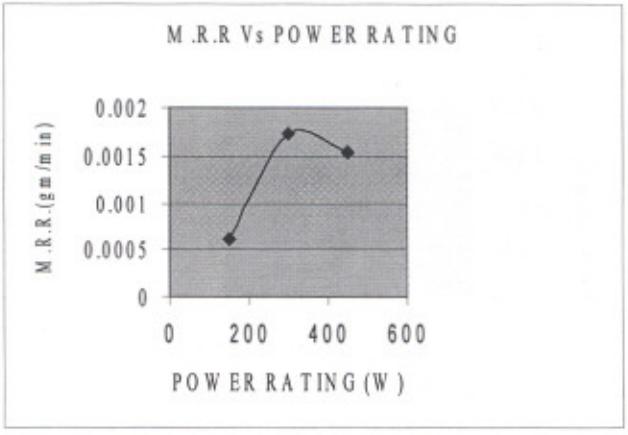

Figure 3.42 M.R.R. Vs Power Rating for Titan15 work piece using WC tool

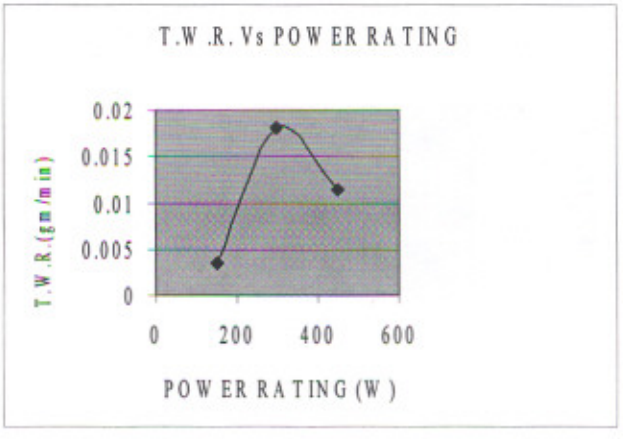

Figure 3.43 T.W.R. Vs Power Rating for WC tool while machining Titan15 work piece

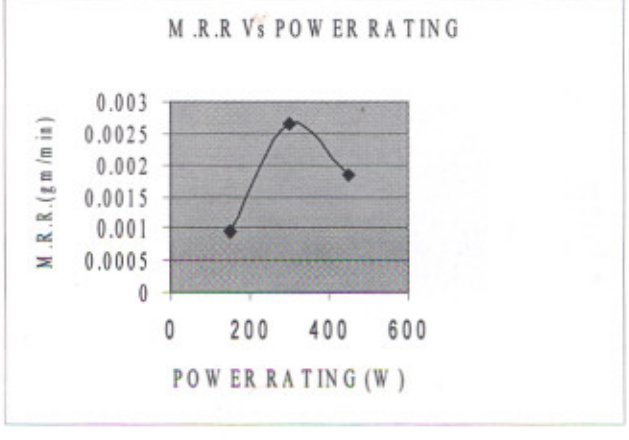

Figure 3.44 M.R.R. Vs Power Rating for Titan15 work piece using H.S.S tool

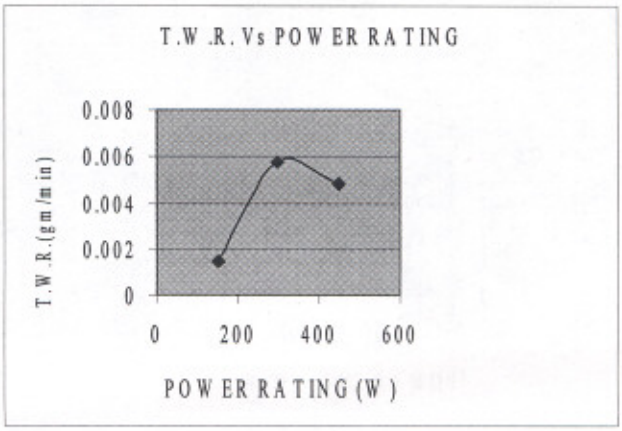

Figure 3.45 T.W.R. Vs Power Rating for H.S.S tool while machining Titan15 work piece

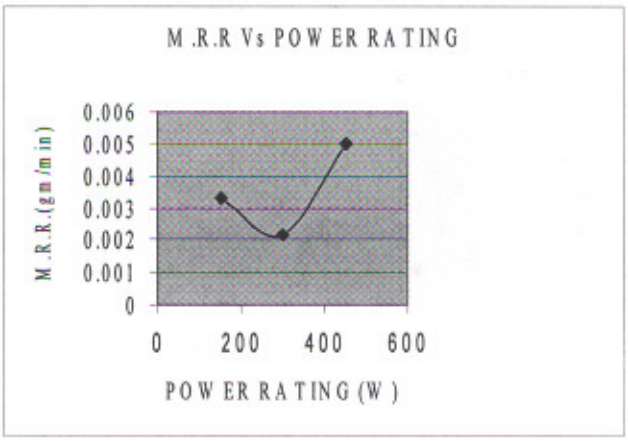

Figure 3.46 M.R.R. Vs Power Rating for Titan15 work piece using S.S tool

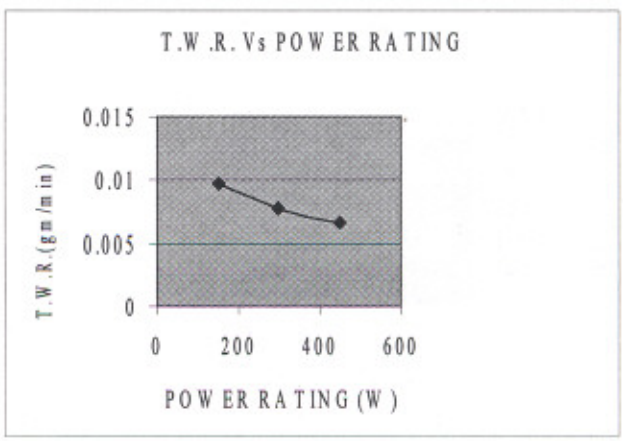

Figure 3.47 T.W.R. Vs Power Rating for S.S tool while machining Titan15 work piece

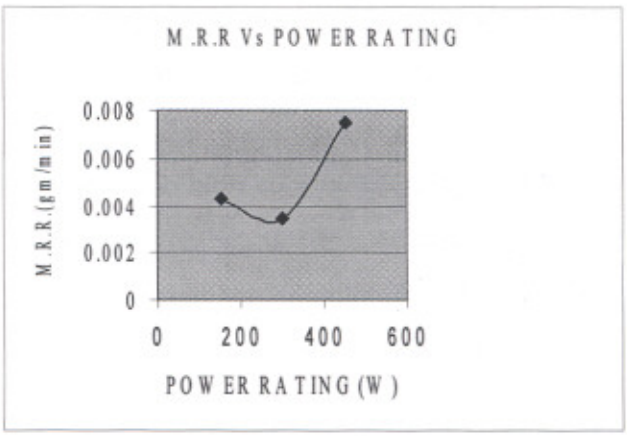

Figure 3.48 M.R.R. Vs Power Rating for Titan15 work piece using Ti tool

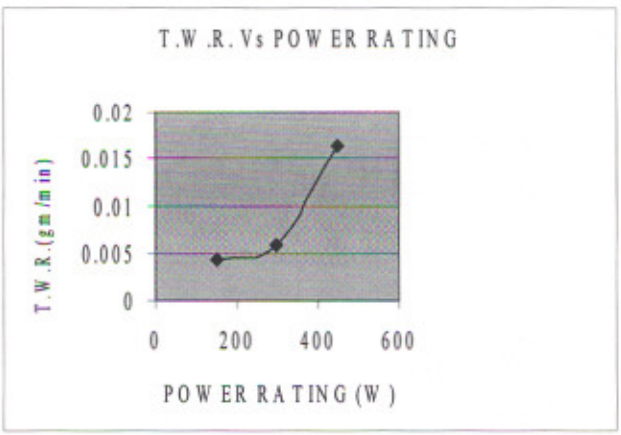

Figure 3.49 T.W.R. Vs Power Rating for Ti tool while machining Titan15 work piece

From the experiments conducted in case1, case2 and case3 following conclusions can be drawn:

1. It is not always necessary that if work piece of higher hardness is machined, it will have more MRR; like in case of ceramics and other hard materials, rather it is combination effect of material composition (hardness of work piece) relative to tool, resulting in work hardening of work piece or tool. In other words selection of operating parameter levels is critical in order to achieve acceptable productivity.
2. More-over the trend of MRR and TWR variation with ultrasonic power rating is not uniform, in some cases with increase in power rating MRR/TWR increases;

but after reaching certain limit of ultrasonic power rating, with further increase, MRR/TWR decreases. This may be because of relative strain hardening of work/ tool material.

3. Also the different tool/ work material combination results in different trends of MRR and TWR, so there is a need of comprehensive study for specific tool-work material combinations. In other words there is requirement of finding optimized machining conditions for a specific work material with specific tool material in relation to other input parameters.
4. It is possible to ultrasonically drill holes in commercially pure titanium, Ti15 (ASTM Grade 2) and titanium alloy, Ti31 (ASTM Grade.5) without causing excessive surface damage, specifically cracking using ultrasonic assisted drilling.
5. The choice of tool material is one of the most important decisions for optimization of metal removal and tool cost. Also mass, length of tool poses difficulty as tool material absorbs much of ultrasonic energy; reducing the efficiency. The larger tool causes over stressing.

From these observations it can be concluded that there is a large scope for exploring machining characteristics using different slurry, tool and work material combinations for optimum utilization in manufacturing industry. The experiments conducted in case 1, 2 and 3 explore effect of machining parameters on Titan15 (pure titanium) and Titan31 (titanium alloy) at room temperature. Choice of tool materials, its dimensions (length) and mass of tool pose difficulty as tool material absorbs much of ultrasonic energy, reducing the efficiency. It has been observed that longer tool causes over stressing. For the present experimental setup the cylindrical horn of 25.4 mm was used, with tool weight constraint of 50mg maximum. As observed from experiments the increase of tool weight above 50 mg leads to USM overloading and auto cut-off (Experimental set-up limitation).

In the next case 4, the effect of slurry temperature on machining capabilities of titanium has been explored.

Case 4: Slurry used: Boron Carbide, 320 grit-size at different temperatures

The experiments have been conducted at fix slurry concentration, flow rate, amplitude of vibration and feed rate using boron carbide slurry of 320 grit-size to find out MRR, TWR and SR. (refer figure 3.50-3.52). Photomicrographs of the machined surface have been taken to find out any microstructure changes during the USM (refer figure 3.54-3.62). The photomicrograph suggests refinement of grain micro structure after machining with USM as compared to conventionally ground surface (see figure 3.53).

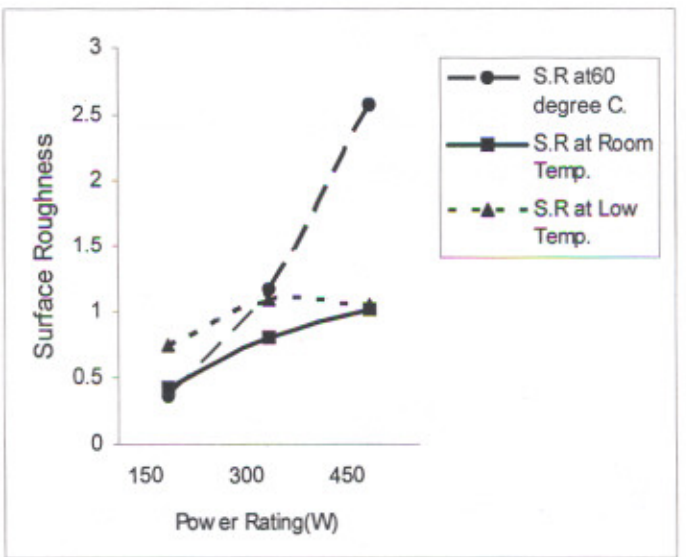

CONSTANT PARAMETERS

1. Slurry Concentration
   Flow rate
   Type
   (Boron Carbide)
   Grit size and shape
2. Amplitude of vibration
3. Work piece and tool material
4. Feed rate

Figure 3.50 Effect of power rating and slurry temperature on surface roughness of Titan15 using H.S.S tool

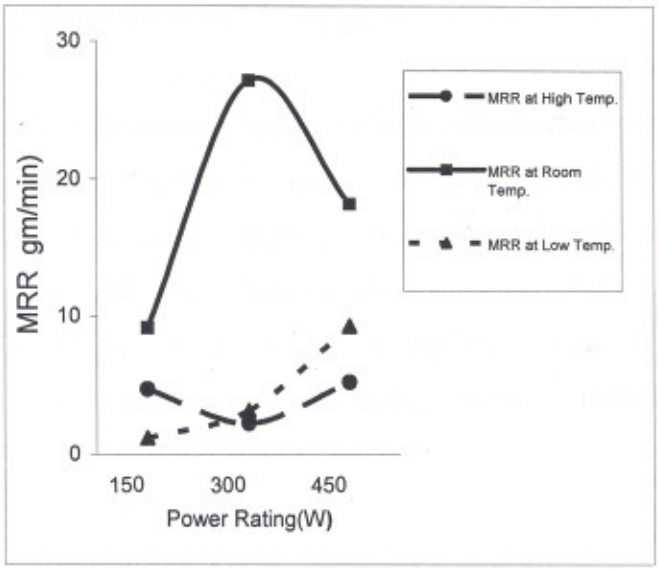

Figure 3.51 Effect of power rating and slurry temperature on material removal rate of Titan15 using H.S.S tool

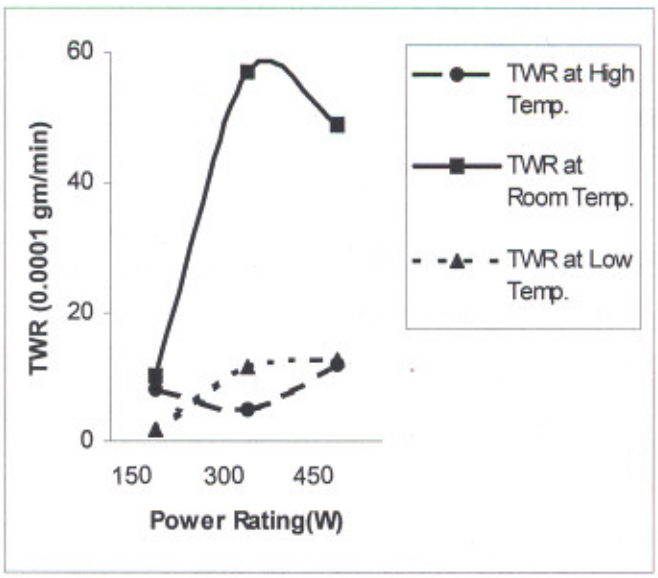

Figure 3.52 Effect of power rating and slurry temperature on tool wear rate of H.S.S. while machining Titan 15

For detailed analysis of microstructure under the machined surface, the region under the tool of Φ5mm has been divided in to three zones. The division in different zones is as under:

1. Zone1: From Center of the tool to Φ1.5mm
2. Zone 2: From Φ1.5mm to Φ3.5mm
3. Zone 3: From Φ3.5mm to Φ5mm

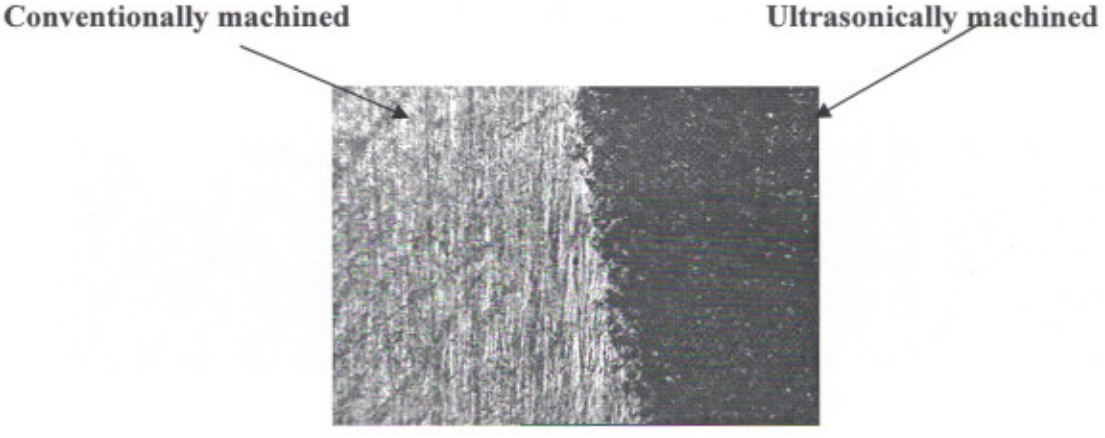

Figure 3.53 Photomicrograph of the machined surface showing comparison of the conventional machining and ultrasonic machining (Magnification; 100x)

These Photomicrographs of surfaces in zone 1, 2 and 3 of Titan15 (pure titanium) at different slurry temperatures, Power ratings (150, 300 and 450W), has been observed with magnification of 100x. For the temperature control of the slurry, three temperature levels; low (10°C), medium (27°C) and high (60°C) were selected, based upon experimental limitations of maintaining the temperature of slurry at the tool tip.

At 60°C **At 27°C** **At 10°C**

(a) **(b)** **(c)**

Figure 3.54 Photomicrographs of machined surface in zone 1 at different slurry temperatures (Power rating: 150W, Magnification; 100x)

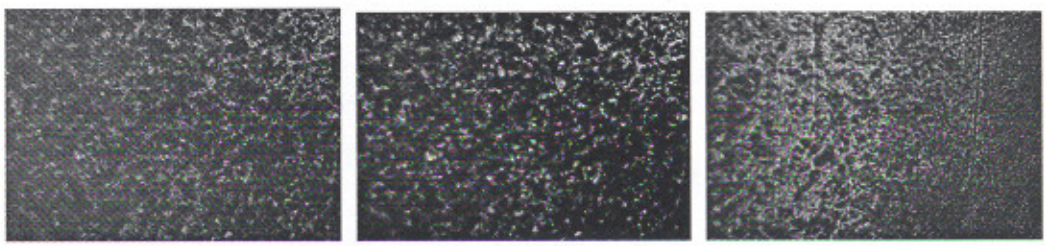

At 60°C **At 27°C** **At 10°C**

(a) **(b)** **(c)**

Figure 3.55 Photomicrographs of surface in zone 2 at different slurry temperatures (Power rating: 150W, Magnification; 100x)

At 60°C **At 27°C** **At 10°C**

(a) **(b)** **(c)**

Figure 3.56 Photomicrographs of surface in zone 3 at different slurry temperatures (Power rating: 150W, Magnification; 100x)

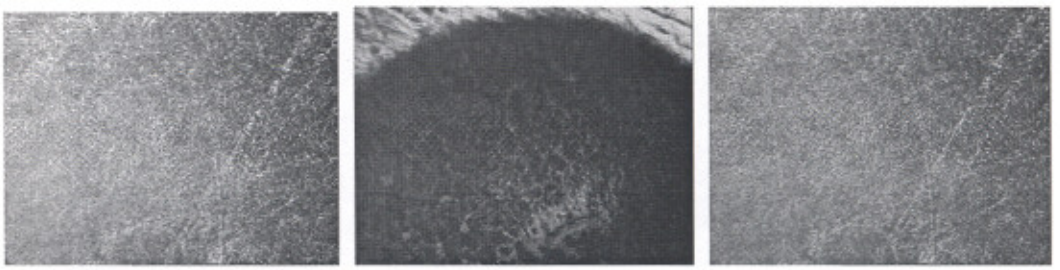

At 60°C **At 27°C** **At 10°C**

(a) **(b)** **(c)**

Figure 3.57 Photomicrographs of surface in zone 1 at different slurry temperatures (Power rating: 300W, Magnification; 100x)

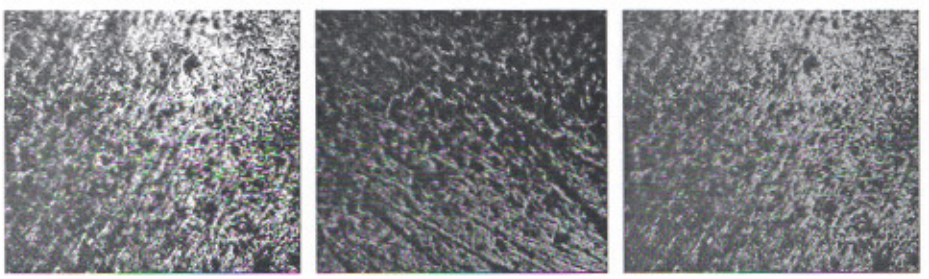

At 60°C **At 27°C** **At 10°C**

(a) **(b)** **(c)**

Figure 3.58 Photomicrographs of surface in zone 2 at different slurry temperatures (Power rating: 300W, Magnification; 100x)

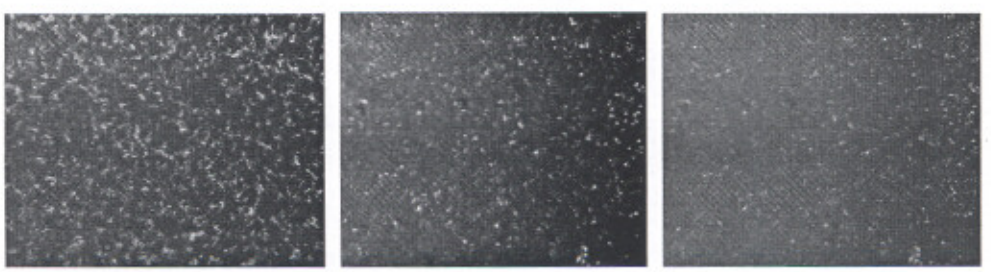

At 60°C **At 27°C** **At 10°C**

(a) **(b)** **(c)**

Figure 3.59 Photomicrographs of surface in zone 3 at different slurry temperatures (Power rating: 300W, Magnification; 100x)

At 60°C **At 27°C** **At 10°C**

(a) **(b)** **(c)**

Figure 3.60 Photomicrographs of surface in zone 1 at different slurry temperatures (Power rating: 450W, Magnification; 100x)

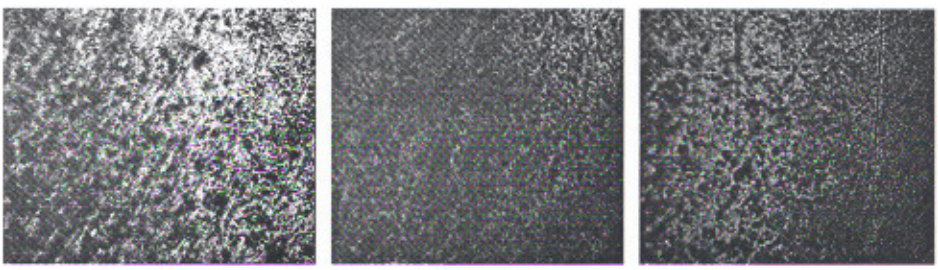

At 60°C **At 27°C** **At 10°C**

(a) **(b)** **(c)**

Figure 3.61 Photomicrographs of surface in zone 2 at different slurry temperatures (Power rating: 450W, Magnification; 100x)

At 60°C **At 27°C** **At 10°C**

(a) **(b)** **(c)**

Figure 3.62 Photomicrographs of surface in zone 3 at different slurry temperatures (Power rating: 450W, Magnification; 100x)

From the experiments conducted in case 4 following conclusions have been drawn:

1. As observed from photomicrographs no major fatigue problems were encountered. Any chipping/ fracture generally being due to tool hole misalignment.
2. Ultrasonic drilling caused little or no deformation of the work piece microstructure.
3. In general at room temperature (27°C) when machining is performed better surface finish is attained than at low temperature (10°C) and at high temperature (60°C) at all power density levels.

3.3.2 Selection of factors level

As the objective of study, is aimed to carry out research on ultrasonic machining of titanium alloys (as work material) using different tool materials to know their impact on material removal rate (MRR), tool wear rate (TWR), and to model these characteristics for their application in manufacturing industry. The following factors have been taken up during this research work.

- Machining properties of commercially pure titanium, (TITAN 15, ASTM Gr.2) and titanium alloy, (TITAN31, ASTM Gr.5) have to be explored in combination with six different tool materials; namely, Stainless Steel (S.S.), High Speed Steel (H.S.S.), High Carbon Steel (H.C.S.), Titanium (Ti), Tungsten Carbide (WC), and Poly Crystalline Diamond (P.C.D.) in ultrasonic machining.
- Tool wear of aforesaid tool materials have to be explored in combination with pure titanium and titanium alloy as work material.
- Relationship between different machining parameters (slurry grit-size, slurry concentration, slurry type, slurry temperature, tool material, work material, power rating) and material properties (material removal rate, tool wear rate and surface roughness) has to be established in this regard.

In light of the above objective, the factors levels have been decided depending upon commercial availability, experimental constraints and machine tool capacity. These in-formations are available from pilot experiments conducted. For example, six levels of

tool were selected because these six commercially available tools resulted in different behaviors of MRR and TWR. So, each tool material has been designated as a level. Similarly three levels of slurry concentration, slurry type, slurry temperature, power rating and slurry grit size were designated. These levels represent threshold points from where change in trend has been observed in pilot tests. Table 3.1 shows different control variables and their levels.

Table 3.1 Control variables and their levels

S.No	Factor Name	Levels	Level 1	Level 2	Level 3	Level 4	Level 5	Level 6
A	Tool	6	S.S	H.S.S	H.C.S	Carbide	Diamond	Titanium
B	Slurry Concentration	3	15 %	20 %	25 %			
C	Slurry Type	3	Boron Carbide	Silicon Carbide	Alumina			
D	Slurry Temperature	3	10°C	27°C	60°C			
E	Power Rating	3	30 %	60 %	90 %			
F	Slurry grit size	3	220	320	500			

For the selection of a particular OA, the number of parameters, the number of levels, and their possible interactions must be taken in to consideration. The case under study involves six parameters, in which one parameter, (tool material) has six levels and rest five parameters have three levels. Now as per requirements of the study L18 'OA' comes out as one of the solution. The standard L18 OA is shown in table 3.2.

Interaction between column 1 and 2 can be estimated without sacrificing any column. Column 1 and 2 can be combined to form a 6-level column. Interactions between any other pair of columns are confounded partially with the remaining columns. Based upon the standard L18 OA, response variables and control log for experimentation has been shown in table 3.3 and 3.4 respectively.

Table 3.2 Standard table for L18 orthogonal arrays

Experiment Number	Column 1	2	3	4	5	6	7	8
1	1	1	1	1	1	1	1	1
2	1	1	2	2	2	2	2	2
3	1	1	3	3	3	3	3	3
4	1	2	1	1	2	2	3	3
5	1	2	2	2	3	3	1	1
6	1	2	3	3	1	1	2	2
7	1	3	1	2	1	3	2	3
8	1	3	2	3	2	1	3	1
9	1	3	3	1	3	2	1	2
10	2	1	1	3	3	2	2	1
11	2	1	2	1	1	3	3	2
12	2	1	3	2	2	1	1	3
13	2	2	1	2	3	1	3	2
14	2	2	2	3	1	2	1	3
15	2	2	3	1	2	3	2	1
16	2	3	1	3	2	3	1	2
17	2	3	2	1	3	1	2	3
18	2	3	3	2	1	2	3	1

Table 3.3 Response variables

Response No.	**Response 1**	**Response 2**	**Response 3**
Response Name	MRR	TWR	S.R.
Response Units	gm/min	gm/min	micron
Response Type	Continuous	Continuous	Continuous

The 18 rows of the L18 array represent the '18' experiments to be conducted. Thus, experiment 1 is to be conducted at level 1 for each six control factors. These levels can be read from table 3.1. However, to make it convenient for the experimenter and to prevent translation errors, the entire matrix of table 3.2 should be translated using definitions in table 3.1 to create the experimenter's log sheet shown in table 3.4.

Table 3.4 Control Log for experimentation

Expt No.	A: Col. 1 Tool	B: Col. 2 Slurry Concentration	C: Col. 3 Slurry Type	D: Col. 4 Slurry Temperature	E: Col. 5 Power Rating	F: Col. 6 Slurry grit size
1	S.S	15 %	Boron Carbide	10°C	30 %	220
2	S.S	20 %	Silicon Carbide	27°C	60 %	320
3	S.S	25 %	Alumina	60°C	90 %	500
4	H.S.S	15 %	Boron Carbide	27°C	60 %	500
5	H.S.S	20 %	Silicon Carbide	60°C	90 %	220
6	H.S.S	25 %	Alumina	10°C	30 %	320
7	H.C.S	15 %	Silicon Carbide	10°C	90 %	320
8	H.C.S	20 %	Alumina	27°C	30 %	500
9	H.C.S	25 %	Boron Carbide	60°C	60 %	220
10	Carbide	15 %	Alumina	60°C	60 %	320
11	Carbide	20 %	Boron Carbide	10°C	90 %	500
12	Carbide	25 %	Silicon Carbide	27°C	30 %	220
13	Diamond	15 %	Silicon Carbide	60°C	30 %	500
14	Diamond	20 %	Alumina	10°C	60 %	220
15	Diamond	25 %	Boron Carbide	27°C	90 %	320
16	Titanium	15 %	Alumina	27°C	90 %	220
17	Titanium	20 %	Boron Carbide	60°C	30 %	320
18	Titanium	25 %	Silicon Carbide	10°C	60 %	500

For conducting final run of experiments all six factors have been denoted by specific letter with suffix representing specific parameter and its level as shown in table 3.5.

The notations used are having following full meanings.

A for Tool

A1 (Tool-1) ---------- S.S
A2 (Tool-2) ---------- H.S.S
A3 (Tool-3) ---------- H.C.S
A4 (Tool-4) ---------- CARBIDE
A5 (Tool-5) ---------- DIAMOND
A6 (Tool-6) ---------- TITANIUM

B for Slurry Concentration by weight

B1 (Concentration-1) = 15%
B2 (Concentration- 2) = 20%
B3 (Concentration- 3) = 25%

C for Slurry Type

C1 (Type-1) = BORON CARBIDE
C2 (Type-2) = SILICON CARBIDE
C3 (Type-3) = ALUMINA

D for Slurry Temperature

D1 (Low Temperature) = 10°C
D2 (Medium Temperature) =27°C
D3 (High Temperature) =60°C

E for Power Rating (Ultrasonic Power)

E1 (Low) = 30% [of 500W] = 150W

E2 (Medium) = 60% [of 500W] = 300W
E3 (High) = 90% [of 500W] = 450W

F for Slurry grit size

F1 = 220 grit size
F2 = 320 grit size
F3 = 500 grit size

Table 3.5 Representation of factor's level

Factor Type	Level 1	Level 2	Level 3	Level 4	Level 5	Level 6
Tool material	A1	A2	A3	A4	A5	A6
Slurry concentration	B1	B2	B3			
Slurry type	C1	C2	C3			
Slurry temperature	D1	D2	D3			
Power rating	E1	E2	E3			
Slurry grit size	F1	F2	F3			

The 18 sets of experiments were performed in order to accommodate all the factors shown in control log of table 3.4. These 18sets of experiments will be repeated at least three times and final conclusion will be made by taking averages of results of three sets of observations. Also the experiments will be performed at random sequence. The observation table for 18sets of experiments is shown in table 3.6.

Table 3.6 Template of observation table

Test Data Experiment No. : 1

Control Factor Settings

A1) Tool
B1) Slurry Concentration
C1) Slurry Type
D1) Slurry Temperature
E1) Power Rating
F1) Slurry grit size

S.NO	Col. 1 Noise Work Piece	Col. 2 Noise Experiment Number	MRR gm/min	TWR gm/min	S.R. Micron	Comments
1	1) TITAN15	1) 1				
2	1) TITAN15	2) 2				
3	1) TITAN15	3) 3				
4	2) TITAN31	1) 1				
5	2) TITAN31	2) 2				
6	2) TITAN31	3) 3				

Test Data Experiment No. : 2

Control Factor Settings
A1) Tool
B2) Slurry Concentration
C2) Slurry Type
D2) Slurry Temperature
E2) Power Rating
F2) Slurry grit size

	Col. 1 Noise Work Piece	Col. 2 Noise Experiment Number	MRR gm/min	TWR gm/min	S.R. Micron	Comments
1	1) TITAN15	1) 1				
2	1) TITAN15	2) 2				
3	1) TITAN15	3) 3				
4	2) TITAN31	1) 1				
5	2) TITAN31	2) 2				
6	2) TITAN31	3) 3				

MRR, TWR and SR will have to be calculated for all 18 sets, as test data table shown in experiment no.1 and 2. The input parameter setting for other test data are shown in table 3.7.

Table 3.7 Template of input parameter setting for Experiment's 3 to 18

Test Data Experiment No. : 3

Control Factor Settings
A1) Tool
B3) Slurry Concentration
C3) Slurry Type
D3) Slurry Temperature
E3) Power Rating
F3) Slurry grit size

Test Data Experiment No. : 4

Control Factor Settings
A2) Tool
B1) Slurry Concentration
C1) Slurry Type
D2) Slurry Temperature
E2) Power Rating
F3) Slurry grit size

Test Data Experiment No. : 5

Control Factor Settings
A2) Tool
B2) Slurry Concentration
C2) Slurry Type
D3) Slurry Temperature
E3) Power Rating
F1) Slurry grit size

Test Data Experiment No. : 6

Control Factor Settings
A2) Tool
C3) Slurry Type
E1) Power Rating
B3) Slurry Concentration
D1) Slurry Temperature
F2) Slurry grit size

Test Data Experiment No. : 7

Control Factor Settings
A3) Tool
C2) Slurry Type
E3) Power Rating
B1) Slurry Concentration
D1) Slurry Temperature
F2) Slurry grit size

Test Data Experiment No. : 8

Control Factor Settings
A3) Tool
C3) Slurry Type
E1) Power Rating
B2) Slurry Concentration
D2) Slurry Temperature
F3) Slurry grit size

Test Data Experiment No. : 9

Control Factor Settings
A3) Tool
C1) Slurry Type
E2) Power Rating
B3) Slurry Concentration
D3) Slurry Temperature
F1) Slurry grit size

Test Data Experiment No. : 10

Control Factor Settings
A4) Tool
C3) Slurry Type
E2) Power Rating
B1) Slurry Concentration
D3) Slurry Temperature
F2) Slurry grit size

Test Data Experiment No. : 11

Control Factor Settings
A4) Tool
C1) Slurry Type
E3) Power Rating
B2) Slurry Concentration
D1) Slurry Temperature
F3) Slurry grit size

Test Data Experiment No. : 12

Control Factor Settings
A4) Tool
C2) Slurry Type
E1) Power Rating
B3) Slurry Concentration
D2) Slurry Temperature
F1) Slurry grit size

Test Data Experiment No. : 13

Control Factor Settings

A5) Tool	B1) Slurry Concentration
C2) Slurry Type	D3) Slurry Temperature
E1) Power Rating	F3) Slurry grit size

Test Data Experiment No. : 14

Control Factor Settings

A5) Tool	B2) Slurry Concentration
C3) Slurry Type	D1) Slurry Temperature
E2) Power Rating	F1) Slurry grit size

Test Data Experiment No. : 15

Control Factor Settings

A5) Tool	B3) Slurry Concentration
C1) Slurry Type	D2) Slurry Temperature
E3) Power Rating	F2) Slurry grit size

Test Data Experiment No. : 16

Control Factor Settings

A6) Tool	B1) Slurry Concentration
C3) Slurry Type	D2) Slurry Temperature
E3) Power Rating	F1) Slurry grit size

Test Data Experiment No. : 17

Control Factor Settings

A6) Tool	B2) Slurry Concentration
C1) Slurry Type	D3) Slurry Temperature
E1) Power Rating	F2) Slurry grit size

Test Data Experiment No. : 18

Control Factor Settings

A6) Tool	B3) Slurry Concentration
C2) Slurry Type	D1) Slurry Temperature
E2) Power Rating	F3) Slurry grit size

3.4 S/N RATIO FOR STATIC PROBLEM

In the Taguchi method, a loss function has been defined to gauge the deviation between the experimental and desired value of a performance characteristics [154-155]. The loss function is further transformed into a signal-to-noise ratio (S/N ratio). Finding a correct objective function to

maximize in an engineering design problem is very important. Failure to do, can lead to great inefficiencies in experimentation and even wrong conclusions about the optimum levels. The task of finding what adjustments are meaningful in a particular problem and determine the correct S/N ratio is not always easy. Three categories of performance characteristics are usually used in the analysis of the S/N ratio, i.e. lower-the-better, higher- the-better, and nominal-the-best. These are described as below:

- Lower-the-better type problem:

For lower the better type problem, the quality characteristics is continuous and non negative- that is, it can take any value from 0 to ∞. Its most desired value is zero. Such problems are characterized by the absence of a scaling factor or any other adjustment factor. Because there is no adjustment factor in these problems, one should simply minimize the quality loss without adjustment- that is, we should minimize:

$$Q = k \text{ (mean square quality characteristics)}$$

$$= k \{1/n. \sum_{i=1}^{n} y_i^2\}$$

Minimizing Q is equivalent to maximizing 'ŋ' defined by the following equation,

$$Ŋ = -10 \log_{10} \{1/n. \sum_{i=1}^{n} y_i^2\}$$

In this case the signal is constant, to make quality characteristics equal to zero. Therefore, the S/N ratio, ŋ, measures merely the effect of noise.

- Higher-the-better type problem:

Here, the quality characteristic is continuous and non-negative and one would like it to be as large as possible. Also, we do not have any adjustment factor. The objective function to be maximized in this case is given by:

$$Ŋ = -10 \log_{10} \text{ (mean square reciprocal quality characteristics)}$$

$$\text{Ɒ} = -10 \log_{10} \{1/n. \sum_{i=1}^{n} 1/y_i^2\}$$

- Nominal-the best type problem:

Here, as in lower-the-better type problem, the quality characteristic is continuous and non-negative- i.e. it can take any value from 0 to ∞. Its target value is non zero and finite. For these problems when the mean becomes zero, the variance also becomes zero. Also, for these problems we can find a scaling factor that can serve as an adjustment factor to move the mean on target.

This type of problem occurs frequently in engineering design. The objective function to be maximized for such problem is:

$$\text{Ɒ} = 10 \log_{10} (\mu^2/\sigma^2)$$

Where

$$\mu = 1/n. \sum_{i=1}^{n} y_i^2$$

$$\sigma^2 = 1/(n-1). \sum_{i=1}^{n} (y_i - \mu)^2$$

In some situations, the scaling factor can be identified readily through engineering expertise. In other situations, we can identify a suitable scaling factor through experimentation.

The optimization of the nominal-the-best problems can be accomplished in two steps:

1. Maximize 'ŋ' or minimize sensitivity to noise. During this step we select the levels of control factors to maximize 'ŋ' while we ignore the mean.
2. Adjust the mean on target. During this step we use the adjustment factor to bring the mean on target without changing 'ŋ'.

In general we should not attempt to minimize 'σ' and then bring the mean on target.

For the case under study nominal-the-best type situation is selected as objective function, as because there were three response parameters namely MRR, TWR and SR and all

these three outputs (responses) are interrelated and have interdependence among each other.

3.5 EXPERIMENTATION

The experiments were conducted in eighteen set-ups. In the first set-up, experiment was undertaken to determine the effect of S.S tool on titanium work piece using boron carbide slurry of 320 grit size with 15% concentration by weight in distilled water as suspension media. The experiment was started by setting power rating of the machine at 30% (of 500W) that is, 150 Watt of ultrasonic drilling machine at 10°C. Figure 3.63 shows the schematic diagram of the USM and slurry tub used for experimentation for eighteen set-ups.

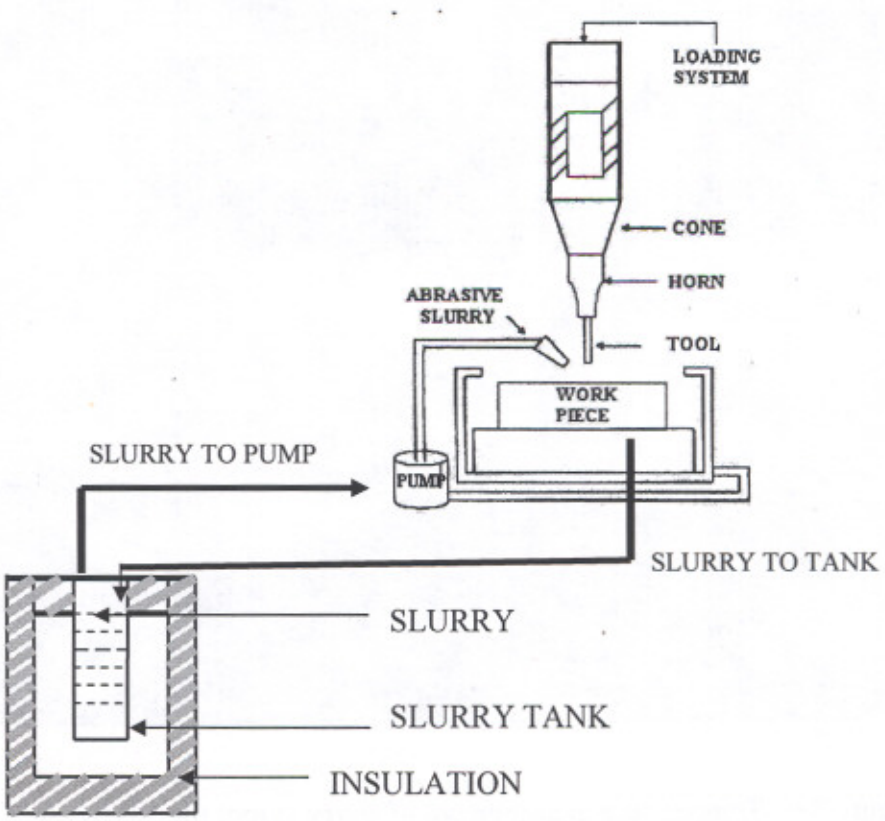

Figure 3.63 Schematic diagram of the USM and Slurry tub

The initial weight of titanium work piece (Titan15 and Titan31) and tool i.e. of S.S was taken. Then machine was allowed to drill for a given depth of 1 mm with constant slurry flow rate and slurry

temperature. The depth was closely watched using dial gauge. Correspondingly, time taken by USM for drilling was measured using stopwatch.

The tool used was of solid cylindrical cross section. After machining was completed, again job (work piece) and tool weight was taken for finding difference in weight loss. Corresponding, material removal rate (MRR) and tool wear rate were (TWR) calculated. After this, titanium work piece was observed for surface roughness and photomicrographs using pertho-meter and metallurgical microscope. The same process was repeated in eighteen set-ups. The pictorial view of different operating conditions on USM has been shown in figures 3.64 to 3.70.

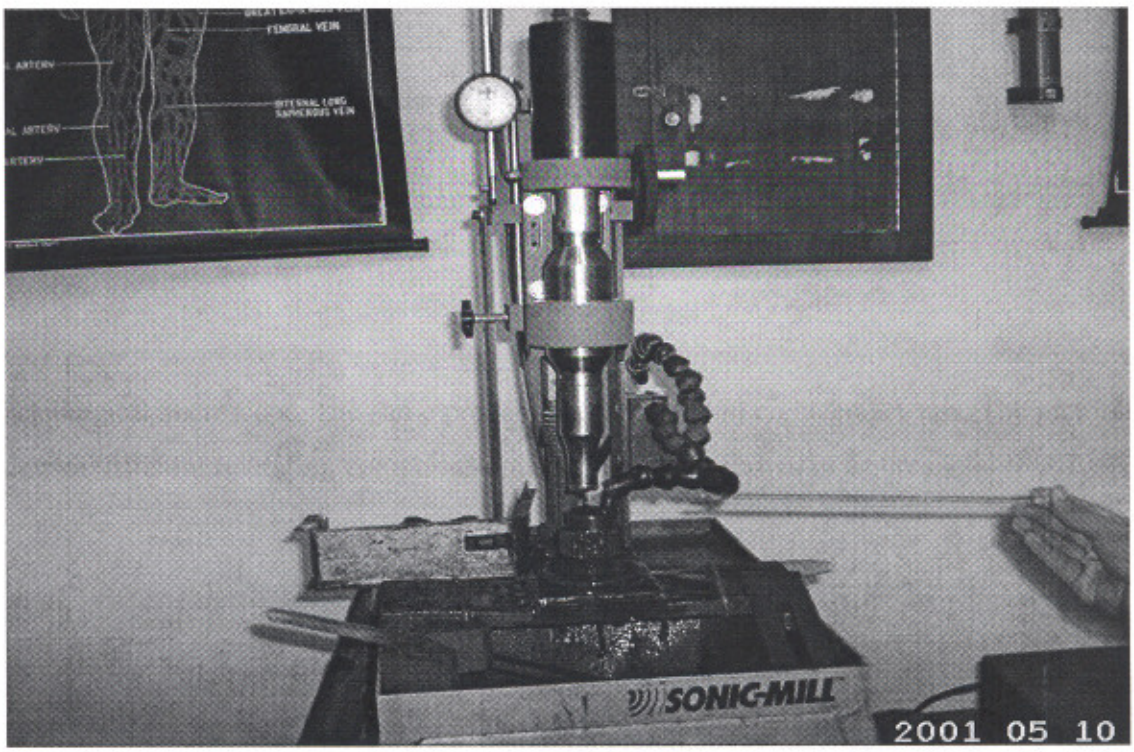

Figure 3.64 Temperature measurement of slurry at tool tip

these three outputs (responses) are interrelated and have interdependence among each other.

3.5 EXPERIMENTATION

The experiments were conducted in eighteen set-ups. In the first set-up, experiment was undertaken to determine the effect of S.S tool on titanium work piece using boron carbide slurry of 320 grit size with 15% concentration by weight in distilled water as suspension media. The experiment was started by setting power rating of the machine at 30% (of 500W) that is, 150 Watt of ultrasonic drilling machine at 10°C. Figure 3.63 shows the schematic diagram of the USM and slurry tub used for experimentation for eighteen set-ups.

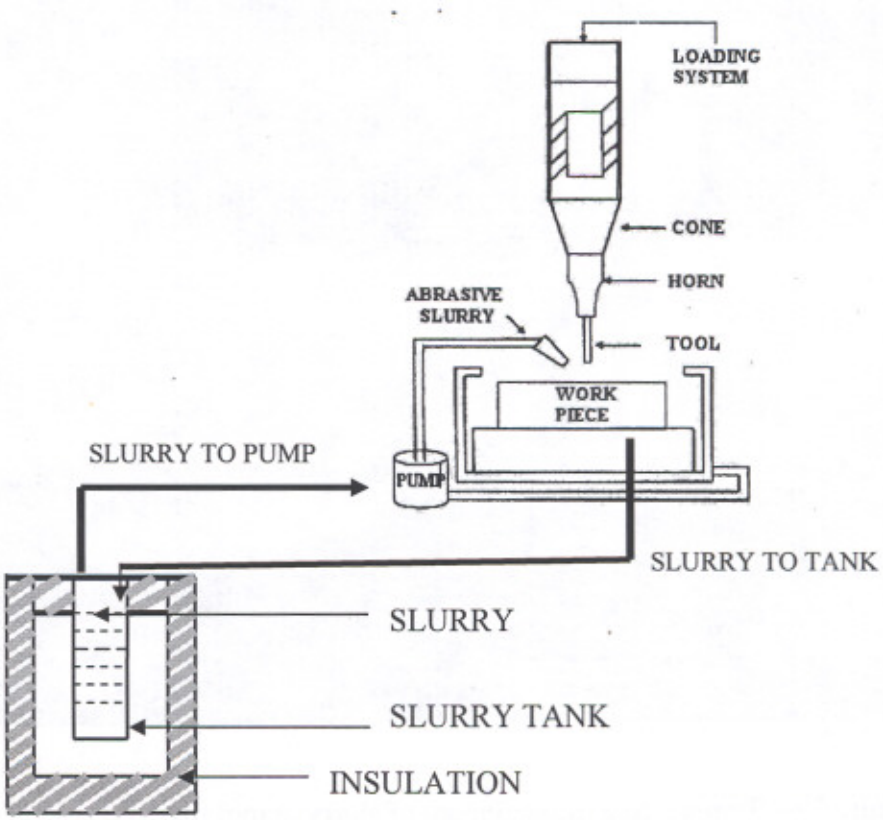

Figure 3.63 Schematic diagram of the USM and Slurry tub

The initial weight of titanium work piece (Titan15 and Titan31) and tool i.e. of S.S was taken. Then machine was allowed to drill for a given depth of 1 mm with constant slurry flow rate and slurry

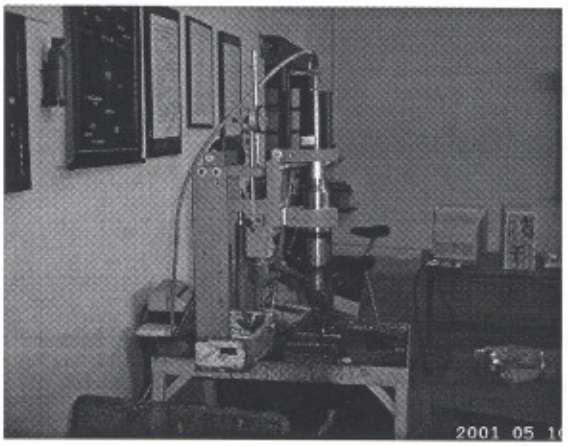

Figure 3.65 Stop watch for measuring MRR

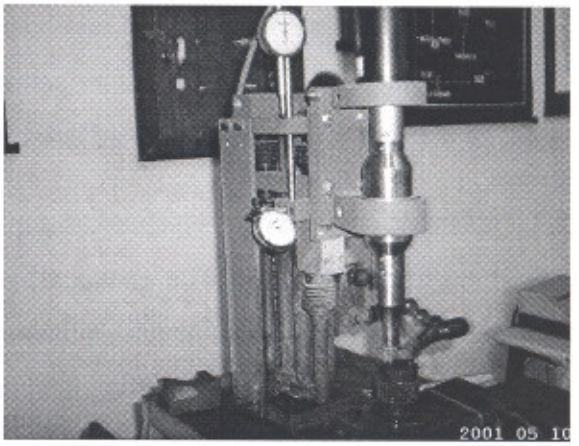

Figure 3.66 3-D pictorial view of USM

Figure 3.67 USM power rating set-up

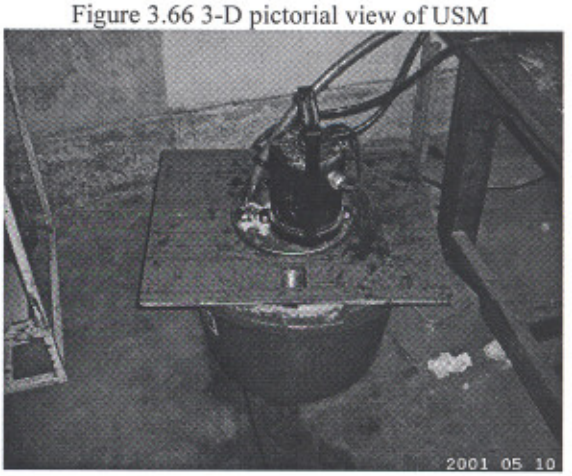

Figure 3.68 Pump for re-circulating slurry

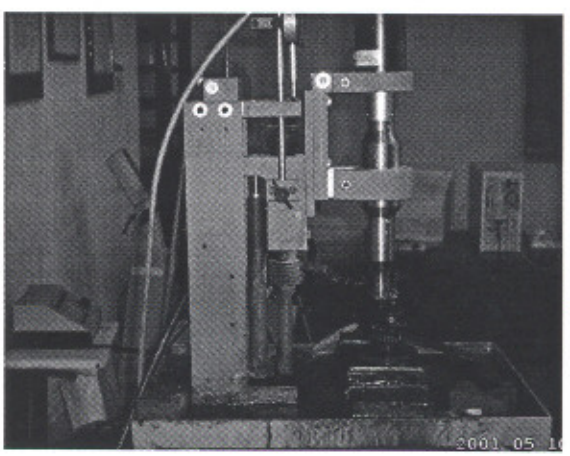

Figure 3.69 3-D pictorial side-view of USM

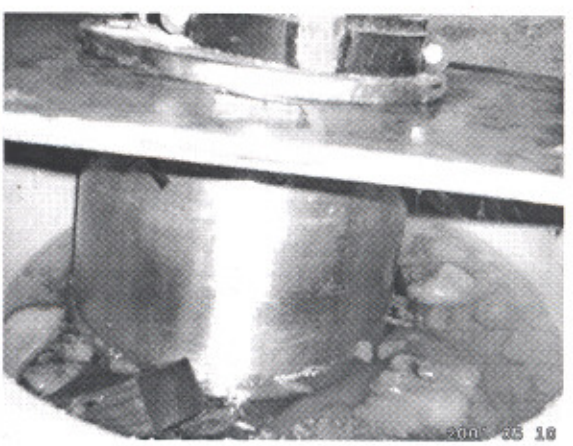

Figure 3.70 Cool slurry condition at 10°C

The experiments were conducted according to order and conditions given in table 3.6 and 3.7. The table 3.8 shows parameter settings for experiment no. 1.Corresponding MRR, TWR, S.R and microstructure were determined and tabulated.

The photomicrographs of machined samples of Titan15 and Titan31, have been analyzed to understand microstructure changes by using 'Image Analyzer' (of Metatech (Pune) India; Model: Metagraph- 1; Magnification: 100x; with in built software calibrated with optical flat from NPL (National physical laboratory) New-Delhi, India).

As observed from photomicrographs for experiment no.1, no micro cracking or surface deformation occurred (see figure 3.71 and 3.72). The use of 220 grit-size, boron carbide slurry with S.S tool at 10°C resulted in non-acicular, small mixed grains with uniform distribution. The comparison of photomicrographs of figure 3.71 and 3.72 with photomicrograph of figure 3.53 (conventionally ground surface) has revealed that grain structure got refined in case of ultrasonically machined surface.

Table 3.8 Observation table for experiment no. 1

Test Data Experiment No. : 1

Control Factor Settings

A1) Tool = S.S

B1) Slurry Concentration = 15 %

C1) Slurry Type = Boron Carbide

D1) Slurry Temperature = Low (10°C)

E3) Power Rating = Low (30%)

F1) Slurry grit size = 220

	A : Col. 1 Noise Work Piece	B : Col. 2 Noise Experiment Number	MRR gm/min (0.001)	TWR gm/min (0.001)	S.R. Microns (micrometer)
1	1) TITAN15	1) 1	2.63	7.13	0.46
2	1) TITAN15	2) 2	1.50	3.20	0.72
3	1) TITAN15	3) 3	2.06	5.14	0.59
4	2) TITAN31	1) 1	2.47	6.63	0.52
5	2) TITAN31	2) 2	2.03	6.63	0.55
6	2) TITAN31	3) 3	2.23	6.61	0.53

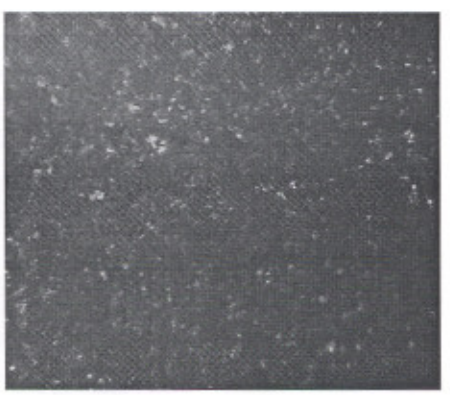

Figure 3.71 Photomicrograph of Ti 15 (100x) [Exp. No.1]

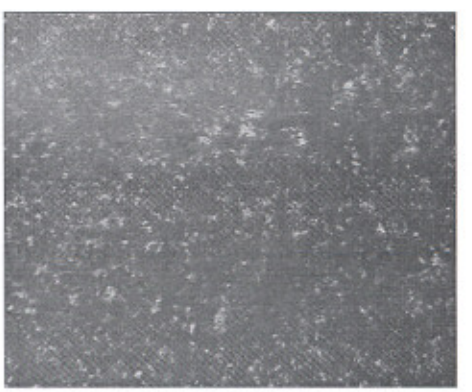

Figure 3.72 Photomicrograph of Ti 31 (100x) [Exp. No.1]

Table 3.9 shows parameter settings for experiment no. 2. Corresponding MRR, TWR, S.R and microstructure were determined and tabulated. The photomicrographs of experiment no. 2 are shown in figure 3.73 and 3.74. The photomicrographs suggest that no cracking of work piece was observed in this case also. The use of 320 grit-size, silicon carbide slurry with S.S tool at 27°C resulted in more refinement of Titan31 grains than Titan15.

Table 3.9 Observation table for experiment no. 2

Test Data Experiment No. : 2

Control Factor Settings

A1) Tool = S.S

B2) Slurry Concentration = 20 %

C2) Slurry Type = Silicon Carbide

D2) Slurry Temperature = Medium (27°C)

E2) Power Rating = Medium (60%)

F2) Slurry grit size = 320

	A : Col. 1 Noise Work Piece	B : Col. 2 Noise Experiment Number	MRR gm/min (0.001)	TWR gm/min (0.001)	S.R. Micron (micrometer)
1	1) TITAN15	1) 1	4.13	9.20	0.31
2	1) TITAN15	2) 2	3.16	8.31	0.40
3	1) TITAN15	3) 3	3.62	8.73	0.35
4	2) TITAN31	1) 1	2.77	5.51	0.46
5	2) TITAN31	2) 2	3.64	5.55	0.46
6	2) TITAN31	3) 3	3.62	5.54	0.45

Figure 3.73 Photomicrograph of Ti 15 (100x) [Exp. No.2]

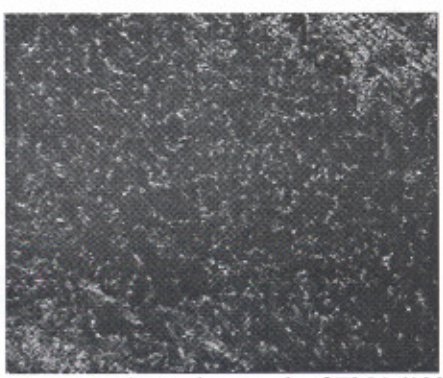

Figure 3.74 Photomicrograph of Ti 31 (100x) [Exp. No.2]

Table 3.10 shows parameter settings for experiment no. 3. Corresponding MRR, TWR, S.R and microstructure were determined and tabulated. The photomicrographs of experiment no. 3 are shown in figure 3.75 and 3.76. The use of 500 grit-size, alumina slurry with S.S tool at 60 °C resulted in almost similar microstructure refinement of both Titan31 and Titan15, with no surface cracking.

Table 3.10 Observation table for experiment no. 3

Test Data Experiment No. : 3

Control Factor Settings

A1) Tool = S.S
B3) Slurry Concentration = 25 %
C3) Slurry Type = Alumina
D3) Slurry Temperature = High (60°C)
E3) Power Rating = High (90%)
F3) Slurry grit size = 500

	A : Col. 1 Noise Work Piece	B : Col. 2 Noise Experiment Number	MRR gm/min (0.001)	TWR gm/min (0.001)	S.R. Micron
1	1) TITAN15	1) 1	5.00	10.10	0.48
2	1) TITAN15	2) 2	4.52	8.94	0.45
3	1) TITAN15	3) 3	4.74	9.50	0.46
4	2) TITAN31	1) 1	4.39	8.01	0.53
5	2) TITAN31	2) 2	3.71	8.38	0.44
6	2) TITAN31	3) 3	4.03	8.17	0.48

Figure 3.75 Photomicrograph of Ti 15 (100x) [Exp. No.3]

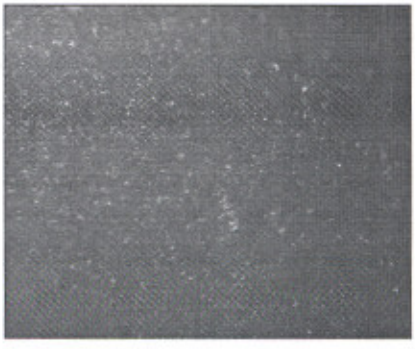

Figure 3.76 Photomicrograph of Ti 31 (100x) [Exp. No.3]

Table 3.11 shows parameter settings for experiment no. 4. Corresponding MRR, TWR, S.R and microstructure were determined and tabulated. The photomicrographs of experiment no. 4 are shown in figure 3.77 and 3.78. As compared to use of S.S tool, the 500 grit-size, boron carbide slurry at 27°C with 'H.S.S tool' resulted in uniform grain distribution and hence better grain refinement of Titan31 and Titan15.

Table 3.11 Observation table for experiment no. 4

Test Data Experiment No. : 4

Control Factor Settings

A2) Tool = H.S.S

B1) Slurry Concentration = 15 %

C1) Slurry Type = Boron carbide

D2) Slurry Temperature = Medium (27°C)

E2) Power Rating = Medium (60%)

F3) Slurry grit size = 500

	A : Col. 1 Noise Work Piece	B : Col. 2 Noise Experiment Number	MRR gm/min (0.001)	TWR gm/min (0.001)	S.R. Micron
1	1) TITAN15	1) 1	0.38	1.12	0.73
2	1) TITAN15	2) 2	1.30	2.21	0.88
3	1) TITAN15	3) 3	0.84	1.53	0.80
4	2) TITAN31	1) 1	1.34	1.95	0.64
5	2) TITAN31	2) 2	0.33	0.78	0.84
6	2) TITAN31	3) 3	0.83	1.34	0.74

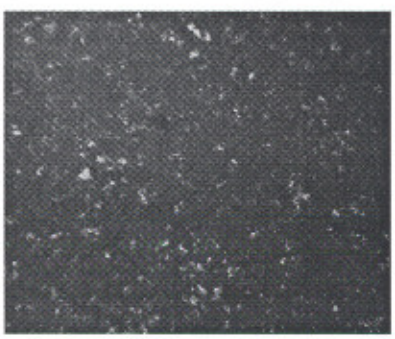

Figure 3.77 Photomicrograph of Ti 15 (100x) [Exp. No.4]

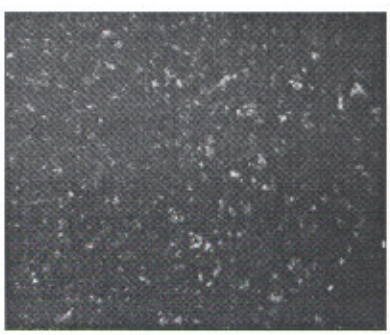

Figure 3.78 Photomicrograph of Ti 31 (100x) [Exp. No.4]

Table 3.12 shows parameter settings for experiment no. 5. Corresponding MRR, TWR, S.R and microstructure were determined and tabulated. The photomicrographs of experiment no. 5 are shown in figure 3.79 and 3.80. The use of 220 grit-size, silicon carbide slurry with H.S.S tool at 60°C resulted in almost similar microstructure of both Titan31 and Titan15.

Table 3.12 Observation table for experiment no. 5

Test Data Experiment No. : 5

Control Factor Settings

A2) Tool = H.S.S

B2) Slurry Concentration = 20 %

C2) Slurry Type = Silicon carbide

D3) Slurry Temperature = High (60°C)

E3) Power Rating = High (90%)

F1) Slurry grit size = 220

	A : Col. 1 Noise Work Piece	B : Col. 2 Noise Experiment Number	MRR gm/min (0.001)	TWR gm/min (0.001)	S.R. Micron
1	1) TITAN15	1) 1	1.50	2.66	1.62
2	1) TITAN15	2) 2	1.05	1.48	0.39
3	1) TITAN15	3) 3	1.25	2.05	0.98
4	2) TITAN31	1) 1	1.00	1.60	0.88
5	2) TITAN31	2) 2	0.68	2.04	1.50
6	2) TITAN31	3) 3	0.84	1.79	1.17

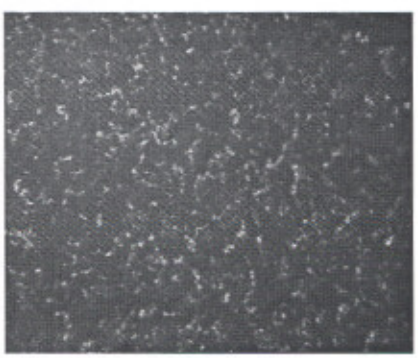

Figure 3.79 Photomicrograph of Ti 15 (100x) [Exp. No.5]

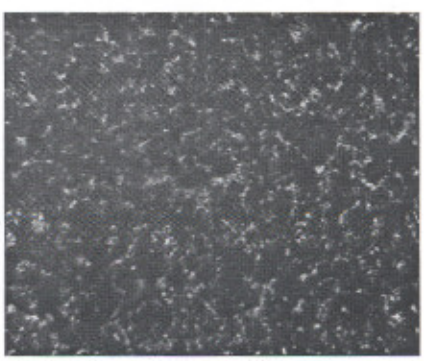

Figure 3.80 Photomicrograph of Ti 31 (100x) [Exp. No.5]

Table 3.13 shows parameter settings for experiment no. 6. Corresponding MRR, TWR, S.R and microstructure were determined and tabulated. The photomicrographs of experiment no. 6 are shown in figure 3.81 and 3.82. The use of 320 grit-size, alumina slurry with H.S.S tool at 10°C resulted in better grain refinement of Titan31 than Titan15.

Table 3.13 Observation table for experiment no. 6

Test Data Experiment No. : 6

Control Factor Settings

A2) Tool = H.S.S
B3) Slurry Concentration = 25 %
C3) Slurry Type = alumina
D1) Slurry Temperature = Low (10°C)
E1) Power Rating = Low (30%)
F2) Slurry grit size = 320

	A : Col. 1 Noise Work Piece	B : Col. 2 Noise Experiment Number	MRR gm/min (0.001)	TWR gm/min (0.001)	S.R. Micron
1	1) TITAN15	1) 1	0.31	0.74	0.65
2	1) TITAN15	2) 2	0.44	0.40	0.61
3	1) TITAN15	3) 3	0.38	0.57	0.63
4	2) TITAN31	1) 1	0.31	0.51	0.45
5	2) TITAN31	2) 2	0.23	0.09	0.46
6	2) TITAN31	3) 3	0.26	0.03	0.45

Figure 3.81 Photomicrograph of Ti 15 (100x) [Exp. No.6]

Figure 3.82 Photomicrograph of Ti 31 (100x) [Exp. No.6]

Table 3.14 shows parameter settings for experiment no. 7. Corresponding MRR, TWR, S.R and microstructure were determined and tabulated. The photomicrographs of experiment no. 7 are shown in figure 3.83 and 3.84. The use of 320 grit-size, silicon carbide slurry with H.C.S tool at 10°C resulted in microstructure refinement of both Titan31 and Titan15.

Table 3.14 Observation table for experiment no.7

Test Data Experiment No. : 7

Control Factor Settings

A3) Tool = H.C.S

B1) Slurry Concentration = 15 %

C2) Slurry Type = Silicon carbide

D1) Slurry Temperature = Low (10°C)

E3) Power Rating = High (90%)

F2) Slurry grit size = 320

	A : Col. 1 Noise Work Piece	B : Col. 2 Noise Experiment Number	MRR gm/min (0.001)	TWR gm/min (0.001)	S.R. Micron
1	1) TITAN15	1) 1	1.46	2.16	0.60
2	1) TITAN15	2) 2	1.44	8.38	0.49
3	1) TITAN15	3) 3	1.43	5.25	0.52
4	2) TITAN31	1) 1	1.35	1.19	0.73
5	2) TITAN31	2) 2	1.31	1.19	0.15
6	2) TITAN31	3) 3	1.35	1.19	0.44

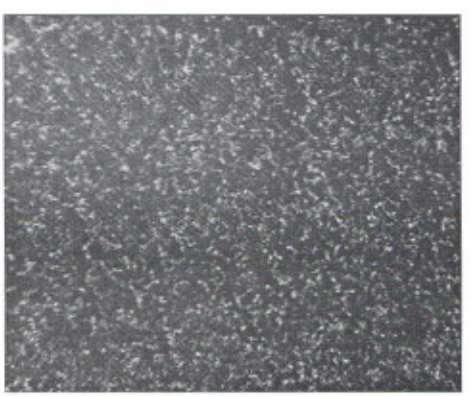

Figure 3.83 Photomicrograph of Ti 15 (100x) [Exp. No.7]

Figure 3.84 Photomicrograph of Ti 31 (100x) [Exp. No.7]

Table 3.15 shows parameter settings for experiment no. 8. Corresponding MRR, TWR, S.R and microstructure were determined and tabulated. The photomicrographs of experiment no. 8 are shown in figure 3.85 and 3.86. The use of 500 grit-size, alumina slurry with H.C.S tool at 27°C resulted in microstructure refinement of both Titan31 and Titan15.

Table 3.15 Observation table for experiment no.8

Test Data Experiment No. : 8

Control Factor Settings

A3) Tool = H.C.S
B2) Slurry Concentration = 20 %
C3) Slurry Type = alumina
D2) Slurry Temperature = Medium (27°C)
E1) Power Rating = low (30%)
F3) Slurry grit size = 500

	A : Col. 1 Noise Work Piece	B : Col. 2 Noise Experiment Number	MRR gm/min (0.001)	TWR gm/min (0.001)	S.R. Micron
1	1) TITAN15	1) 1	0.14	0.08	0.41
2	1) TITAN15	2) 2	0.02	0.01	0.35
3	1) TITAN15	3) 3	0.08	0.05	0.38
4	2) TITAN31	1) 1	0.29	0.03	0.47
5	2) TITAN31	2) 2	0.04	0.06	0.30
6	2) TITAN31	3) 3	0.02	0.04	0.38

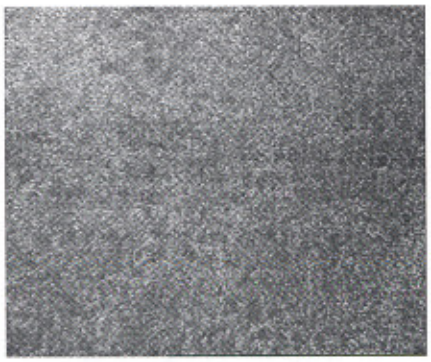

Figure 3.85 Photomicrograph of Ti 15 (100x) [Exp. No.8]

Figure 3.86 Photomicrograph of Ti 31 (100x) [Exp. No.8]

Table 3.16 shows parameter settings for experiment no. 9. Corresponding MRR, TWR, S.R and microstructure were determined and tabulated. The photomicrographs of experiment no. 9 are shown in figure 3.87 and 3.88. The use of 220 grit-size, boron carbide slurry with H.C.S tool at 60°C resulted in better microstructure refinement of Titan31 sample than Titan15.

Table 3.16 Observation table for experiment no.9

Test Data Experiment No. : 9

Control Factor Settings
A3) Tool = H.C.S
C1) Slurry Type = boron carbide
E2) Power Rating = medium (60%)
B3) Slurry Concentration = 25 %
D3) Slurry Temperature = High (60°C)
F1) Slurry grit size = 220

	A : Col. 1 Noise Work Piece	B : Col. 2 Noise Experiment Number	MRR gm/min (0.001)	TWR gm/min (0.001)	S.R. Micron
1	1) TITAN15	1) 1	1.47	8.40	0.56
2	1) TITAN15	2) 2	2.11	3.68	0.80
3	1) TITAN15	3) 3	1.77	6.02	0.66
4	2) TITAN31	1) 1	1.62	2.98	0.86
5	2) TITAN31	2) 2	1.51	2.53	1.00
6	2) TITAN31	3) 3	1.54	2.73	0.93

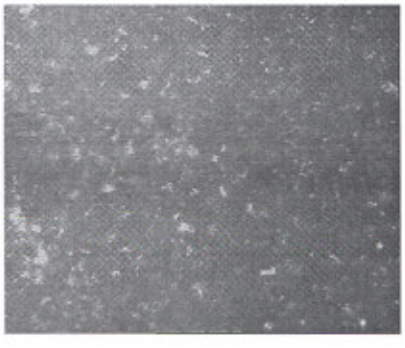

Figure 3.87 Photomicrograph of Ti 15 (100x) [Exp. No.9]

Figure 3.88 Photomicrograph of Ti 31 (100x) [Exp. No.9]

Table 3.17 shows parameter settings for experiment no. 10. Corresponding MRR, TWR, S.R and microstructure were determined and tabulated. The photomicrographs of experiment no. 10 are shown in figure 3.89 and 3.90. The use of 320 grit-size, alumina slurry with carbide tool at 60°C resulted in almost similar micro-grain distributions of both Titan31 and Titan15.

Table 3.17 Observation table for experiment no.10

Test Data Experiment No. : 10

Control Factor Settings
A4) Tool = Carbide
C3) Slurry Type = Alumina
E2) Power Rating = medium (60%)
B1) Slurry Concentration = 15 %
D3) Slurry Temperature = High (60°C)
F2) Slurry grit size = 320

	A : Col. 1 Noise Work Piece	B : Col. 2 Noise Experiment Number	MRR gm/min (0.001)	TWR gm/min (0.001)	S.R. Micron
1	1) TITAN15	1) 1	0.16	0.52	1.04
2	1) TITAN15	2) 2	0.19	0.23	0.69
3	1) TITAN15	3) 3	0.18	0.37	0.86
4	2) TITAN31	1) 1	0.01	0.02	0.46
5	2) TITAN31	2) 2	0.01	0.03	0.56
6	2) TITAN31	3) 3	0.01	0.03	0.51

Figure 3.89 Photomicrograph of Ti 15 (100x) [Exp. No.10]

Figure 3.90 Photomicrograph of Ti 31 (100x) [Exp. No.10]

Table 3.18 shows parameter settings for experiment no. 11. Corresponding MRR, TWR, S.R and microstructure were determined and tabulated. The photomicrographs of experiment no. 11 are shown in figure 3.91 and 3.92. The use of 500 grit-size, boron carbide slurry with carbide tool at 10°C resulted in more grain refinement of Titan31 sample than Titan15.

Table 3.18 Observation table for experiment no.11

Test Data Experiment No. : 11

Control Factor Settings
A4) Tool = Carbide
C1) Slurry Type = Boron Carbide
E3) Power Rating = High (90%)
B2) Slurry Concentration = 20 %
D1) Slurry Temperature = low (10°C)
F3) Slurry grit size = 500

	A : Col. 1 Noise Work Piece	B : Col. 2 Noise Experiment Number	MRR gm/min (0.001)	TWR gm/min (0.001)	S.R. Micron
1	1) TITAN15	1) 1	1.07	5.20	0.65
2	1) TITAN15	2) 2	1.54	7.44	0.43
3	1) TITAN15	3) 3	1.28	6.30	0.54
4	2) TITAN31	1) 1	1.35	6.77	0.57
5	2) TITAN31	2) 2	1.15	6.36	0.88
6	2) TITAN31	3) 3	1.23	6.54	0.72

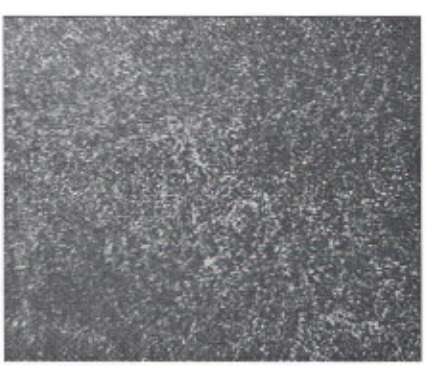

Figure 3.91 Photomicrograph of Ti 15 (100x) [Exp. No.11]

Figure 3.92 Photomicrograph of Ti 31 (100x) [Exp. No.11]

Table 3.19 shows parameter settings for experiment no. 12. Corresponding MRR, TWR, S.R and microstructure were determined and tabulated. The photomicrographs of experiment no. 12 are shown in figure 3.93 and 3.94. The use of 220 grit-size, silicon carbide slurry with carbide tool at 27°C resulted in almost similar grain refinement of both Titan31 and Titan15.

Table 3.19 Observation table for experiment no.12

Test Data Experiment No. : 12

Control Factor Settings
A4) Tool = Carbide
B3) Slurry Concentration = 25 %
C2) Slurry Type = Silicon Carbide
D2) Slurry Temperature = Medium (27°C)
E1) Power Rating = Low (30%)
F1) Slurry grit size = 220

	A : Col. 1 Noise Work Piece	B : Col. 2 Noise Experiment Number	MRR gm/min (0.001)	TWR gm/min (0.001)	S.R. Micron
1	1) TITAN15	1) 1	0.29	1.76	1.29
2	1) TITAN15	2) 2	0.29	1.56	1.33
3	1) TITAN15	3) 3	0.29	1.64	1.31
4	2) TITAN31	1) 1	0.54	2.58	1.15
5	2) TITAN31	2) 2	0.65	4.22	1.06
6	2) TITAN31	3) 3	0.60	3.40	1.10

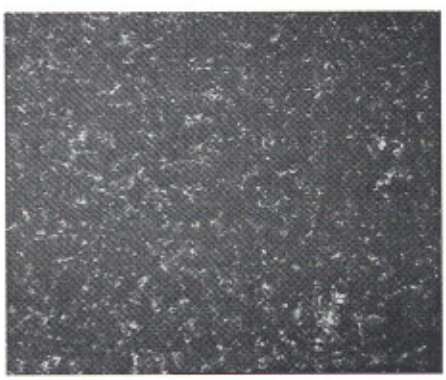

Figure 3.93 Photomicrograph of Ti 15 (100x) [Exp. No.12]

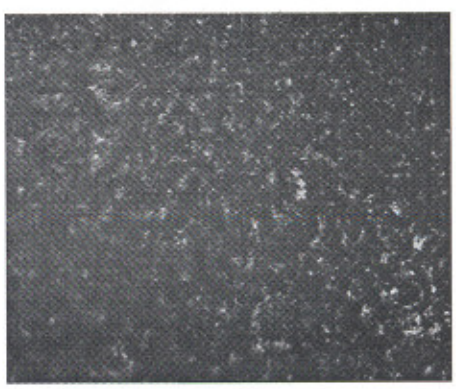

Figure 3.94 Photomicrograph of Ti 31 (100x) [Exp. No.12]

Table 3.20 shows parameter settings for experiment no. 13. Corresponding MRR, TWR, S.R and microstructure were determined and tabulated. The photomicrographs of experiment no. 13 are shown in figure 3.95 and 3.96. The use of 500 grit-size, silicon carbide slurry with diamond tool at 60°C resulted in almost similar grain refinement of both Titan31 and Titan15.

Table 3.20 Observation table for experiment no.13

Test Data Experiment No. : 13

Control Factor Settings

A5) Tool = Diamond
B1) Slurry Concentration = 15 %
C2) Slurry Type = Silicon Carbide
D3) Slurry Temperature = High (60°C)
E1) Power Rating = Low (30%)
F3) Slurry grit size = 500

	A : Col. 1 Noise Work Piece	B : Col. 2 Noise Experiment Number	MRR gm/min (0.001)	TWR gm/min (0.001)	S.R. Micron
1	1) TITAN15	1) 1	0.53	0.53	0.73
2	1) TITAN15	2) 2	0.28	0.28	0.87
3	1) TITAN15	3) 3	0.40	0.40	0.80
4	2) TITAN31	1) 1	0.49	0.62	0.72
5	2) TITAN31	2) 2	0.62	0.27	0.38
6	2) TITAN31	3) 3	0.56	0.44	0.55

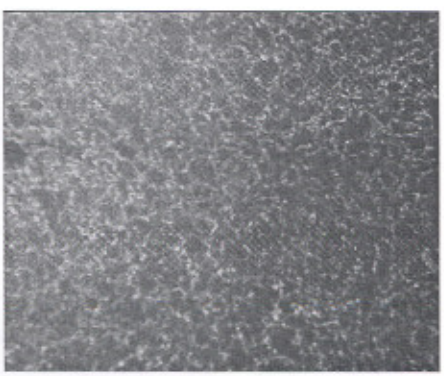

Figure 3.95 Photomicrograph of Ti 15 (100x) [Exp. No.13]

Figure 3.96 Photomicrograph of Ti 31 (100x) [Exp. No.13]

Table 3.21 shows parameter settings for experiment no. 14. Corresponding MRR, TWR, S.R and microstructure were determined and tabulated. The photomicrographs of experiment no. 14 are shown in figure 3.97 and 3.98. The use of 220 grit-size, alumina slurry with diamond tool at 10°C resulted in more grain refinement of Titan31 sample as compared to Titan15.

Table 3.21 Observation table for experiment no.14

Test Data Experiment No. : 14

Control Factor Settings

A5) Tool = Diamond

B2) Slurry Concentration = 20 %

C3) Slurry Type = Alumina

D1) Slurry Temperature = Low (10°C)

E2) Power Rating = Medium (60%)

F1) Slurry grit size = 220

	A : Col. 1 Noise Work Piece	B : Col. 2 Noise Experiment Number	MRR gm/min (0.001)	TWR gm/min (0.001)	S.R. Micron
1	1) TITAN15	1) 1	0.65	0.16	0.56
2	1) TITAN15	2) 2	1.25	0.47	0.90
3	1) TITAN15	3) 3	0.95	0.32	0.73
4	2) TITAN31	1) 1	0.06	0.50	0.34
5	2) TITAN31	2) 2	0.14	0.68	0.19
6	2) TITAN31	3) 3	0.99	0.59	0.26

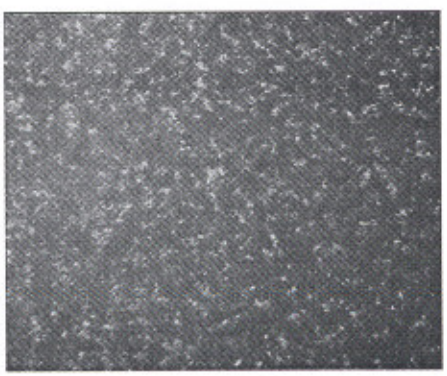

Figure 3.97 Photomicrograph of Ti 15 (100x) [Exp. No.14]

Figure 3.98 Photomicrograph of Ti 31 (100x) [Exp. No.14]

Table 3.22 shows parameter settings for experiment no. 15. Corresponding MRR, TWR, S.R and microstructure were determined and tabulated. The photomicrographs of experiment no. 15 are shown in figure 3.99 and 3.100. The use of 320 grit-size, boron carbide slurry with diamond tool at 27°C resulted in almost similar grain refinement of both Titan31 and Titan15.

Table 3.22 Observation table for experiment no.15

Test Data Experiment No. : 15

Control Factor Settings

A5) Tool = Diamond

B3) Slurry Concentration = 25 %

C1) Slurry Type = boron carbide

D2) Slurry Temperature = Medium (27°C)

E3) Power Rating = High (90%)

F2) Slurry grit size = 320

	A : Col. 1 Noise Work Piece	B : Col. 2 Noise Experiment Number	MRR gm/min (0.001)	TWR gm/min (0.001)	S.R. Micron
1	1) TITAN15	1) 1	2.32	8.99	0.82
2	1) TITAN15	2) 2	3.77	5.80	0.94
3	1) TITAN15	3) 3	3.04	7.39	0.88
4	2) TITAN31	1) 1	3.43	0.95	0.77
5	2) TITAN31	2) 2	4.34	2.77	0.60
6	2) TITAN31	3) 3	3.88	6.11	0.68

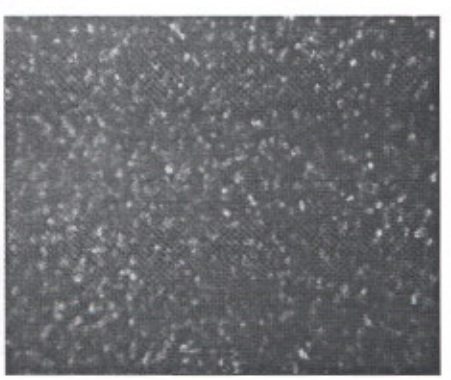

Figure 3.99 Photomicrograph of Ti 15 (100x) [Exp. No.15]

Figure 3.100 Photomicrograph of Ti 31 (100x) [Exp. No.15]

Table 3.23 shows parameter settings for experiment no. 16. Corresponding MRR, TWR, S.R and microstructure were determined and tabulated. The photomicrographs of experiment no. 16 are shown in figure 3.101 and 3.102. The use of 220 grit-size, alumina slurry with titanium tool at 27°C resulted in almost similar grain refinement of both Titan31 and Titan15 samples.

Table 3.23 Observation table for experiment no.16

Test Data Experiment No. : 16

Control Factor Settings

A6) Tool = Titanium

C3) Slurry Type = Alumina

E3) Power Rating = 90 %

B1) Slurry Concentration = 15 %

D2) Slurry Temperature = 27°C

F1) Slurry grit size = 220

	A : Col. 1 Noise Work Piece	B : Col. 2 Noise Experiment Number	MRR (0.001) gm/min	TWR (0.001) gm/min	S.R. Micron
1	1) TITAN15	1) 1	4.03	6.43	0.95
2	1) TITAN15	2) 2	4.03	6.44	0.94
3	1) TITAN15	3) 3	4.03	6.43	0.95
4	2) TITAN31	1) 1	8.17	3.71	0.90
5	2) TITAN31	2) 2	8.16	3.70	0.89
6	2) TITAN31	3) 3	8.17	3.71	0.90

Figure 3.101 Photomicrograph of Ti 15 (100x) [Exp. No.16]

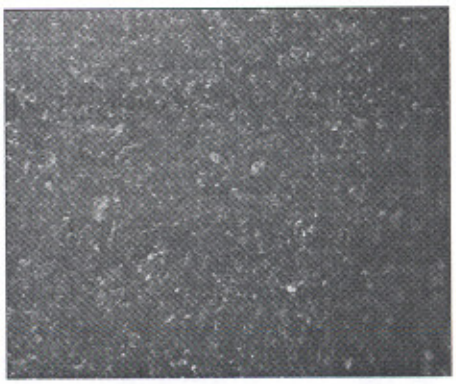

Figure 3.102 Photomicrograph of Ti 31 (100x) [Exp. No.16]

Table 3.24 shows parameter settings for experiment no. 17. Corresponding MRR, TWR, S.R and microstructure were determined and tabulated. The photomicrographs of experiment no. 17 are shown in figure 3.103 and 3.104. The use of 320 grit-size, boron carbide slurry with titanium tool at 60°C resulted in better grain refinement of Titan31 sample than Titan15.

Table 3.24 Observation table for experiment no.17

Test Data Experiment No. : 17

Control Factor Settings

A6) Tool = Titanium
B2) Slurry Concentration = 20 %
C1) Slurry Type = Boron Carbide
D3) Slurry Temperature = 60°C
E1) Power Rating = 30 %
F2) Slurry grit size = 320

	A : Col. 1 Noise Work Piece	B : Col. 2 Noise Experiment Number	MRR (0.001) gm/min	TWR (0.001) gm/min	S.R. Micron
1	1) TITAN15	1) 1	2.22	2.22	1.53
2	1) TITAN15	2) 2	3.66	0.92	0.45
3	1) TITAN15	3) 3	2.92	1.54	0.99
4	2) TITAN31	1) 1	4.81	9.44	0.39
5	2) TITAN31	2) 2	3.13	2.55	0.70
6	2) TITAN31	3) 3	3.97	5.97	0.54

Figure 3.103 Photomicrograph of Ti 15 (100x) [Exp. No.17]

Figure 3.104 Photomicrograph of Ti 31 (100x) [Exp. No.17]

Table 3.25 shows parameter settings for experiment no. 18. Corresponding MRR, TWR, S.R and microstructure were determined and tabulated. The photomicrographs of experiment no. 18 are shown in figure 3.105 and 3.106. The use of 500 grit-size, silicon carbide slurry with titanium tool at 10°C resulted in better refinement of grain microstructure of Titan31 sample than Titan15.

Table 3.25 Observation table for experiment no.18

Test Data Experiment No. : 18

Control Factor Settings

A6) Tool = Titanium
B3) Slurry Concentration = 25 %
C2) Slurry Type = Silicon Carbide
D1) Slurry Temperature = 10°C
E2) Power Rating = 60 %
F3) Slurry grit size = 500

	A : Col. 1 Noise Work Piece	B : Col. 2 Noise Experiment Number	MRR (0.001) gm/min	TWR (0.001) gm/min	S.R. Micron
1	1) TITAN15	1) 1	8.63	9.26	0.55
2	1) TITAN15	2) 2	1.00	1.47	0.40
3	1) TITAN15	3) 3	4.79	5.34	0.47
4	2) TITAN31	1) 1	0.26	1.28	0.38
5	2) TITAN31	2) 2	1.76	1.32	0.55
6	2) TITAN31	3) 3	1.01	1.30	0.46

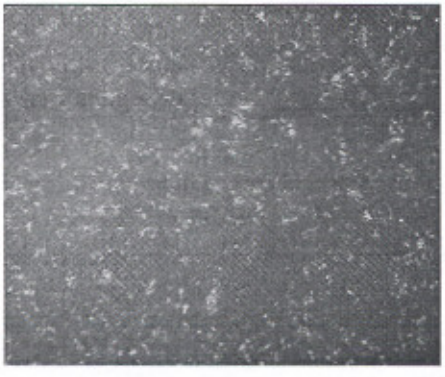

Figure 3.105 Photomicrograph of Ti 15 (100x) [Exp. No.18]

Figure 3.106 Photomicrograph of Ti 31 (100x) [Exp. No.18]

The outcome of the Taguchi designed experiments for MRR, TWR and SR of Titan15 and Titan31, while machining with USM has been recorded. **Eighteen sets** of experiments were repeated **three times** for reducing the experimentation errors. Photomicrographs of eighteen sets of experiments have been observed for further analysis.

CHAPTER 4

RESULTS AND DISCUSSION

4.1 INTRODUCTION

Experiments were conducted at various settings of slurry temperature, slurry concentration, slurry type, slurry grit-size, tool types and power ratings of USM. Material removal rate, tool wear rate and surface roughness has been recorded and plotted as per Taguchi design. Following are the results of experimentation.

4.2 EFFECT ON MATERIAL REMOVAL RATE

As observed from figure 3.51 (Pilot experimentation, 'Titan15-H.S.S' work-tool combination), the material removal rate at slurry temperature 27°C was better than the material removal rate at 10°C and at 60°C. But similar trend was not observed in table 3.8 to 3.25, as the set of process parameters used in these tables were different. From these tables it was observed that the effect of slurry temperature on MRR was insignificant. The main factors that contributed to MRR were power rating, tool type and type of slurry. The impact of these factors on MRR was evident from tables 3.8 to 3.25. For analyzing the effect of these process parameters on MRR, 'Nominal the best' type situation was judicially selected, because if 'Larger the better' type situation would have been selected; MRR, TWR and SR would have been automatically higher. Accordingly, it was concluded from table 3.8 to 3.25 that ***'input parameter settings of ultrasonic power rating at 450W, with S.S tool and boron carbide slurry had shown the best results for MRR; when titanium and its alloys were machined'.*** The parametric settings at 450W resulted in higher momentum strikes of abrasive particles on work piece; S.S tool resulted in less strain hardening with work piece combination, and boron carbide being the hardest abrasive slurry, resulted in best output.

In pilot experimentation (refer figure 3.51) material removal rate increased with increase in power rating from 150W to 300W for slurry temperature 27°C and decreased with increase in ultrasonic power from 300W-450W, whereas for slurry temperature 10°C, the

450W, tool wear rate increased. But in designed experiments (refer table 3.8 to 3.25) the role played by slurry temperature was insignificant; whereas the power rating affected the TWR appreciably.

4.4 EFFECT ON SURFACE ROUGHNESS

The surface roughness increased with increase in power rating for all the slurry temperature that is at 10°C, 27°C and 60°C (refer figure 3.50). The increase in surface roughness was sharp at slurry temperature 60°C; however for slurry temperature 27°C and 10°C the increase in surface roughness appeared to be moderate. Further, at 10°C slurry temperature there was even fall in surface roughness at power rating of 450W. The reason for increase in surface roughness with increase in power rating may be explained on the basis that with increase in power rating, momentum of the abrasive particle increases and thus they strike the work piece with greater impact and haphazardly resulting in increased surface roughness. Also the sharp increase in surface roughness with increase in power rating at slurry temperature 60°C may be explained on the basis that the particle movement becomes less restricted due to fall in viscosity of slurry. As a result, the abrasive particles attack the surface with more impact causing sharp increase in surface roughness with rise in temperature of slurry. On further increasing the ultrasonic power from 300W to 450W at slurry temperature 10°C, the surface roughness decreased or almost remained constant. This trend may be explained on the basis that at such a high power rating and low slurry temperature the abrasive particles are more compactly packed. This resulted in more precise and controlled hitting of abrasive particles on the work piece, which causes better surface finish.

To get more insight into the machining characteristics of work piece (Titan15 and Titan31), microphotographs of all the machined cavities were obtained at various values of power rating and slurry temperature as per Taguchi designed matrix. It can be observed from the microphotographs (figures 3.71 to 3.106) that the grains are uniformly packed with high density. These refined grain structure, resulting from ultrasonic machining, can give better strength and mechanical properties. It becomes clear from photomicrographs that at 150W, the grains were more uniformly packed in case of

machining at slurry temperature 60°C followed machining at 27°C and machining at 10°C respectively. At 300W, it was very clear from the photomicrographs that grains in case of machining at slurry temperature 27°C were very densely packed resulting in very fine surface and lower value of the surface roughness followed by machining at 10°C and 60°C. Further from the photomicrographs at 450W it clearly shows that grains were loosely packed in case of machining at 60°C resulting in maximum value of surface roughness followed by machining at 10°C and 27°C. As observed from table 3.8 to 3.25; slurry temperature at 27°C, with slurry concentration at 25% and S.S tool was giving the best results for SR.

4.5 ANALYSIS

For analysis purpose, software for robust deign (rdExpert™ V 7.0 for Test Planning Lite) has been used for generating efficient orthogonal test plans. The *rdExpert* engine can accommodate test parameters having up to 17 levels. It provides balanced, pair wise coverage.

Table 4.1 shows 'test data summary' for S/N ratio and SEN (Sensitivity, which is reciprocal of S/N) for MRR, TWR and SR.

Table 4.1: Test Data Summary

S.No	Material Removal Rate S/N	Material Removal Rate SEN	Tool Wear Rate S/N	Tool Wear Rate SEN	Surface Roughness S/N	Surface Roughness SEN
1	14.71	6.66	12.00	15.40	16.06	-5.01
2	17.46	10.86	12.05	17.07	16.10	-7.85
3	19.43	12.87	20.64	18.94	23.39	-6.50
4	5.70	-1.56	9.00	3.45	19.02	-2.25
5	11.15	0.45	13.24	5.74	7.73	0.75
6	12.43	-9.88	2.92	-8.18	14.88	-5.33
7	27.15	2.86	0.71	10.17	8.01	-6.23
8	-0.54	-20.13	6.21	-27.15	16.51	-8.37
9	16.84	4.45	5.45	12.85	13.68	-1.92
10	0.28	-20.46	-0.49	-13.99	9.73	-3.28
11	17.75	2.08	18.88	16.17	12.11	-3.99
12	8.30	-7.05	7.30	8.05	20.24	1.63
13	11.81	-6.37	9.62	-7.48	11.50	-3.41
14	2.84	-3.47	7.65	-6.89	4.94	-6.08
15	13.76	10.79	5.07	14.54	15.84	-2.14
16	8.60	15.70	10.62	14.10	30.39	-0.71
17	11.66	10.76	1.20	11.53	4.99	-2.31
18	-0.89	9.27	0.03	10.44	16.27	-6.59
Average	11.02	0.99	7.89	5.27	14.52	-3.86
Std.Dev.	7.57	10.66	6.08	12.80	6.45	2.85
Maximum	27.15	15.70	20.64	18.94	30.39	1.63
Minimum	-0.89	-20.46	-0.49	-27.15	4.94	-8.37

The factor effects of different six input parameters with their corresponding levels on S/N ratio of MRR, TWR and SR is shown in table 4.2.

Table 4.2 Factor Effects

Factor	Level	Material Removal Rate S/N	Tool Wear Rate S/N	Surface Roughness S/N
A) Tool	**A1) S.S**	17.20	14.90	18.51
	A2) H.S.S	9.76	8.39	13.88
	A3) H.C.S	14.48	4.12	12.73
	A4) Carbide	8.78	8.56	14.03
	A5) Diamond	9.47	7.45	10.76
	A6) Titanium	6.46	3.95	17.22
B) Slurry Concentration	**B1) 15 %**	11.37	6.91	15.79
	B2) 20 %	10.05	9.87	10.40
	B3) 25 %	11.65	6.90	17.38
C) Slurry Type	**C1) Boron Carbide**	13.40	8.60	13.62
	C2) Silicon Carbide	12.50	7.16	13.31
	C3) Alumina	7.17	7.93	16.64
D) Slurry Temperature	**D1) 10°C**	12.33	7.03	12.04
	D2) 27°C	8.88	8.38	19.68
	D3) 60°C	11.86	8.28	11.84
E) Power Rating	**E1) 30 %**	9.73	6.54	14.03
	E2) 60 %	7.04	5.62	13.29
	E3) 90 %	16.31	11.53	16.24
F) Slurry grit size	**F1) 220**	10.41	9.38	15.51
	F2) 320	13.79	3.58	11.59
	F3) 500	8.88	10.73	16.47
Average		11.02	7.89	14.52
Error Variance		99.82	23.07	16.72

As regards to M.R.R., figure 4.1 represents Signal to Noise ration (S/N) Vs different input parameters and table 4.3 shows the F-test values and %age sum of squares. The ideal function selected here is 'nominal the best' type case.

Name: 1) Material Removal Rate **Type: Nominal the Best (Ideal Function)**
Response: [MRR]

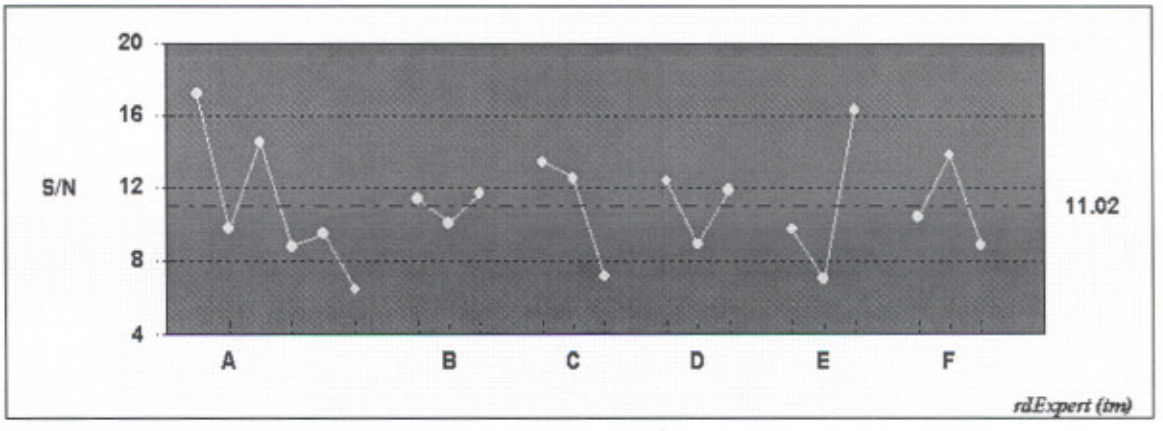

Figure 4.1 S/N Vs Input parameters

Table 4.3 Factor F Value

F Value	0.5	0.0	0.7	0.2	1.4	0.4
%SS	24.6	0.9	13.9	4.3	28.0	7.8

Figure 4.2 represents SEN for M.R.R. Vs different input parameters and table 4.4 shows the F-test values and %age sum of squares for M.R.R. response case.

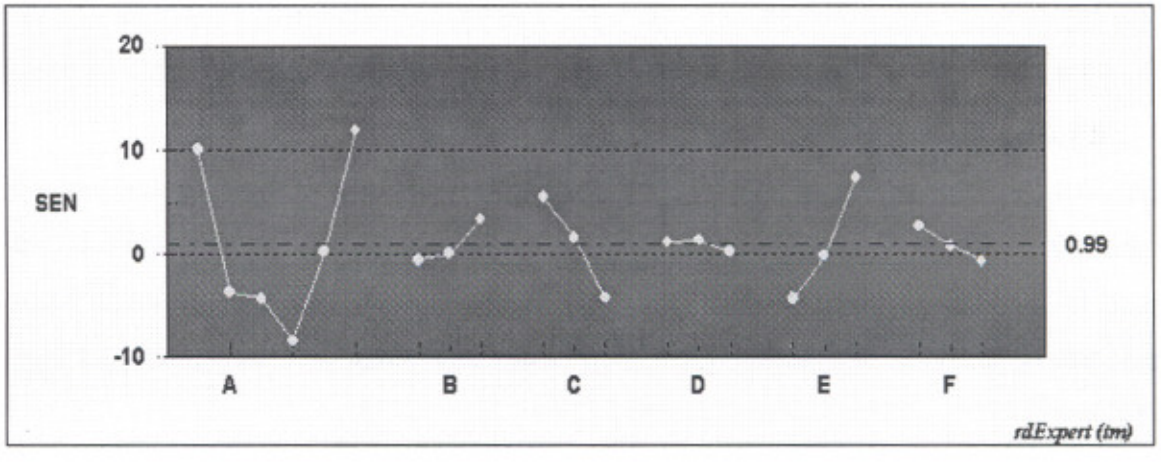

Figure 4.2 SEN Vs Input parameters

Table 4.4 Factor F Value

F Value	4.4	0.6	3.1	0.0	4.6	0.4
%SS	53.1	2.8	15.0	0.2	22.2	1.8

Figure 4.3 represents T.W.R Signal to noise ration (S/N) Vs different input parameters and table 4.5 shows the F-test values and %age sum of squares. The ideal function selected here also is nominal the best type.

Name: 2) Tool Wear Rate **Type: Nominal the Best (Ideal Function)**
Response: [TWR]

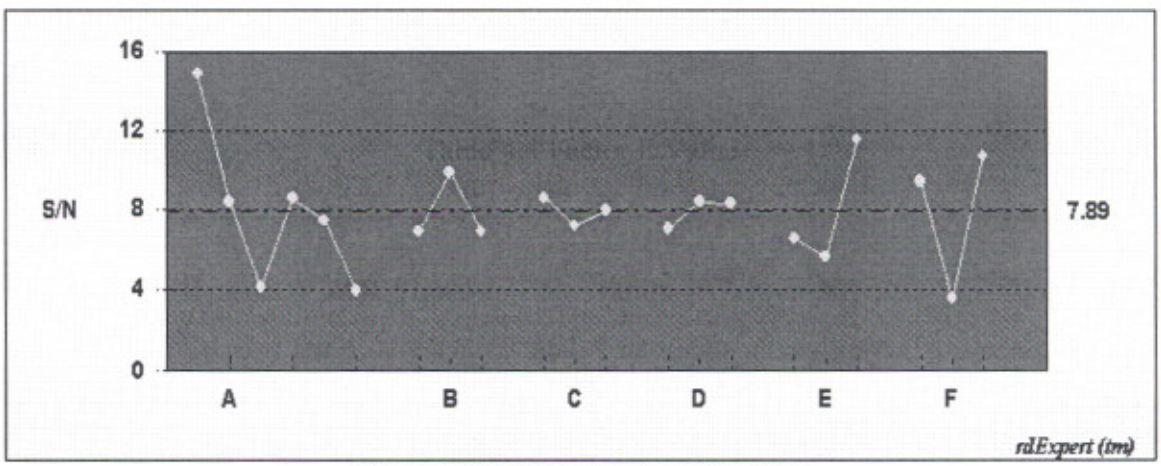

Figure 4.3 S/N Vs Input parameters

Table 4.5 Factor F Value

F Value	2.1	0.8	0.1	0.1	2.6	3.8
%SS	38.1	5.6	1.0	1.1	19.3	27.6

Figure 4.4 represents T.W.R. SEN Vs different input parameters and table 4.6 shows the F-test values and %age sum of squares for T.W.R response.

Figure 4.5 represents S.R. Signal to noise ration (S/N) Vs different input parameters and table 4.7 shows the F-test values and %age sum of squares. The ideal function selected here is nominal the best type. Figure 4.6 represents S.R. SEN Vs different input parameters and table 4.8 shows the F-test values and %age sum of squares for S.R response.

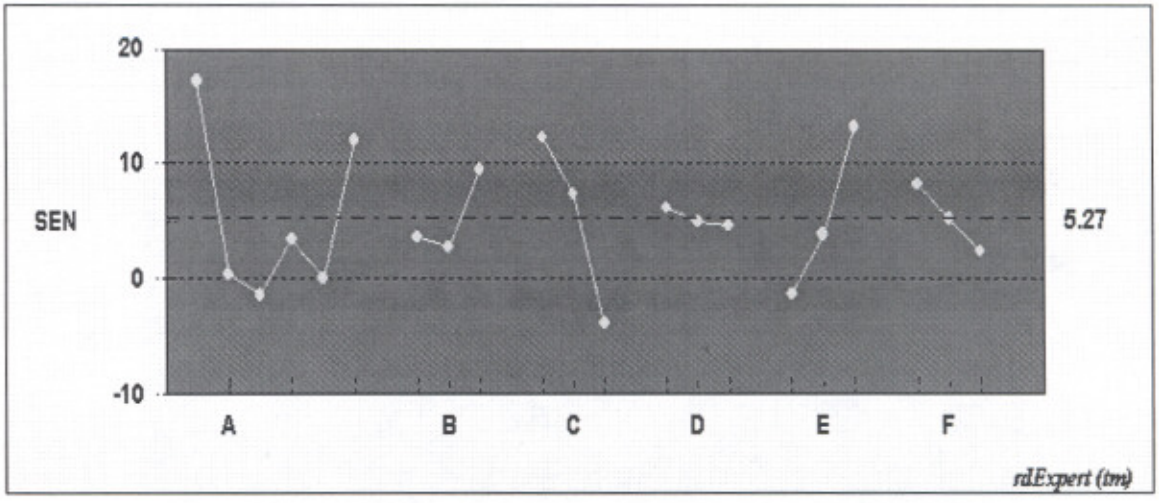

Figure 4.4 SEN Vs Input parameters

Table 4.6 Factor F Value

F Value	1.9	0.9	4.7	0.0	3.7	0.6
%SS	30.8	5.7	29.6	0.3	23.6	3.6

Name: 3) Surface Roughness **Type: Nominal the Best (Ideal Function)**
Response: [S.R. Micron]

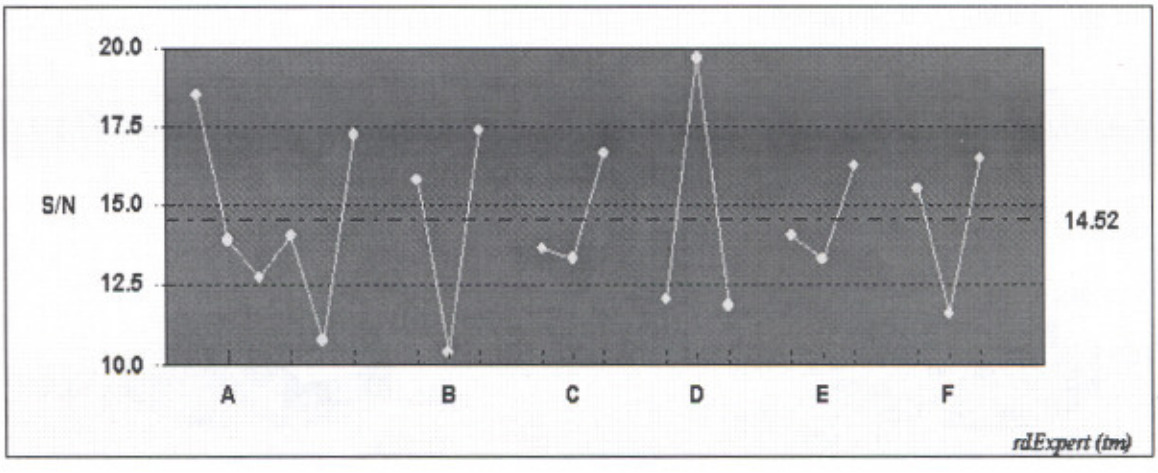

Figure 4.5 S/N Vs Input parameters

Table 4.7 Factor F Value

F Value	1.5	4.8	1.2	7.2	0.8	2.4
%SS	17.5	22.8	5.8	33.9	4.0	11.3

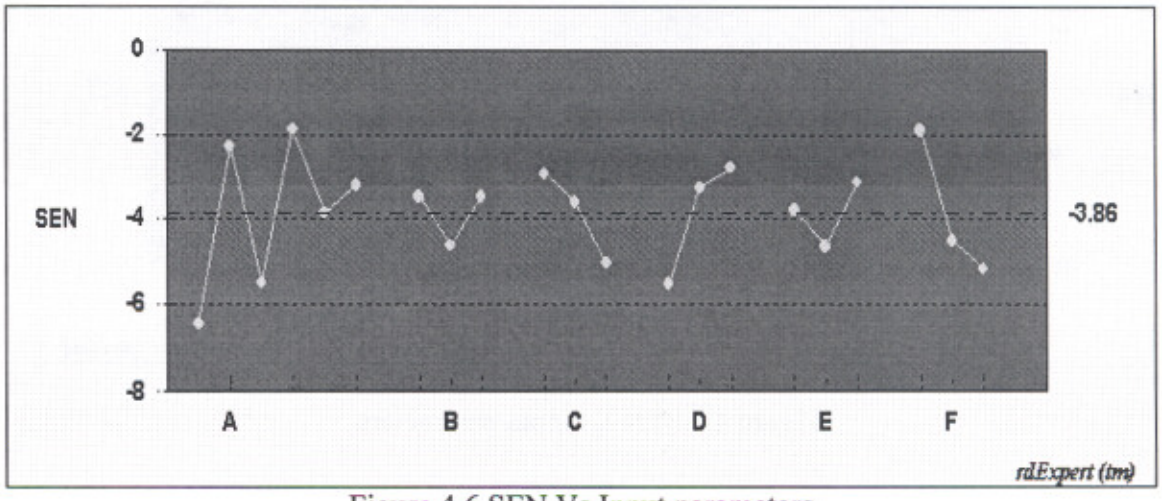

Figure 4.6 SEN Vs Input parameters

Table 4.8 Factor F Value

F Value	27.8	7.7	19.7	36.9	10.0	51.9
%SS	35.4	3.9	10.0	18.7	5.1	26.4

Figure 4.7 to 4.12 represents Pie chart to understand %age contribution of each factor effect for M.R.R., T.W.R. and S.R.

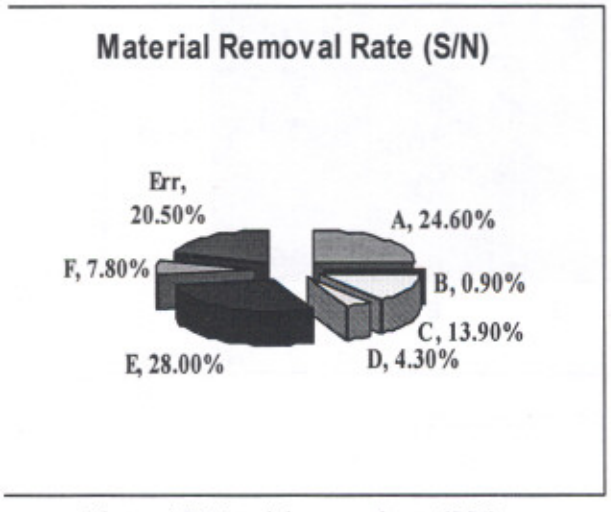

Figure 4.7 Material removal rate (S/N)

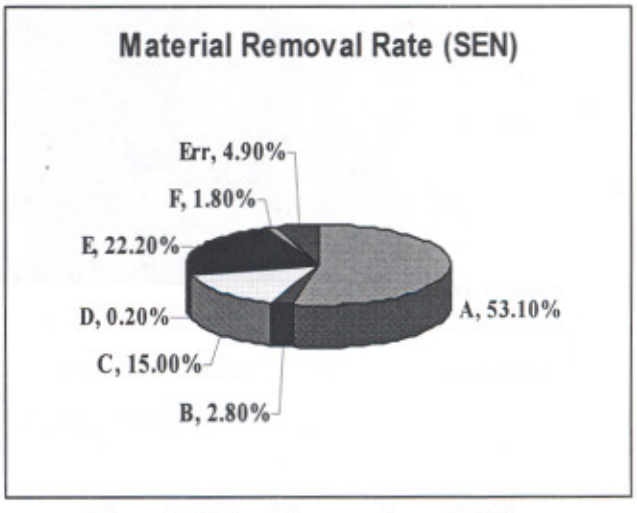

Figure 4.8 Material removal rate (SEN)

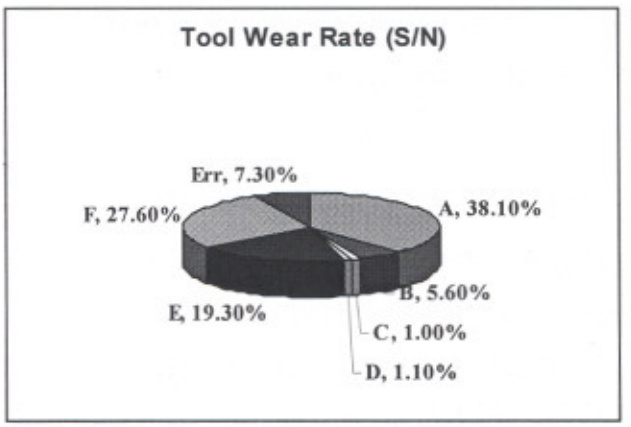

Figure 4.9 Tool wear rate (S/N)

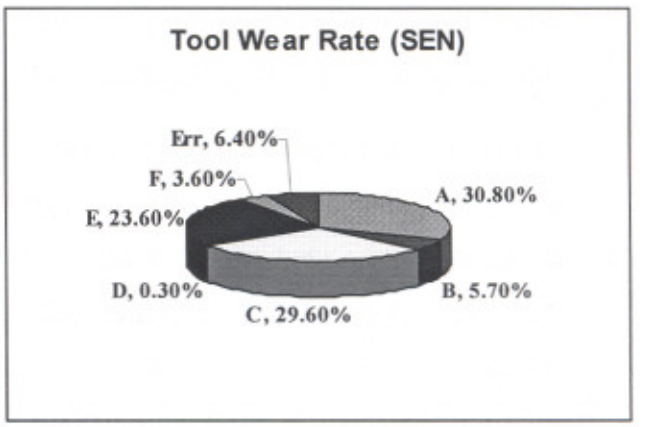

Figure 4.10 Tool wear rate (SEN)

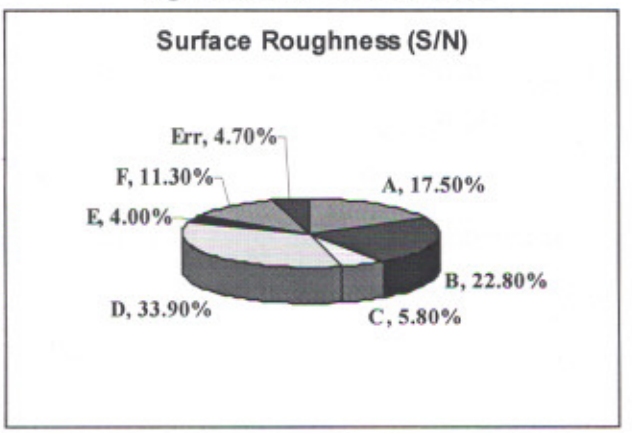

Figure 4.11 Surface Roughness (S/N)

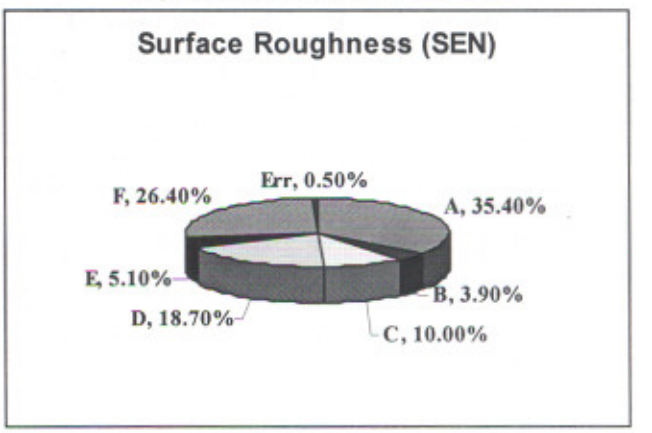

Figure 4.12 Surface Roughness (SEN)

4.5.1 Verification experiment and future plans

Conducting a verification experiment is a crucial final step of a robust design project. Its purpose is to verify that the optimum conditions suggested by the matrix experiment do indeed give the projected improvement. If the observed S/N ratios under the optimum conditions are close to their respective predictions, then we conclude that the additive model on which the matrix experiment was based is a good approximation of the reality. Then, we adopt the recommended optimum conditions for our process or product, as the case may be. However, if the observed S/N ratios under the optimum conditions differ drastically from their respective predictions, there is an evidence of failure of the additive model. There can be many reasons for failure and, thus, there are many ways of dealing with it. The failure of additive model generally indicates that choice of the objective

function or the S/N ratio is inappropriate, the observed quality characteristics was chosen incorrectly, or the levels of the control factors were chosen inappropriately.

The verification experiment has two aspects:

The first is that the prediction must agree under the laboratory conditions; the second aspect is that the predictions should be valid under actual manufacturing conditions for the process design and under actual field conditions for the product design. A judicious choice of both the noise factors to be included in the experiment and the testing conditions is essential for the predictions made through the laboratory experiment to be valid under both manufacturing and field conditions.

For the case study of titanium and its alloys machining characteristics optimization using USM process, three final observations were made under both the optimum condition and under the starting conditions. The results are tabulated in Table 4.9. It is clear that the data agree very well with the predictions about the improvement in the S/N ratios and the deposition rate. So, we could adopt the optimum settings as the new process settings and proceed to implement these settings. The comparison can also be seen in figure 4.13.

Table 4.9 Results of Verification Experiment

Response type		Starting condition value	Optimum condition Value
MRR	gm/min	$3.29*10^{-3}$	$5.02*10^{-3}$
TWR	gm/min	$9.68*10^{-3}$	$8.94*10^{-3}$
SR	microns	0.46	0.31

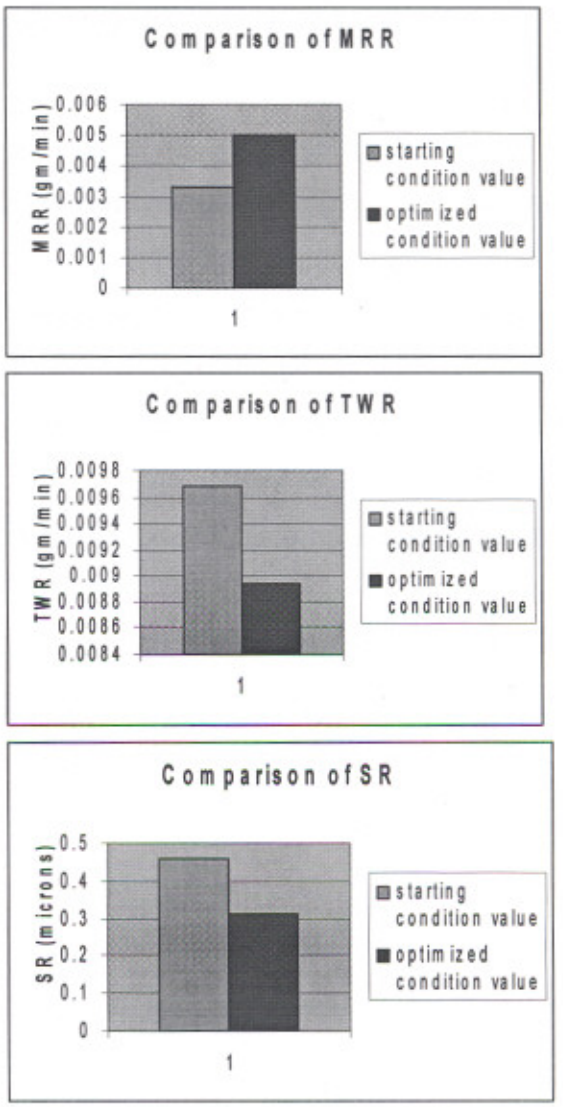

Figure 4.13 Comparison of initial Vs optimized condition

4.5.2 Follow-up experiments

Optimization of a process or a product need not be completed in a single matrix experiment. Several matrix experiments may have to be conducted in sequence before completing a product or process design. The information learned in one matrix experiment is used to plan the subsequent matrix experiments for achieving even more improvement in the process or the product. The factors studied in such subsequent

experiments, or the levels of the factors, were typically different from those studied in the earlier experiments.

From the case-study data on the machining characteristics of titanium and its alloy as regard to MRR; Ultrasonic power rating, type of tool and type of slurry stood out as the most important factors- both for quality and productivity. Ultrasonic power rating at 90% i.e. at 450W, with S.S tool and boron carbide slurry was giving the best results for MRR; when titanium and its alloys were machined with USM.

Type of tool, ultrasonic power rating, and slurry grit-size significantly affect the TWR in USM. Ultrasonic power rating at 90% i.e. at 450W, with S.S tool and 500grit-size slurry was giving the best results for TWR; when titanium and its alloys were machined with USM.

Slurry temperature, slurry concentration and type of tool significantly affect the SR in USM. The slurry temperature at 27°C, with slurry concentration as 25% and S.S tool was giving the best results for SR; when titanium and its alloys were machined with USM.

4.5.3 Range of applicability

In any development activity, it is highly desirable that the conclusions continue to be valid when we advance to a new generation of technology. In the case study of the machining characteristics optimization, this means that having developed the process with Titan15 (ASTM Gr2) and Titan31 (ASTM Gr5) titanium work pieces, one would want it to be valid when we advance to more grades of titanium and its alloys. The present results are valid for 90-95% confidence interval.

The process developed for one application should be valid for other applications. Processes and products developed by the robust design method generally possess this characteristic of design transferability.

In the case study, going from two grades of titanium work pieces to other grades can be achieved by making minor changes dictated by response variable calculations. Thus, a significant amount of development effort may be saved in transferring the process to the settings of new control factors that will handle new grades of titanium work pieces.

CHAPTER 5

MODELING OF THE RESULTS

5.1 INTRODUCTION

There are two broad approaches for optimizing a complex system such as machining characteristics of titanium and its alloys.

1. Micro-modeling
2. Macro-modeling

The both of these approaches are explained next.

1. Micro-modeling: As the name suggests, micro-modeling is based on an in-depth understanding of the system. It begins by developing a mathematical model of the system, which, in this case, would be of the MRR of titanium and its alloys while machining with USM. When systems are complex, as in the case study, we must make assumption that simplify the operation, as well as put forth considerable effort to develop the model. Furthermore, the more simplifying we do, the less realistic the model will be, and, hence, the less adequate it will be for precise optimization. But once an adequate model is constructed, a number of well-known optimization methods, can be used to find the best system configuration.

For developing a micro-model in the case under study, initially a macro-model based upon concept of robust design has been made and out put of this macro-model has been used for developing a micro-model.

2. In macro-modeling, we bypass the step of building a mathematical model of the system. The concern is primarily with obtaining the optimum system configuration, not with obtaining a detailed understanding of the system itself. As such, macro-modeling gives faster and more efficient results. It gives the specific information needed for optimization with a minimum expenditure of experimental resources.

Both of these approaches have been used in study presented here for modeling the machining characteristics of titanium and its alloys. The macro-model is based upon Taguchi design for optimization and micro-model is based upon dimensional analysis as per Buckingham's-Π theorem.

5.2 MACRO-MODEL FOR PREDICTING MACHINING CHARACTERISTICS OF TITANIUM AND IT'S ALLOYS IN USM

The case study under consideration deals primarily with obtaining the optimum system configuration in terms of response parameters with minimum expenditure of experimental resources. The P-diagram (Process diagram) for the process has been shown in figure 2.18.The titanium and its alloys machining was viewed as "black box". The parameters that influence the output were identified and divided in to two classes: Noise factors and Control Factors. Figure 5.1 shows details of noise factors and signal factors for P-diagram representing machining conditions of titanium and its alloys. The best settings of control factors have been determined through experiments as shown in table 5.1 as macro model.

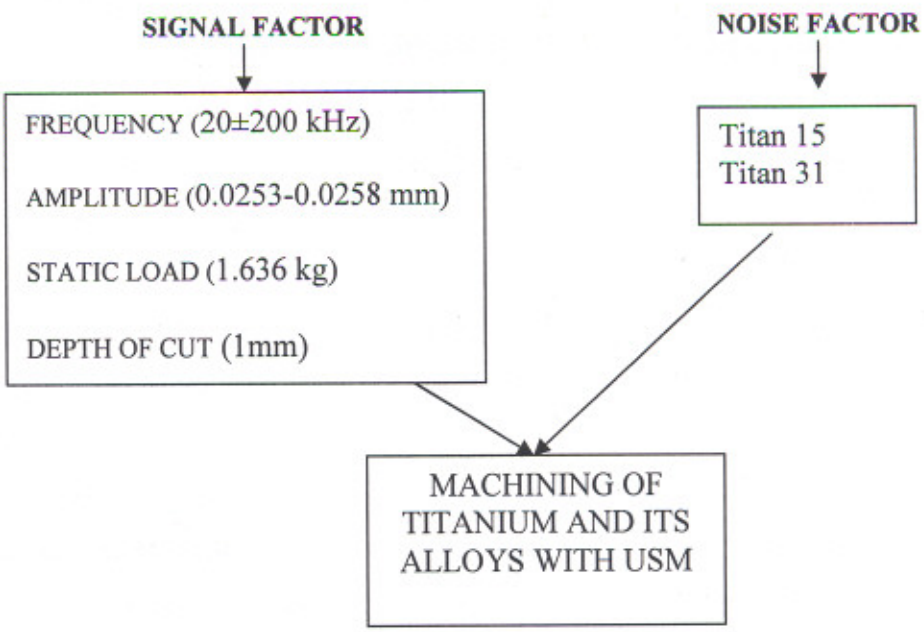

Figure 5.1 Signal and Noise factors for P-diagram

Table 5.1 Macro model

OPTIMIZED MRR CONDITIONS	
Power Rating	90% i.e.450W
Tool	S.S
Slurry	Boron Carbide
OPTIMIZED TWR CONDITIONS	
Tool	S.S
Grit-size	500
Power Rating	90% i.e.450W
OPTIMIZED SR CONDITIONS	
Slurry temperature	27°C
Slurry concentration	25%
Tool	S.S

Large and complex systems, such as the machining characteristics of titanium and its alloys using USM, are often managed by single factor optimization approach. This traditional approach results in to optimization with out considering the factors interactions.

In the present case, success in improving the MRR, TWR and SR of titanium and its alloys using USM suggests that the robust design approach could be used successfully to improve other machining characteristics. This robust design approach involves all experiments conducted on a live system involving multi factor interactions. Running robust design experiments on live systems involves a methodological problem that the noise conditions (which are different work materials in machining characteristics optimization problem) are not the same for every row of matrix experiments. Consequently, the estimated error variance can be large compared to the estimated factor effects. Also, the predicted response under the optimum condition can have large variance. Standardized S/N ratio can be used to reduce the adverse effect of changing noise conditions, which is encountered in running robust design experiments on live system.

5.3 MICRO-MODEL FOR PREDICTING MACHINING CHARACTERISTICS OF TITANIUM AND ITS ALLOYS IN USM

The micro model presented in this section has been based on macro model using robust design technique. The out come of previously developed macro model using Taguchi design highlights:

- MRR in USM is dependent on ultrasonic power, type of tool, and type of slurry.
- TWR in USM is dependent on type of tool, USM power rating followed by slurry grit size.
- SR in USM is dependent on slurry temperature, followed by slurry concentration and type of tool.

Taking these results of macro model as input; an attempt has been made to develop micro model using dimensionless analysis approach (Buckingham's π-theorem). Following assumptions have been made while developing the mathematical micro model for the given situation.

1. Frequency of ultrasonic vibration is fixed through out the experimentation and it is of the order of 20 kHz ± 200 Hz.
2. Amplitude of vibration is constant throughout the experimentation and is of the order of 0.0253-0.0258mm.
3. Feed force is also constant and maintained equal to 1.636 kg throughout the experiment.
4. Parameters resulting insignificant by Taguchi analysis has been omitted for developing a mathematical relationship.

The Buckingham's π-theorem proves that, in a physical problem including "n" quantities in which there are "m" dimensions, the quantities can be arranged in to "n-m" independent dimensionless parameters. In this approach dimensional analysis is used for developing the relations [156-162].

5.3.1 Micro-model for predicting MRR

MRR "Z" depends upon six input parameters namely ultrasonic power, Elastic modulus of tool, slurry hardness factor, slurry temperature, slurry concentration and grit size of slurry.

Now by selecting:

- M (mass);
- L (length);
- T (time); and
- θ (temperature)

Basic dimensions, the dimensions of the foregoing quantities would then be:-

1. The MRR "Z" (gm/min)	$M L^0 T^{-1}$
2. Power rating "P" (Watt)	$M L^2 T^{-3}$
3. Elastic modulus of tool "Y" (G Pa)	$M L^{-1} T^{-2}$
4. Slurry hardness factor "μ_s" (kgf/mm^2) knoop hardness	$M L^{-1} T^{-2}$
5. Temperature "θ" (°C)	θ
6. Slurry concentration "η" (gm/mm^3)	ML^{-3}
7. Grit size "ρ" (mm)	L

Now

$$Z = f(P, Y, \mu_s, \theta, \eta, \rho)$$

In this case n is 7 and m is 4. So, we can have (n-m = 3) π_1, π_2, and π_3 three dimensionless groups.

Taking Z, P and Y as the quantities which directly go in π_1, π_2 and π_3 respectively, we obtain:

$$\pi_1 = Z.\ (\mu_s)^{\alpha 1}.\ (\theta)^{\beta 1}.\ (\eta)^{\gamma 1}.\ (\rho)^{\delta 1}$$

$$\pi_2 = P.\ (\mu_s)^{\alpha 2}.\ (\theta)^{\beta 2}.\ (\eta)^{\gamma 2}.\ (\rho)^{\delta 2}$$

$$\pi_3 = Y.\ (\mu_s)^{\alpha 3}.\ (\theta)^{\beta 3}.\ (\eta)^{\gamma 3}.\ (\rho)^{\delta 3}$$

Substituting the dimensions of each quantity and equating to zero, the ultimate exponent of each basic dimension is achieved, since the "π_is" are dimensionless groups. Thus αi, βi, γi, δi, where i= 1, 2, 3, can be solved.

Solving for π_1, we get

$$\pi_1 = (M\,T^{-1}).\,(M\,L^{-1}T^{-2})^{\alpha 1}.\,(\theta)^{\beta 1}.\,(M\,L^{-3})^{\gamma 1}.\,(L)^{\delta 1}$$

Here,

$1+\alpha_1+\gamma_1=0$

$-\alpha_1-3\gamma_1+\delta_1=0$

$-1-2\alpha_1=0$

$\beta_1=0$

Solving, we get:

$\alpha_1=-1/2$, $\beta_1=0$, $\gamma_1=-1/2$, $\delta_1=-2$

Thus

$$\pi_1 = Z.\,(\mu_s)^{-1/2}.\,(\theta)^0.\,(\eta)^{-1/2}.\,(\rho)^{-2}$$

$$\boldsymbol{\pi_1 = Z/\mu_s^{1/2}.\eta^{1/2}.\rho^2}$$

Similarly we get:

$$\pi_2 = (M\,L^2\,T^{-3}).\,(M\,L^{-1}T^{-2})^{\alpha 2}.\,(\theta)^{\beta 2}.\,(M\,L^{-3})^{\gamma 2}.\,(L)^{\delta 2}$$

Here,

$1+\alpha_2+\gamma_2=0$

$2-\alpha_2-3\gamma_2+\delta_2=0$

$-3-2\alpha_2=0$

$\beta_2=0$

Solving, we get:

$\alpha_2=-3/2$, $\beta_2=0$, $\gamma_2=1/2$, $\delta_2=-2$

Thus

$$\pi_2 = P.\,(\mu_s)^{-3/2}.\,(\theta)^0.\,(\eta)^{1/2}.\,(\rho)^{-2}$$

$$\boldsymbol{\pi_2 = P.\eta^{1/2}/\mu_s^{3/2}.\rho^2}$$

Similarly we get:

$$\pi_3 = (M\,L^{-1}\,T^{-2}).\,(M\,L^{-1}T^{-2})^{\alpha 3}.\,(\theta)^{\beta 3}.\,(M\,L^{-3})^{\gamma 3}.\,(L)^{\delta 3}$$

Here,

$1+ \alpha_3+ \gamma_3= 0$

$-1-\alpha_3 -3\gamma_3+ \delta_3= 0$

$-2-2\alpha_3= 0$

$\beta_3= 0$

Solving, we get:

$\alpha_3= -1, \quad \beta_3= 0, \quad \gamma_3= 0, \quad \delta_3= 0$

Thus

$$\pi_3= Y. (\mu_s)^{-1}$$

$$\boldsymbol{\pi_3= Y/\mu_s}$$

The ultimate relationship can be assumed to be of the form

$$\pi_i = f(\pi_j , \pi_k)$$

Let's assume i =1, j = 2, k =3 Then the functional relationship is of the form

$$\pi_1 = f(\pi_2 , \pi_3)$$

Or

$$Z /\mu_s^{1/2} .\eta^{1/2}.\rho^2 = f(P .\eta^{1/2}/\mu_s^{3/2}.\rho^2, Y/\mu_s)$$

It has been experimentally found that Z directly goes with P [2].

Thus the equation becomes

$$Z /\mu_s^{1/2} .\eta^{1/2}.\rho^2 = P .\eta^{1/2}/\mu_s^{3/2}.\rho^2. f(Y/\mu_s)$$

$$\boldsymbol{Z = C \{P. \eta. Y /\mu_s^2\}}$$

Where "C" is a constant of proportionality.

Calculation for "C" Constant of proportionality:-

By keeping $\eta. Y /\mu_s^2$ fixed, experiments were performed for different values of P, to find out Z.

Case 1 (S.S. tool, Boron carbide slurry 320-grit size)

- For titanium alloy; Titan31 (ASTM Gr.5)

The actual experimental data has been collected and plotted in figure 5.2. The data collected has been further used for finding the best fitting curve. The second degree

polynomial equation is coming out to be best fitted curve with regression analysis coming equals to "1". Thus the equation of MRR for this case is given as:-

$$Z = (-4^{*}\ 10^{-8}\ P^{2} + 3^{*}\ 10^{-5}P + 0.0003)\ \eta.\ Y/\mu_s^{2}$$

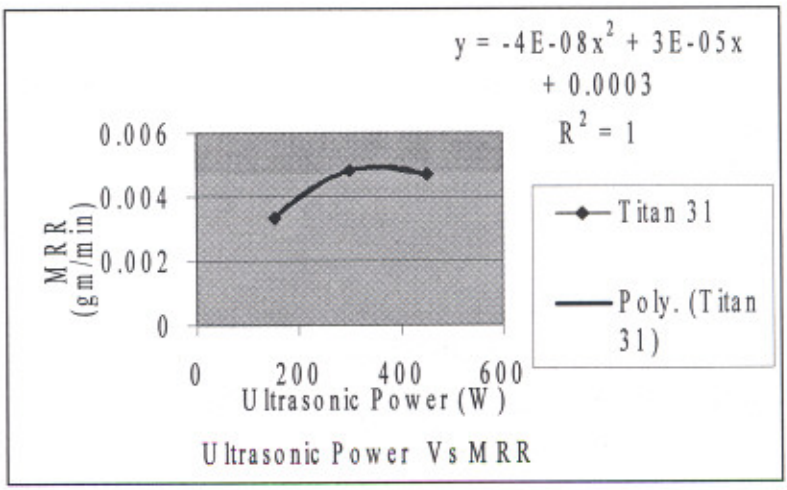

Figure 5.2 Ultrasonic Power Vs MRR for Titan31 using S.S tool

- For commercially pure titanium; Titan15 (ASTM Gr.2)

The variation of Z Vs P is plotted in figure 5.3. The equation with best fitted curve and regression analysis equals to "1" thus obtained in this case is:

$$Z = (9^{*}\ 10^{-8}\ P^{2} - 5^{*}\ 10^{-5}P + 0.0085)\ \eta.\ Y/\mu_s^{2}$$

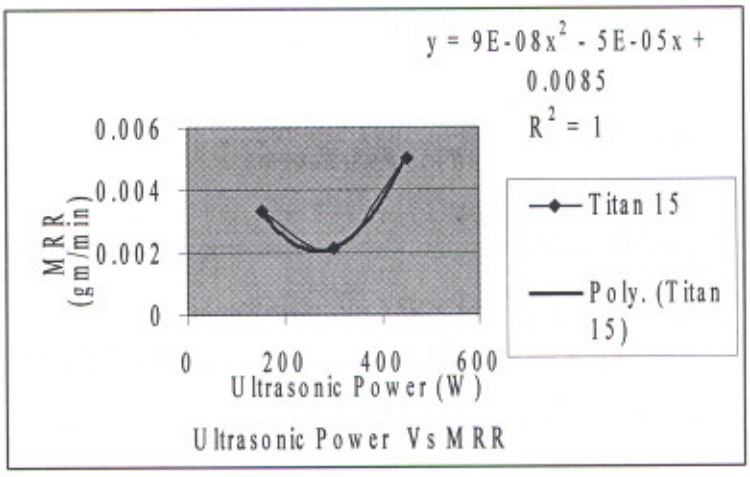

Figure 5.3 Ultrasonic Power Vs MRR for Titan15 using S.S tool

As the results of macro model based upon the concept of robust design, Taguchi analysis highlights that MRR is affected by power rating; elastic modulus of tool and slurry hardness factor and optimized results for the said case comes up with use of S.S tool, boron carbide slurry at 450W of ultrasonic power [2, 27-30]. These two equations sufficiently express the variations of MRR as a function of input parameters selected in specific cases.

However for different tool materials the same methodology can be used.

Case 2 (H.S.S. tool, Boron carbide slurry 320-grit size)

- For titanium alloy; Titan 31 (ASTM Gr.5)

The actual experimental data has been plotted in figure 5.4. So the equation of MRR in this case becomes:

$$Z = (-3* 10^{-8} P^2 + 2* 10^{-5} P - 0.0009)\, \eta .\, Y / \mu_s^2$$

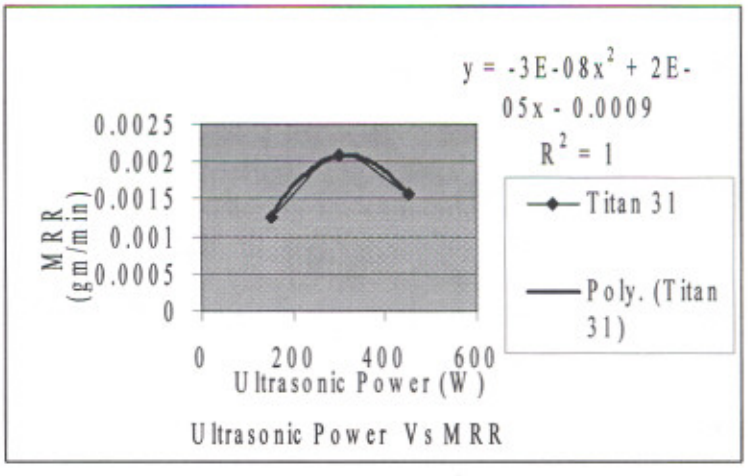

Figure 5.4 Ultrasonic Power Vs MRR for Titan31 using H.S.S tool

- For commercially pure titanium Titan15 (ASTM Gr.2)

The actual experimental data has been plotted in figure 5.5. So the equation of MRR in this case becomes:-

$$Z = (-6* 10^{-8} P^2 + 4* 10^{-5} P - 0.0032)\, \eta .\, Y / \mu_s^2$$

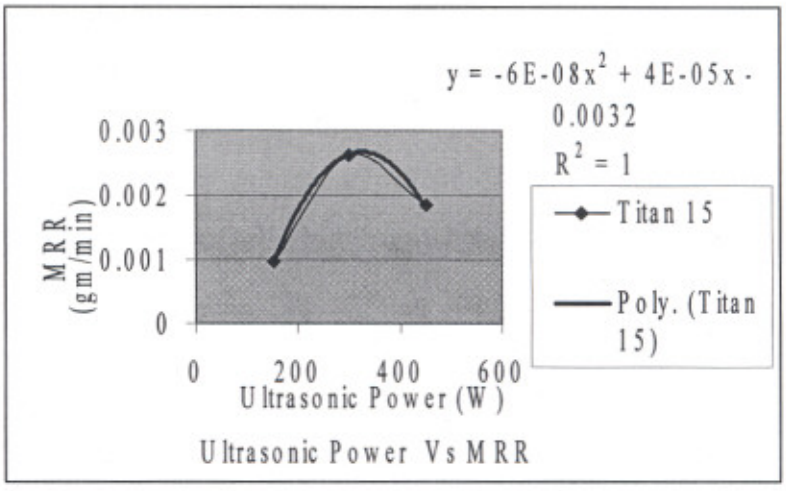

Figure 5.5 Ultrasonic Power Vs MRR for Titan15 using H.S.S tool

The two cases described here express MRR of both Titan15 and Titan31 at a specific power rating; for particular slurry type by varying elastic modulus of tool, i.e. by selecting different tool materials. The same methodology can be further enhanced for developing mathematical model using optimum input parametric settings based upon macro model.

5.3.2 Micro-model for predicting TWR

TWR "υ" depends upon six input parameters namely ultrasonic power, tool hardness factor, slurry hardness factor, slurry temperature, slurry concentration and grit size of slurry.

Now again by selecting:

- M (mass);
- L (length);
- T (time); and
- θ (temperature)

Basic dimensions, the dimensions of the foregoing quantities would then be:-

1. The TWR "υ" (gm/min) $M L^0 T^{-1}$
2. Power rating "P" (Watt) $M L^2 T^{-3}$
3. Tool hardness factor "H" (kgf/mm^2) Vickers hardness $M L^{-1} T^{-2}$

4. Slurry hardness factor "μ_s" (kgf/mm^2) knoop hardness — $M L^{-1} T^{-2}$
5. Temperature "θ" (°C) — θ
6. Slurry concentration "η" (gm/mm^3) — ML^{-3}
7. Grit size "ρ" (mm) — L

$$\text{Now, } \upsilon = f(P, H, \mu_s, \theta, \eta, \rho)$$

As discussed in article 5.3.1 'micro-model for predicting MRR' similar equation has been derived for TWR using Buckingham's π-theorem.

$$\upsilon = C \{P. \eta. H / \mu_s^2\}$$

Where "C" is a constant of proportionality.

Calculation for "C" Constant of proportionality:-

By keeping $\eta. P / \mu_s^2$ fixed, experiments were performed for different values of H, to find out υ.

Case 1 (150W Power rating, Silicon carbide slurry 320-grit size)

- For titanium alloy; Titan15 (ASTM Gr.2)

The actual experimental data for six tools have been collected and plotted in figure 5.6.

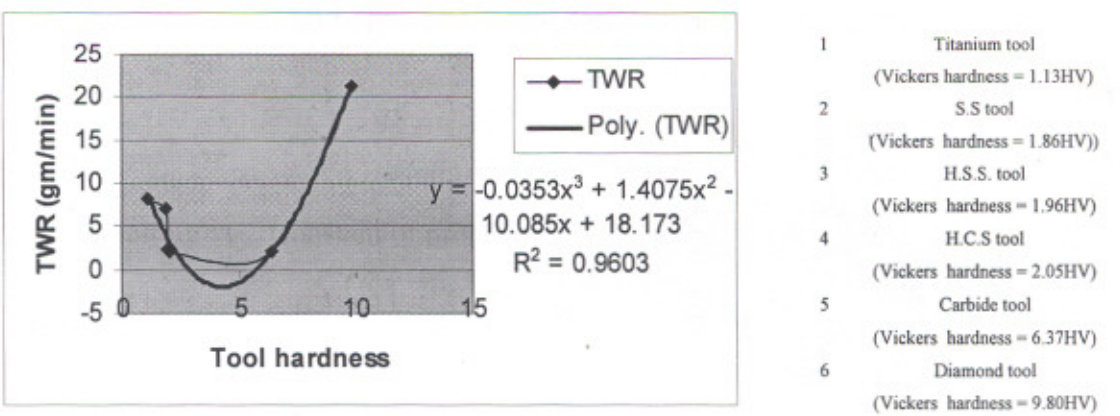

Figure 5.6 TWR Vs tool hardness for Titan15 at 150W

The data collected has been further used for finding the best fitting curve. The third degree polynomial equation comes out to be best fitted curve with regression analysis coming equals to "0.96". Thus the equation of TWR for this case is given as:-

$$\upsilon = (-0.0353H^3 + 1.4075H^2 - 10.085H + 18.173)\, \eta. P / \mu_s^2$$

- For titanium alloy; Titan31 (ASTM Gr.5)

The variation of υ Vs H is plotted in figure 5.7.

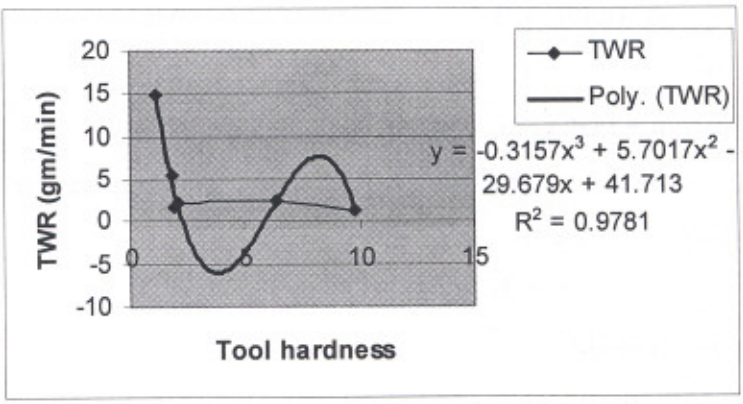

1 Titanium tool (Vickers hardness = 1.13HV)
2 S.S tool (Vickers hardness = 1.86HV))
3 H.S.S. tool (Vickers hardness = 1.96HV)
4 H.C.S tool (Vickers hardness = 2.05HV)
5 Carbide tool (Vickers hardness = 6.37HV)
6 Diamond tool (Vickers hardness = 9.80HV)

Figure 5.7 TWR Vs tool hardness for Titan31 at 150W

The third degree polynomial equation with best fitted curve and regression analysis equals to "0.97" thus obtained in this case is:

$$\upsilon = (-0.3157H^3 + 5.7017H^2 - 29.679H + 41.713)\,\eta.\,P/\mu_s^2$$

Case 2 (150W Power rating, Boron carbide slurry 320-grit size)

- For commercially pure titanium; Titan 15 (ASTM Gr.2)

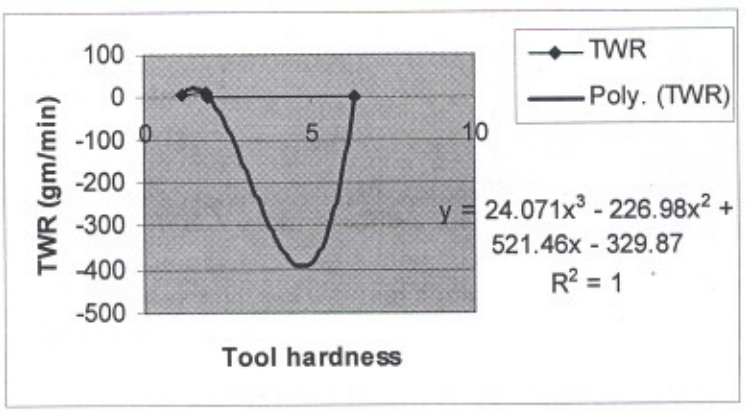

1 Titanium tool (Vickers hardness =1.13HV)
2 S.S tool (Vickers hardness=1.86HV)
3 H.S.S. tool (Vickers hardness=1.96HV)
4 Carbide tool (Vickers hardness =6.37HV)

Figure 5.8 TWR Vs tool hardness for Titan15 at 150W

The actual experimental data for four tool materials have been plotted in figure 5.8. So the equation of TWR in this case becomes:

$$\upsilon = (24.071H^3 - 226.98H^2 + 521.46H - 329.87)\,\eta.\,P/\mu_s^2$$

The third degree polynomial equation comes out to be best fitted curve with regression analysis coming equals to "1" for the given case.

- For titanium alloy; Titan31 (ASTM Gr.5)

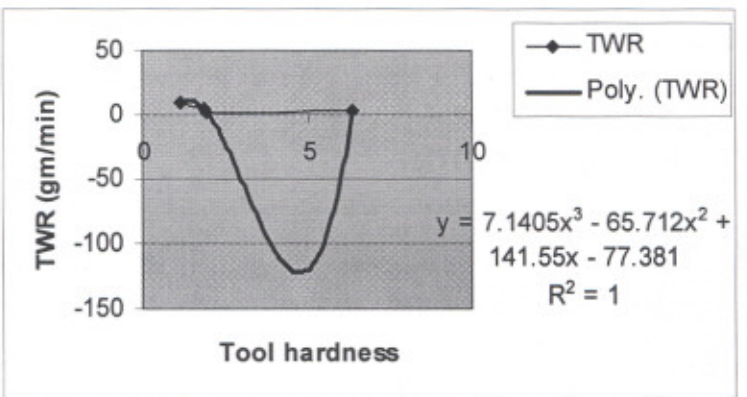

Figure 5.9 TWR Vs tool hardness for Titan31 at 150W

The variation of υ Vs H is plotted in figure 5.9. So the equation of TWR in this case becomes:

$$\upsilon = (7.14H^3 - 65.712H^2 + 141.55H - 77.381)\,\eta.\,P/\mu_s^2$$

Case 3 (150W Power rating, Aluminum oxide slurry 320-grit size)

- For commercially pure titanium; Titan 15 (ASTM Gr.2)

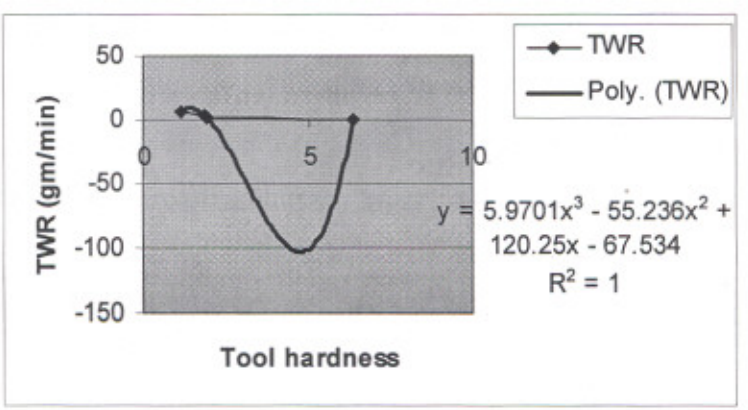

Figure 5.10 TWR Vs tool hardness for Titan15 at 150W

The actual experimental data for four tool materials have been plotted in figure 5.10. The third degree polynomial equation comes out to be best fitted curve with regression

analysis coming equals to "1" for the given case. So the equation of TWR in this case becomes:-

$$\upsilon = (5.97H^3 - 55.236H^2 + 120.25H - 67.534)\ \eta.\ P/\mu_s^2$$

- For titanium alloy; Titan31 (ASTM Gr.5)

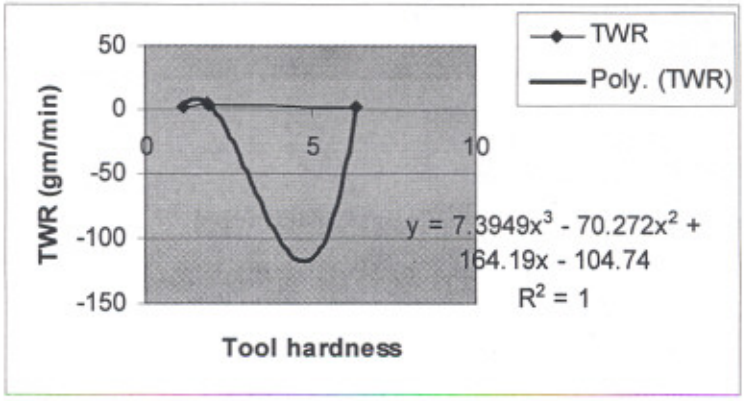

1	Titanium tool (Tool hardness = 1.13HV)
2	S.S tool (Tool hardness = 1.86HV)
3	H.S.S. tool (Tool hardness = 1.96HV)
4	Carbide tool (Tool hardness = 6.37HV)

Figure 5.11 TWR Vs tool hardness for Titan31 at 150W

The variation of υ Vs H is plotted in figure 5.11. So the equation of TWR in this case becomes:-

$$\upsilon = (7.39H^3 - 70.272H^2 + 164.19H - 104.74)\ \eta.\ P/\mu_s^2$$

The three cases described here express TWR of both Titan15 and Titan31 at a specific power rating; for particular slurry type by varying tool hardness factor, i.e. by selecting different tool materials. The third degree polynomial equation of 'H' is expressing the effect of strain hardening of different tool materials. The same methodology can be further enhanced for developing mathematical model using optimum input parametric settings based upon macro model.

CHAPTER 6

CONCLUSIONS AND SCOPE FOR FUTURE WORK

6.1 CONCLUSIONS

Based on the experiments conducted in the present study, the following conclusions have been drawn.

1. Ultrasonic power rating, type of tool and type of slurry significantly affect the MRR in USM. The most significant factor is ultrasonic power rating with contribution of 28%, followed by type of tool with contribution of 24.6%. The third significant factor is type of slurry with contribution of 13.3%. Ultrasonic power rating at 90% that is at 450W, with S.S tool and boron carbide slurry is giving the best MRR, when titanium and its alloys are machined with USM. This is consistent with the conclusions from the study of other investigators. The remaining three input parameters namely slurry concentration, slurry grit size and temperature are in-significant.
2. Type of tool, ultrasonic power rating, and slurry grit-size significantly affect the TWR in USM. The most significant factor is type of tool with contribution of 38.1%, followed by slurry grit-size with contribution of 27.6%. The third significant factor is ultrasonic power rating with contribution of 19.3%. Ultrasonic power rating at 90% i.e. at 450W, with S.S tool and 500grit-size slurry is giving the best TWR, when titanium and its alloys are machined with USM. The remaining three input parameters namely slurry concentration, slurry type and temperature are in-significant.
3. Slurry temperature, slurry concentration and type of tool significantly affect the SR in USM. The most significant factor is slurry temperature with contribution of 33.9%, followed by slurry concentration with contribution of 22.8%. The third significant factor is type of tool with contribution of 17.5%. The slurry temperature at 27°C, with slurry concentration as 25% and S.S tool is giving the best SR, when titanium and its alloys are machined with USM. The remaining

three input parameters namely slurry grit-size, slurry type and ultrasonic power rating are in-significant.

4. It is possible to ultrasonically drill holes in titanium without causing excessive surface damage that is, cracking. The relative toughness of the tool and work piece material plays an important role in MRR and TWR of ultrasonic machining.
5. The selection of the tool material is one of the critical factors for optimizing MRR, TWR and SR. Initial weight of the tool is another critical factor. Tool weight more than 50mg results in auto-cut of the machine for the present set-up. Improper silver-brazing of the tool and its excessive length leads to fatigue failure.
6. While comparing the photomicrographs of conventionally ground surface, and ultrasonically machined surface of titanium, it was observed that the microstructure deformation of work piece was negligible in the later case. Material removal process in ultrasonic machining is the individual or combined effect of; material abrasion by direct hammering, micro chipping by impact of abrasive particles, and cavitation effect of abrasive slurry. Overall mechanism of material removal involves shear or fracture (after work hardening) and plastic deformation (before work hardening), which occurs simultaneously at the transient surface.

6.2 LIMITATIONS

1. The results are valid within the specified range of the process parameters. In the present work, 500W piezoelectric transducer based USM apparatus was used. The depth of cut was limited as excessive length of the tool was adding to tool weight, and tool weight more than 50mg was resulting in auto-cut for machine. Hence results are limited in present form to machine comparatively small sized work pieces.
2. The use of solid tool leads to the problem of flushing of slurry particles from the machined surface after a certain depth of cut. Because of this reason, the depth of cut was limited to 1.0 mm in the present work. Also the fabrication of hollow tool was a constraint especially for diamond tool.
3. Maintaining slurry temperature below 10°C at tool-work interface was a problem in the present set up. Experimentation below slurry temperature of 10°C was not done.

6.3 SCOPE OF FUTURE WORK

1. In the present work, only six process parameters viz. work piece, tool, slurry concentration, ultrasonic power rating, slurry grit size and slurry temperature were investigated. Study of other process parameters like frequency of vibration, static load, flow rate of slurry, depth of cut and type of horns can be done.
2. The further study can be focused on magnetized flow of abrasive slurry while machining with USM on titanium and its alloys. The magnetic field direction can be so adjusted to check effect of magnetic field on surface quality of work piece, in the same direction or counter direction of slurry flow.
3. Although effect of ultrasonic power rating has been established in this study in terms of machinability, it can be further investigated with different combinations of process parameters on high power machines.

4. The same study can be implemented on other tough/soft materials like aluminum, copper etc for their commercial application in manufacturing industry.

REFERENCES

1 Benedict Gary F. (1987), "Non traditional manufacturing processes", Marcel Dekker, Inc., ISBN 0-8247-7352-7, pp 67-86.

2 Gilmore R. (1990), "Ultrasonic machining of ceramics", SME Paper, MS90-346, pp12.

3 Rozenberg L. D. and Kazantsev V. F. (1964), "Ultrasonic cutting", Consultants Bureau, New York.

4 Kohls, J. B. (1984), "Ultrasonic-manufacturing process: Ultrasonic machining (USM) and ultrasonic impact grinding (US1G)", *The Carbide and Tool J.*, Vol.16, No.5, pp 12-15.

5 Haslehurst M. (1981), "Manufacturing technology (3rd Edn.)", Arnold Australia, ISBN: 0340405910, pp 270-271.

6 Soundararajan, V. and Radhakrishnan, V. (1986), "An experimental investigation on the basic mechanisms involved in ultrasonic machining", *Int. J. MTDR*, Vol.26, No.3, pp 307-321.

7 Satyanarayana, A. and Krishna Reddy, B. G. (1984), "Design of velocity transformers for ultrasonic machining", *Electrical India*, Vol.24, No.14, pp 11-20.

8 Drozda T. J. and Wick C. (1983), "Tool and manufacturing engineers handbook (Desk Ed.)", Soc. Manuf Engrs, Dearborn, MI, ISBN No. 0872633519, pp. 1-23.

9 Thoe T.B., Aspinwall D.K. and Wise M.L.H. (1998), "Review on Ultrasonic Machining", *International Journal of Machine Tools Manufacture*, Vol.38, No.4, pp. 239-255.

10 Scab, K. H. W. (1990), "Parametric studies of ultrasonic machining", SME Tech. paper, MR90-294, pp 11.

11 Neppiras, E. A. (1972), "Macrosonics in industry", *Ultrasonics*, Vol.10, pp 9-13.

12 Farago, F. T. (1980), "Abrasive methods engineering", Industrial Press, Vol.2, pp 480-481.

13 Balamuth, L. (1964), "Ultrasonic vibrations assist cutting tools", *Metalworking Prod*, Vol.108, No.24, pp 75-77.

14 Perkins J. (1972), "An outline of power ultrasonics", Technical report on ultrasonics, pp7.

15 Kennedy D. C. and Grieve, R. J. (1975), "Ultrasonic machining - A review". *The Prod. Engineer*, Vol.54, No.9, pp 481-486.

16 Kremer D. (1991), "New developments on ultrasonic machining", SME Technical Paper, MR91-522, pp 13.

17 Clifton D., Imal Y. and McGeough J. A. (1993), "Some ultrasonic effects on machining materials encountered in the offshore industries", Proc. 30th Int. MATADOR Conf., pp. 119-123.

18 Shaw M. C. (1956), "Ultrasonic grinding", Microtechnic, Vol.10, No.6, pp 257-265.

19 Moreland M. A. (1991), "ASM International, Engineering Material Handbook", ISBN 0871702827, Vol.4, pp. 359-362.

20 Guzzo P. L., Shinohara A. H. and Raslan A. A. (2004), "A comparative study on ultrasonic machining of hard and brittle materials", *Journal of Brazil Soc. Mech. Sci. & Eng.,* Vol.26, No.1 Rio de Janeiro, pp56-61.

21 Komaraiah M., Manan M. A., Narasimha Reddy, P. and Victor S. (1988), "Investigation of surface roughness and accuracy in ultrasonic machining", *Precision Engg*, Vol.10, No.2, pp 59-65.

22 Seah K. H. W., Wong Y. S. and Lee L. C. (1993), "Design of tool holders for ultrasonic machining using FEM", *J. Materials Processing Technology,* Vol.37, No.1-4, pp 801-816.

23 Neppiras E. A. (1964), "Ultrasonic machining and forming", *Ultrasonics*, Vol.2, pp167-173.

24 Isaev A. I. (1962), "Learning with ultrasonically vibrated reamers", *Machines and Tooling*, Vol.33, No.6, pp27-30.

25 Singh Rupinder (2002), "Ultrasonic machining for tough materials and its application in mechanical industry", Proceedings of fourth national symposium of research scholars on metal and materials at IIT Madras (INDIA), pp31.

26 RTI International metals (2002), "Titanium alloy guide", Ohio, U.S.A.

27 Verma D. R. S. V., NandaGopal B.G., Srinivasulu K. and Reddy S. Sudhakar (2003), "Effect of pre- drilled holes on tool life in turning of aerospace titanium alloys", Proceedings of national conference on advances in manufacturing system (AMS-03), Prod. Engg. Dept. Jadavpur University, Kolkata (India), pp 42-47.

28 Dornfeld D.A, Kim J. S., Dechow H., Hewsow J. and Chen L.J. (1999), "Drilling burr formation in titanium alloy Ti-6Al-4V", *Annals of CIRP,* Vol. 48/1 pp 73-76.

29 SME (1985), "Tool and Manufacturing Engineers hand- book", Vol.3.

30 Mantle A.L and Aspinwall D.K. (1995), "Single point turning of titanium aluminide intermetallic", Proceedings of the eight world conference on Titanium, Vol.1, pp 248-255.

31 Ezugwa. E.O. and Wang. Z. M. (1997), "Titanium alloys and their machinability - A review", *Journal of Material processing technology,* Vol. 68, pp 262-274.

32 Khamba J.S and Singh Rupinder (2003), "Effect of Alumina (White fused) Slurry in Ultrasonic Assisted Drilling of Titanium Alloys (TITAN 15)", Proceedings of national conference on materials and related technologies (NCMRT-2003), TIET, Patiala, India, pp 75-79.

33 Singh Rupinder and Khamba J.S. (2003), "A Frame-work for modeling the machining characteristics of titanium alloys using USM", Proceedings of international conference on digital aided modeling and simulation, CIT, Coimbatore, INDIA, pp.31.

34 Cherng Lin Yan, Bing Yan, Chang Hwa, Song Yong (2000), "Machining characteristics of titanium alloys (Ti-6Al-4V) using a combination process of EDM and USM", *Journal of Material Processing technology,* Vol.104, No.3, pp 171-177.

35 Singh Rupinder, Khamba J.S. and Grewal J.S (2005), "Machining Characteristics optimization using Taguchi Technique Ultrasonic Drilling of Titanium Alloys", Proceedings of international conf. on emerging technologies in intelligent system and control (EISCO-2005), Kumaraguru College of Technology, Coimbatore, India, Jan.5-7, 2005, pp.81-87.

36 Singh Rupinder and Khamba J.S. (2004), "Study of Machining characteristics of Titanium Alloys in Ultrasonic Machining", Proceedings of the 21st AIMTDR conference, Vellore Institute of Tech. (Tamilnadu) India, Dec 20-22, 2004, pp 155-160.

37 Singh Rupinder and Khamba J.S. (2004), "Machining Characteristics comparison of Titanium Alloys in Ultrasonic Assisted Drilling", Proceedings of international conf. on recent advances in composite materials (ICRACM2004), Institute of Technology, B.H.U, India, Dec. 17-19, 2004, pp.438-442.

38 Nishimura G. (1954), "Ultrasonic machining - Part I". *J. Fac. Engg.* Tokyo Univ., Vol.24, No.3, pp 65-100.

39 Neppiras E. A.(1956) , "Report on ultrasonic machining", Metalworking Prod., 100, pp 1283-1288, 1333-1336, 1377-1382, 1420-1424, 1464-1468, 1554-1560, 1599-1604.

40 Weller E. J. (1984), "Non-traditional machining processes (2nd Edn.)", Soc. of Manuf. Engineers, pp. 15-71.

41 Fairer J. O. (1948), English Patent No. 602801 from 3.6.1948 - USM.

42 Singh Rupinder and Khamba J.S. (2003), "Silver brazing for tool preparation in USM process", Proceedings of national workshop of welding technology in India-Present status and future trends, S.L.I.E.T. Longowal (Pb.) India, pp 61-63.

43 Singh Rupinder and Khamba J.S. (2004), "Tool Manufacturing Technique in Ultrasonic Drilling Machine", *Journal of Manufacturing Technology Today*, Vol-3, Issue-1, pp. 05-07.

44 Technical Staff' of the Machinability Data (1980), "Centre Machining data handbook (3rd Edn.)", Cincinnati Metcut Research Associates Inc., Vol.2, pp 43-63.

45 Halm R. and Schulz P. (1993), "Ultrasonic machining of complex ceramic components", Erosion AC Report, DKG 70. No. 7, pp 6.

46 Graff K. F. (1975), "Macrosonics in industry: ultrasonic machining", *Ultrasonics*, Vol.13, pp103-109.

47 Moreland M. A. (1988), "Ultrasonic advantages revealed in the hole story", *Cer. Appl. Manuf.*, Vol. 187, pp 156-162.

48 Rutan H.L. (1984), "Ultrasonic machining (Impact grinding)", Proceedings of topical meetings on optical fabrication and test, U.S. Department of Energy.

49 Technical Staff' of the Machinability Data center (1984), "Machining briefs", Metcut research Assoc., Inc., Cincinnati, Ohio, Issue No.3.

50 Gilmore R. (1989), "Ultrasonic machining and orbital abrasion techniques", SME Technical Paper (Series) AIR, NM89-419, pp. 1-20.

51 Moore D. (1985), "Ultrasonic impact grinding", Proc. Non-traditional Machining Conf, Cincinnati, pp. 137-139.

52 Black P. (1985), "An ultrasonic impact grinding technique for electrode-forming and redressing", Proc. Non-traditional Machining Conf., Cincinnati, Ohio, ASM, pp. 129-136.

53 Kremer D., Bazine G. and Moison A. (1983), "Ultrasonic machining improves EDM. technology, Electro machining", Proc. 7th Int. Symp., Birmingham, UK, pp. 67-76.

54 Ghabrial S. R. (1986), "Trends towards improving surfaces produced by modem processes", Proc. of 3rd Int. Conf. on Metrol, pp. 113-118.

55 Robare M.W. and Richerson D.W. (1977), "Review at Rotor blade machining development", Proceedings of ARPA/NAVSEA-Garrett/Ai Research Ceramic Gas Turbine Engine Demonstration Program, Marine Maritime Academy.

56 Richerson D. W. and Robare M.W. (1978), "Turbine component machining development", Proceedings of conference on ceramic machining and surface finishing II, Naval Research Lab., Gaithersburg, Md.

57 SONIC-MILL 500W model (2002), "Instruction manual for stationary ultrasonic machining", U.S.A.

58 Singh Rupinder and Khamba J.S. (2004), "Comparison of Machining characteristics of Titanium Alloys: Effect of Slurry in Ultrasonic Machining Process", Proceedings of global congress on manufacturing and management, The

international conference on manufacturing and management (GCMM-2004),Vellore Institute of Tech. (Tamilnadu) India, Dec.8-10, 2004, pp 54-58.

59 Legge P. (1966), "Machining without abrasive slurry" *Ultrasonics*, Vol.4, pp 157-162.

60 Rozenberg L. D. (1973), "Physical principles of ultrasonic technology", Vol.1-2, Plenum Press, N.Y.

61 Frederick J. R. (1965), "Ultrasonic engineering", John Wiley and Sons Inc., New York, ISBN 0471277258.

62 Jay F. (1984), "IEEE standard dictionary of electrical and electronics terms, 3rd edition", pp. 405 and 519.

63 Balamuth L. A. (1966), "Ultrasonic assistance to conventional metal removal" *Ultrasonics*, Vol.4, pp125-130.

64 Gilmore R. (1989), "Ultrasonic machining", SME Technical Paper, EM89-123, pp l0.

65 Kaczmarek I. (1976), "Principles of machining by cutting, abrasion and erosion", Peter Peregrinus Ltd., Stevenage, ISBN 0901223662, pp. 448-462.

66 Kremer D. (1981), "The state of the art of ultrasonic machining", *Annals of the CIRP,* Vol.30, No.1, pp 107-110.

67 Singh Rupinder and Khamba J.S. (2006), "Ultrasonic machining of titanium and its alloys: A review", *Journal of material processing technology*, Vol. 173, No.2, pp 125-135.

68 Neppiras E. A. and Foskett R. D. (1957), "Ultrasonic machining - II. Operating conditions and performance of ultrasonic drills", Philips Tech. Rev., Vol.18, No.12, pp 368-379.

69 US400 (1994), "Ultrasonic machining system", Brochure from Erosonic AG.

70 Rumyantsev E. and Davydev A. (1989), "A electrochemical machining of metals", MIR publishers, Moscow.

71 Thoe T. B., Aspinwall D. K. and Wise M. L. H., (1995), "The effect of operating parameters on ultrasonic contour machining", Proc. of Twelfth Annual

Conference of the Irish Manufacturing Committee (IMC-12), Cork, Ireland, September 1995, pp. 305-312.

72 Prabhakar D. and Haselkorn M. (1992), "An experimental investigation of material removal rates in rotary ultrasonic machining", *Trans. of NAMRI/SME*, Vol.20, pp 211-218.

73 Wojchiechowski M. P. (1972), "Ultrasonic machining: Past, present and future", SME Paper, MR72-188, pp 12.

74 Adithan M. (1974), "Tool wear studies in ultrasonic drilling", *Wear*, Vol.29, pp 81-93.

75 Kumehara H. (1984), "Characteristics of threaded joints in ultrasonic vibrating system", *Bull of JSME*, Vol.27, No.223, pp117-123.

76 Adithan M. (1976), "Production accuracy of holes in ultrasonic drilling", *Wear*, Vol.40, No.3, pp 309-318.

77 Kazantsev V. F. (1966), "Improving the output and accuracy of ultrasonic machining", *Machines and Tooling*, Vol. 37, No.4, pp 33-39.

78 Pentland E. W. and Ektermanis J. A. (1965), "Improving ultrasonic machining rates - some feasibility studies", *J. Engineering for Ind., Trans. of the ASME,* 87(Series B), pp 39-46.

79 Miller G. E. (1957), "Special theory of ultrasonic machining", *J. Appl. Phy*, Vol.28, No.2, pp 149-156.

80 Cook N. H. (1966), "Manufacturing analysis", Addison-Wesley, New York, pp. 133-138.

81 Kainth G. S., Nandy Amitav and Singh Kuldeep (1979), "On the mechanics of material removal in ultrasonic machining" *Int. J. MTDR,* Pergamon Press, Vol. 19, pp 33-41.

82 Neppiras E. A. and Foskett R. D. (1957), "Ultrasonic machining - I. Technique and equipment." Philips Tech. Rev., Vol.18, No.11, pp 325-334.

83 Khairy A. B. E. (1990), "Assessment of some dynamic parameters for the ultrasonic machining process", *Wear*, Vol.137, pp 187-198.

84 Ghabriel S. R., Saleh S. M., Kohail A. and Moisan A. (1982), "Problems associated with electro-discharge machined, electro-chemically machined and ultrasonically machined surfaces", *Wear*, Vol. 83, pp 275—283.

85 Bhattacharya A. (1973), "New Technology", The institution of engineers (I), Calcutta.

86 Saha J., Bhattacharya A. and Mishra P.K. (1988), "Estimation of material removal in USM process- A theoretical and experimental study", Proceedings of 27th International matador conference, Manchester, England.

87 Zhao Jr., Wang Li-Jiang and Li Hua (1991), "A new side clamped ultrasonic vibration in cutting system with two stage amplification", *International Journal of Machine tool manufacture*, Vol.31, No.3, pp 249-256.

88 Riddie V and Roch G. (1975), "Cavitation erosion, A survey of literature 1942-70", *Wear*, pp 133-136.

89 Bulat T.J. (1974), "Micro-Sonics in Industry, Ultrasonic cleaning", Bendix and life supports division publication 120.10.153, USA.

90 Willard G.W. (1953), "Ultrasonically induced cavitation", *Journal of accousticate society of America*, pp 669.

91 Goetze D. (1956), "Effect of vibration amplitude, frequency and composition of the abrasive slurry on the rate of ultrasonic machining in Ketos tool steel", *The J. Acoust. Soc. of Am.*, Vol. 28, No.6, pp 1033-1037.

92 Markov A.I (1977), "Ultrasonic drilling and milling of hard non-metallic materials with diamond tools", *Mach. Tooling*, Vol.48, No.9, pp45-47.

93 McGeough J.A (1988), "Advanced methods of machining", Chapman and Hall, London, ISBN 0412319705, pp. 170-198.

94 Koops L. (1964), "Investigation into the influence of the wear of the abrasive powder on the technological indices of ultrasonic machining", *CIRP Annals*, Vol.13, No.3, pp 151-157.

95 Smith T. L. (1971), "Parameter influence in ultrasonic machining", B.Sc. (Hon) Diss., The Nottingham Trent University.

96 Ghabrial S. R., Saleh S. M., Moisan A. and Kremer D. (1984), "Some aids towards improving performance in U.S.M.", Proc. of 12th NAMRC Conf., SME Manuf Engg. Trans., 1984, pp. 227-232.

97 Kremer D. and Mackie J (1988), "Ultrasonic machining applied to ceramic materials", *Industrial Ceramics*, No.830, pp 632-637.

98 Zhang Q.H and Zhixin Jia (1999), "Material removal rate analysis in the ultrasonic machining of engineering ceramics", *Journal of material processing technology*, Vol.88, pp.180-184.

99 Rajurkar K.P and Wang Z. Y. (1999), "Micro removal of ceramic material (Al_2O_3) in the precision ultrasonic machining", *Precision Engineering*, Vol.23, No.2, pp 73-78.

100 Kennedy W.J. Jr. and Skaar Eric C. (1989), "Improving the machining of ceramics", Technical paper- Society of manufacturing engineers, Orlando, USA.

101 Spur G., Brueker Th., and Holl S.E (1997), "Ultrasonic machining of ceramics", *Industrial Ceramics*, Vol. 17, No.1, pp 29-34.

102 Haun R. and Schulze P. (1994), "New ultrasonic machining route to create complex ceramic components", Proceedings of IEEE ultrasonic symposium, NJ, USA, Vol. 3, pp. 1389-1392.

103 Hocheng H., Tai N.H. and Liu C.S. (2000), "Assessment of ultrasonic drilling of C/SiC composite material, Composites-Part A", *Applied Science and Manufacturing*, Vol. 31, No.2, pp 133-142.

104 Thoe T.B., Masuzawa T. and Fujino M. (1999), "Combined ultrasonic and electric discharge machining of ceramic coated nickel alloy", *Journal of material processing technology*, Vol.92-93, pp 323-328.

105 Guzzo Pedro L., Raslan Alberto A., De Mello and Jose Daniel B. (1999), "Relationship between quartz crystal orientation and the surface quality obtained by the ultrasonic machining", Proceedings of annual IEEE international frequency control symposium, Vol.2, pp. 792-795.

106 Kai Egashira and Takahira Masuzawa (1999), "Micro ultrasonic machining (MUSM) by application of work-piece vibration", *CIRP annals manufacturing technology*, Vol.48, No.1, pp.131-134.

107 Zhixin Jia, Zhang and Xing Ai (1995), "Combined machining of USM and EDM for advanced ceramics", *Journal of advanced materials*, Vol. 26, No.3, pp16-20.

108 Zhixin Jia, Zhang and Xing Ai (1997), "Study on a new kind of machining technology of USM and EDM", *International journal of machine tool and manufacture*, Vol.37, No. 2, pp193-199.

109 Sun Xi Qing (1996), "Micro ultrasonic machining and its application in MEMS, sensors and actuators", Vol.57, No.2, pp159-164.

110 Pei Z.J., Khanna N. and Ferreia P.M (1995), "Rotary ultrasonic machining of structural ceramics a review", Proc. of Ceramic engineering and science, Vol.16, No.1, KY, USA, pp.259-278.

111 Deng Jianxin and Lee Taichin (2000), "Surface integrity in electro-discharge machining, ultrasonic machining and diamond saw cutting of ceramic composites", *Ceramic International*, Vol. 26, No.8, pp 825-830.

112 Ya G., Qin H.W, Xu Y.W. and Zhang Y.S (2001), "An experimental investigation on rotary ultrasonic machining", *Key engineering materials*, Vol.202-203, pp277-280.

113 Diepoled T. and Obermeier E. (1996), "Smoothing of ultrasonically drilled holes in borosilicate glass by wet chemical etching", *Journal of micro mechanics and micro engineering*, Vol.6, No.1, pp 29-32.

114 Anatha Ramu, Krishnamurthy R. and Gokularathnam C.V (1989), "Machining performance of toughened ceramic and cold compact alumina in ultrasonic drilling", *Journal of mechanical working technology*, Vol. 20, pp 365-375.

115 Abu Zahra, Nidal H. and Nayfeh Taysir H. (1997), "Calibrated methods for ultrasonic on line monitoring of gradual wear during turning operation", *International journal of machine tool and manufacture*, Vol.37, No.10, pp 1475-1484.

116 Xu W.L. and Han L. (1999), "Piezoelectric actuator based active error compensation of precision machining", *Measurement science and technology*, Vol. 10, No.2, pp. 106-111.

117 Dam Henrik, Quist Schreiber and Mads Peter (1995), "Productivity, surface quality and tolerances in ultrasonic machining of ceramics", *Journal of material processing technology*, Vol.51, No.1-4, pp 825-830.

118 Wang Z. Y. and Rajurkar K.P. (1995), "Dynamic analysis of USM process", Proceedings of the ASME international mechanical engineering congress and exposition, San Francisco, USA.

119 Wang Hsueh-Ming S., Plebani Louis J. and Sathyanarayanan G. (1998), "Modelling considerations for ultrasonic machining", *Abrasive,* pp8.

120 Markov A.I. (1959), "Kinematics of the dimensional ultrasonic machining method. Machines and Tooling", Vol. 30, No.10, pp 28-31.

121 Kubota M., Tamura Y. and Shimamura, N. (1977), "Ultrasonic machining with a diamond impregnated tool", *Bull. Japan. Soc. of Free. Engg*, Vol.11 No.3, pp 127-132.

122 Kazantsev V. F. (1963), "The relationship between output and machining conditions in ultrasonic machining", *Machines and Tooling*, Vol.34, pp 14-17.

123 Pandey P. C. and Shan, H. S. (1980), "Modern machining processes", Tata McGraw-Hill, pp. 7-38.

124 Adithan M. (1981), "Tool wear characteristics in ultrasonic drilling", *Tribology Int.*, Vol.14, No.6, pp 351-356.

125Markov A. I. (1966), Ultrasonic machining of intractable materials Iliffe Books Ltd., London.

126 Smith T. L. (1973), "Parameter influence in ultrasonic machining", *Ultrasonics*, Vol.11, No.5, pp 196-198.

127 Technical report (1964), "Ultrasonic machining of glass" N. P.L., Machinery, pp. 1172-1176.

128Adithan M. (1983), "Abrasive wear in ultrasonic drilling", *Tribology International,* Vol.16, No.5, pp 253-255.

129Adithan M. and Venkatesh V. C. (1974), "Parameter influence on tool wear in ultrasonic drilling", *Tribology International.*, Vol.7, No.6, pp 260-264.

130 Venkatesh V. C. (1983), "Machining of glass by impact processes", *J. Mech. Working Technology*, Vol. 8, pp 247-260.

131 Iwanek H., Grathwohl G., Hamminger, R. and Brugger N. (1986), "Machining of ceramics by different methods", Proc. 2nd Int. Symp. on Cer. Mat'Is and Components for Engines, pp. 417-423.

132 Komaraiah M and Narasimha Reddy P. (1993), "A study on the influence of work piece properties in ultrasonic machining", *Int. J. Mach. Tools Manuf,* Vol.33, No.3, pp 495-505.

133 Koval'chenko M. S., Paustovskii A. V. and Perevyazko V. A. (1986), "Influence of properties of abrasive materials on the effectiveness of ultrasonic machining of ceramics", Sov. Powder Metallurgy and Metal Cer, Vol.25, No.7, pp 560-562.

134 Dam H. (1993), "Surface characterization of ultrasonic machined ceramics with diamond impregnated sonotrode", Proc. the international conference on machining of advanced materials, Gaithersburg, Maryland, pp. 125-133.

135 Amin S. G., Ahmed M. H. M. and Youssef H. A. (1993), "Optimum design charts of acoustic horns for ultrasonic machining", Proc. of Int. Conf on AMPT'93, pp 139-147.

136 Amin S. G., Ahmed M. H. M. and Youssef H. A. (1993), "Computer aided design of acoustic horns for ultrasonic machining using finite element analysis", Proc. AMPT93 Conf., Vol.2, pp 1455-1465.

137Jain V.K (2002), "Advanced machining process", Allied Publisher Pvt. Limited, India, pp. 28-56.

138Ultrasonic assembly of thermoplastic mouldings and semi-finished product - Recommendations on methods, construction and applications. Manual written by German Electrical Manufacturers Association ZVEI, Germany.

139Merkulov L. G. (1957), "Design of ultrasonic concentrations", *Akusticheskiy Zhurnal*, Vol.3, pp 246-255.

140Adithan M. and Venkatesh V. C. (1975), "Study of the performance characteristics of an ultrasonic drilling head", *Wear*, Vol. 33, pp 261-270.

141 Hahn R. (1993), "Ultrasonic machining of glass and ceramics", *Am. Cer. Soc. Bull.*, Vol.72, No.8, pp 103-106.

142Sharma Anurag; Mishiro Shoji; Suzuki Kiyoshi; Imai Tomoyasu; Uematsu Tetsutaro; and Iwai Manabu (2003), "A new longitudinal mode ultrasonic transducer with an eccentric horn for micro machining", *Key Engineering Materials*, , Vol. 238-239, pp 147-152.

143 Bellows G. and Kohls J.B. (1982), "Drilling without drills", Am. Machinist, Special Rep. No. 743, Mar, 1982, pp187.

144 Babitsky V.I.; Mitrofanov A.V. and Silberschmidt, V.V. (2004), "Ultrasonically assisted turning of aviation materials: Simulations and experimental study", *Ultrasonic*, Vol. 42, No. 1-9, pp 81-86.

145Murakawa Masao and Jin Masahiko (1998), "Turning of beta-titanium alloys by means of ultrasonic vibration", Proceedings of the 1998 XXXVI NAMRC conference, Atlanta, USA.

146 Mishra P.K. (2005), "Non conventional machining", Narosa publishing house, New Delhi, ISBN 81-7319-192-1, pp 22-44.

147Laroyia S.C.; Adithan M. and Dell K. Allen (1993), "Tool wear in machining of advanced ceramics", Proceedings of International symposium on Tribology, Tsingua University, Beijing, China, Oct. 18-23, 1993, pp 1100-1109 (International academic publishers, Beijing, China).

148 Laroyia S.C. and Adithan M. (1992), "Machining of advanced ceramics", Proceedings of Sunderland advanced manufacturing technology international conference 92 (SAMT-92), Sunderland, U.K., April 27-30, 1992, pp 13.4.1-13.4.14.

149 Bagchi T.P. (1993), "Taguchi methods explained: Practical steps to robust design", Prentice-Hall of India private limited, ISBN-0-87692-808-4.

150 Roy R. K. (1990), "A primer on the Taguchi method", Van Nostrand Reinhold, New York, ISBN-0-442-23729-4.

151 Rose Phillip J. (1988), "Taguchi techniques for quality engineering", McGraw-Hill Book Company, ISBN-0-07-053866-2.

152Phadke Madhav S.(1989), "Quality engineering using robust design", AT & T Bell laboratories, P T R Prentice-Hall, Inc., NJ, U.S.A., pp 231-249.

153 Phadke M.S. (1982), "Quality engineering using design of experiments", Proceedings of the American statistical association, Section on statistical education, Aug.1982, Cincinnati, OH, pp 11-20.

154 Phadke M.S. (1986), "Design optimization case study", AT& T technical journal, Mar-Apr.1986, Vol.65, No.2, pp 51-68.

155 Singh Sehijpal, Shan H.S. and Kumar Pradeep (2002), "Parametric optimization of magnetic-field-assisted abrasive flow machining by the Taguchi method", *Journal of Quality and reliability engineering international,* Vol. 18, pp 273-283.

156 Garde R.J. and Mirajgaoker A.G. (1988), "Engineering fluid mechanics", New Chand & Bros. publishers, Roorkee (India), ISBN: 81-85240-11-6, pp 235-236.

157 Bansal R.K. (1998), "A text book of fluid mechanics and hydraulic machines", Laxmi publications (P) ltd., New Delhi, 1998, ISBN: 81-7008, pp 595-600.

158Kumar D.S. (1987), "Fluid mechanics and fluid power engineering", B.D. Kataria & Sons, India, 1987, pp 323-326.

159Modi P.N. and Seth S.M. (1998), "Hydraulics and fluid mechanics", Standard book house, New Delhi, 1998, ISBN: 81-900893-7-4, pp 830-833.

160Streeter V.L. and Wylie E. Benjamin (1983), "Fluid Mechanics", International student edition, McGraw-Hill International book company, Japan, pp 160-169.

161 Buckingham E. (1915), "Model experiments and the form of empirical equations", *Trans. ASME,* Vol.37, pp 263-296.

162Ghosh Amitabha and Mallik A. K. (1996), "Manufacturing Science", East-West Press private limited, India, pp 335-353, 409-411.

APPENDIX I

Introduction to Titanium

1. Titanium and its characteristics

Titanium was discovered in 1910 and got its name from "Titan", a giant Greek mythology. Titanium is a light metal composed of 60% iron, 4.5g/cm^3. It is strong and highly resistant to corrosion. Titanium is bio-compatible because it is non allergenic.

2. Familiar material

Chinese woks: Titanium is highly resistant to heat with a melting temperature as high as 1668 °C. Its melting point is higher than that of steel. Although heat conductivity of titanium is almost the same as that of stainless steel, its weight is almost half of stainless steel. Titanium is non-toxic and easy to clean.

Piercing, watches and eye glasses: Titanium appears many colors and is used in piercing, for brooches, tie pins and cuff links. It is very light and allergic reactions are almost nil.

Golf clubs: With a titanium driver head, it is possible for the ball to travel longer distances. Changing the design of the golf courses is being considered due to this reason. The unit weight of the club is light and because the driver head has a thinner skull, the total weight of the club is light. With a light-weight club, one can aim for a higher speed swing. Many golfers agree that because of a larger head and consequently, a wider sweet spot, titanium clubs are unbeatable. In 1997 iron clubs and putters made from titanium were introduced.

Recently, many kinds of new titanium alloy heads have been developed. There are new applications for titanium being studied.

Foods and tableware: Titanium is non-toxic and since it does not dissolve in salt water, it does not change the taste of foods. Titanium is most appropriate for

processing food and tableware. It is light strong and is a high-grade material. Titanium is being used for some types of outdoor equipment and will be used even more in this area in the future.

Automobiles: Titanium is being tested mainly in connecting rods and is very effective when used for moving parts. The use of titanium has resulted in significant fuel efficiency.

Architecture and Building Materials:

The Naya Temple in Fukui is famous in Matsuo Basho's 'Oku no Hosomichi'. (Matsuo Basho is a famous Japanese poet from the 17th century.) The roof of the Naya Temple, the Fukuoka Dome, the Miyazaki-Ocean-Dome and the International Conference building at Tokyo Big Site are some of the buildings made from titanium.

3. Most Common Applications

Chemical plants: Titanium is highly corrosion resistant. It is used in many types of chemical equipment. About 30% of titanium used domestically is for chemical plants.

Seawater usage: Titanium is greatly used in nuclear and fossil power stations. It is used for the big heat exchanger, Condenser, which cools the steam form the turbine with seawater which does not corrode so the wall thickness of the tube is as thin as 0.5 mm. Condenser tubes consume about 20% of domestic titanium consumption.

Titanium in daily life: Recently, titanium is being used in many goods we use such as in sports, building material, medical applications and accessories. This amounts to about 30% of domestic consumption.

Aerospace: In the USA, about 70% of titanium produced is used for aerospace parts. In Japan only 2-3% of the titanium is consumed for aerospace usage. Thus, there is a big difference of market structure between Japan and USA.

Types and properties of titanium

From a materials science viewpoint, titanium has three types:α-titanium, $\alpha+\beta$-titanium and β-titanium. The typical α-titanium is high purity commercially pure unalloyed titanium; $\alpha+\beta$-titanium is represented by the Ti-6Al-4V alloy; and β-titanium includes the Ti-15V-3Cr-3Sn-3Al alloy.

$\alpha+\beta$-titanium and β-titanium are generally called titanium alloys. As unalloyed titanium is softer than stainless steel, golf club heads made of this material give golfers a tender feeling at the time of hitting. It is also an indispensable material when sophisticated fabrications are required. Titanium alloys, materials with other metals added to titanium, exceed stainless steel in strength and are used to manufacture cast or forged club heads. There are various titanium alloys, having specific characteristics. By using the right titanium alloy for the right application, thus making optimum use of the properties of each material, new golf clubs with even better performance are being developed. The chemical composition of some titanium alloys used for golf club heads is shown in the table below.

Type of Ti	Chemical composition (weight %)							
(crystal structure)	Ti	Al	V	Mo	Sn	Fe	Cr	Others
Unalloyed titanium(α)	100	-	-	-	-	-	-	-
Ti-6Al-4V($\alpha+\beta$)	90	6	4	-	-	-	-	-
Ti-4.5Al-3V-2Fe-2Mo($\alpha+\beta$)	88.5	4.5	3	2	-	2	-	-
Ti-15V-3Cr-3Sn-3Al(β)	76	3	15	-	3	-	3	-
Ti-20V-4Al-1SN(β)	75	4	20	-	1	-	-	-
Ti-22V-4Al(β)	74	4	22	-	-	-	-	-
Ti-16V-4Sn-3Al-3Nb(β)	74	3	16	-	4	-	-	3(Nb)

Physical properties of commercially pure Titanium (Titan15) ASTM Gr.2

Density (gm/cm^3)	**Melt Range** (°C±15)	**Spec. Heat** (J/gm K)	**Elec. Resist.** (μΩ cm)	**Yield Str/ Density** ($*10^6$N m/ kg)	
4.51	1677	0.54	56	78	
UTS (MPa)	**Therm. Cond.** (W/m K)	**Beta Transus** (°C±15)	**0.2% Proof** (MPa)	**Th. Exp. Coeff. 0-100°C** (10^{-6} K^{-1})	**Th. Exp. Coeff. 0-300°C** (10^{-6} K^{-1})
491	16.3	913	276	8.6	9.2
Elong. (%)	**Fatigue Limit** (% of Tens. Strength)	**Tensile Str.** (MPa)	**Poisson's Ratio**	**Tensile Str./ Density** ($*10^6$ $NmKg^{-1}$)	**Fracture Toughness** MPa-$m^{1/2}$)
20	50	345	0.36	107	66

Physical properties of Ti-6%Al-4%V (Titan31) ASTM Gr.5

Density (gm/cm^3)	**Melt Range** (°C±15)	**Spec. Heat** (J/gm K)	**Elec. Resist.** (μΩ cm)	**Yield Str/ Density** ($*10^6$N m/ kg)	
4.42	1649	0.56	170	206	
UTS (MPa)	**Therm. Cond.** (W/m K)	**Beta Transus** (°C±15)	**0.2% Proof** (MPa)	**Th. Exp. Coeff. 0-100°C** (10^{-6} K^{-1})	**Th. Exp. Coeff. 0-300°C** (10^{-6} K^{-1})
994	7.2	999	828	8.8	9.2
Elong. (%)	**Fatigue Limit** (% of Tens. Strength)	**Tensile Str.** (MPa)	**Poisson's Ratio**	**Tensile Str./ Density** ($*10^6$ $NmKg^{-1}$)	**Fracture Toughness** MPa-$m^{1/2}$)
10	55-60	345	0.31	226	75

APPENDIX II

Labeled 3-D Pictorial View of Sonic mill Ultrasonic Drilling Machine and Slurry Tank

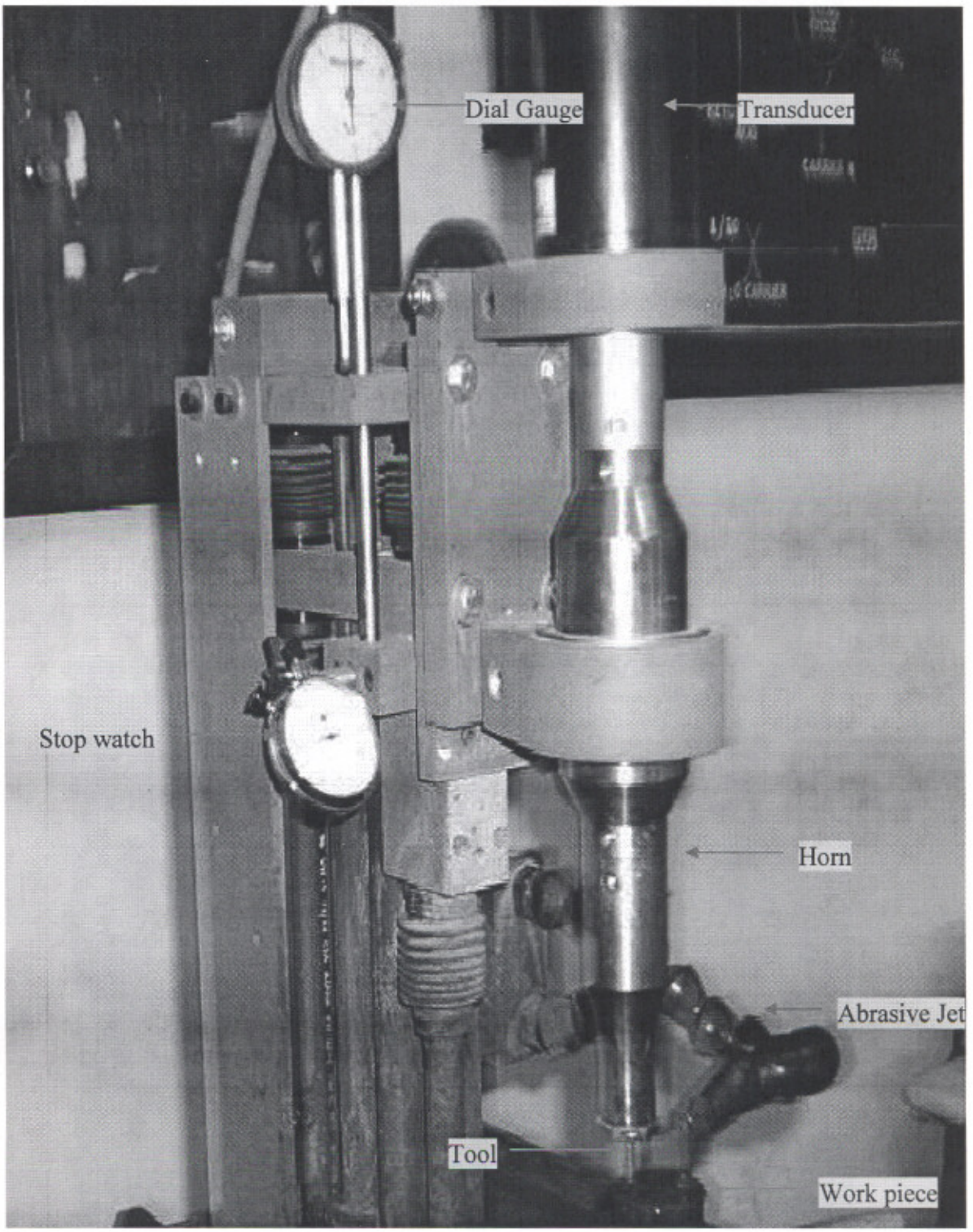

Figure AII-a: 3-D Pictorial view of Sonic ultrasonic drilling machine

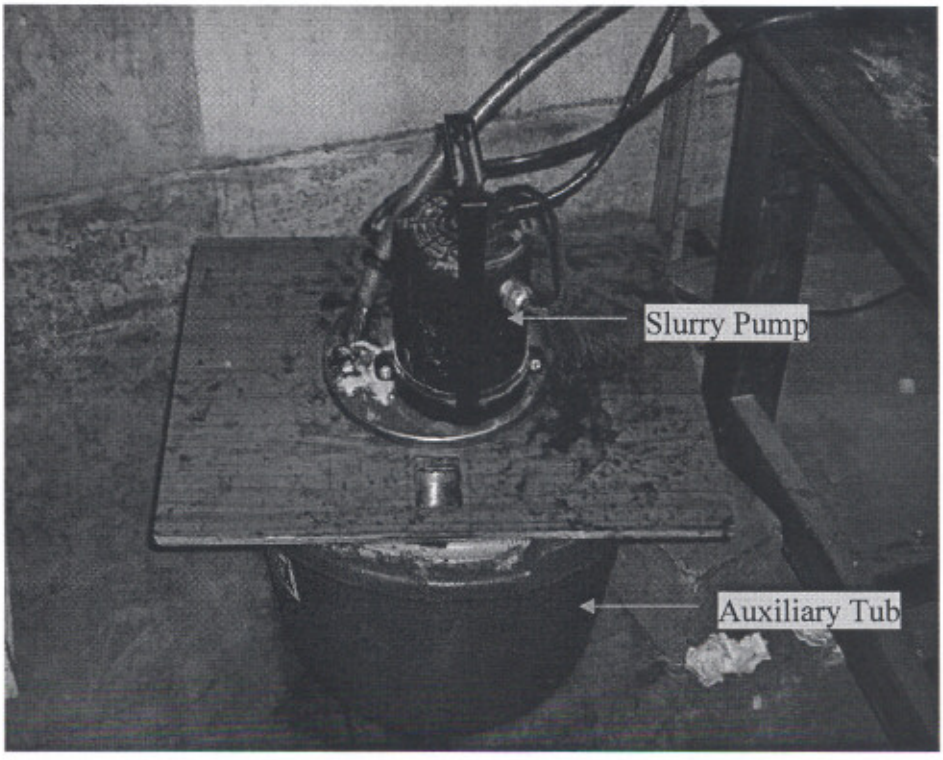

Figure A II-b: 3-D Pictorial view of slurry pump with auxiliary tub

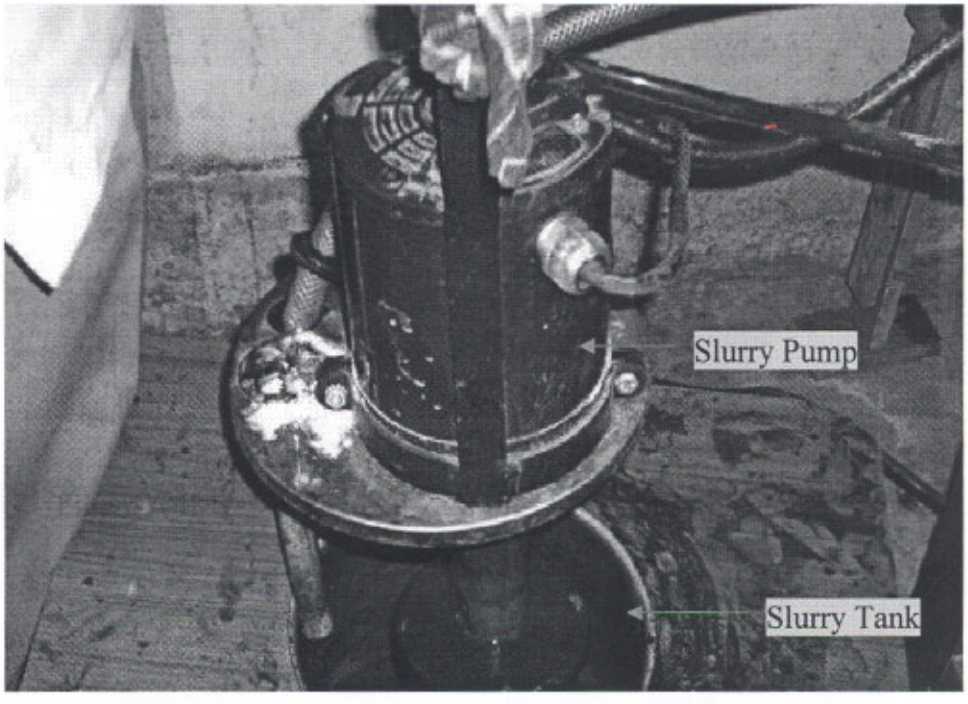

Figure A II-c: 3-D Pictorial view of slurry pump and slurry tank